

# Surface Grafted Polymer Brushes: A Versatile Platform for Antibacterial Applications

THÈSE N° 6565 (2015)

PRÉSENTÉE LE 2 AVRIL 2015

À LA FACULTÉ DES SCIENCES ET TECHNIQUES DE L'INGÉNIEUR  
LABORATOIRE DES POLYMÈRES  
PROGRAMME DOCTORAL EN SCIENCE ET GÉNIE DES MATÉRIAUX

ÉCOLE POLYTECHNIQUE FÉDÉRALE DE LAUSANNE

POUR L'OBTENTION DU GRADE DE DOCTEUR ÈS SCIENCES

PAR

**Sorin Alexandru IBANESCU**

acceptée sur proposition du jury:

Prof. P. Muralt, président du jury  
Prof. H.-A. Klok, directeur de thèse  
Dr Y. Simon, rapporteur  
Prof. G. J. Vancso, rapporteur  
Dr C. Wandrey, rapporteuse



ÉCOLE POLYTECHNIQUE  
FÉDÉRALE DE LAUSANNE

Suisse  
2015



The work described in this Thesis has been performed at the École Polytechnique Fédérale de Lausanne from May 2010 until December 2014 under the supervision of Prof. Harm-Anton Klok

*This work was financially supported by the CCMX Competence Centre for Materials Science and Technology, Lausanne, Switzerland*





*For Simina*



*The more you know who you are, and what you want, the less you let things upset you.*

*Bob Harris*



## Acknowledgments

First of all, I would like to thank Prof. Harm-Anton Klok for his supervision on my PhD thesis and for providing all the conditions to perform the research. Moreover, I sincerely appreciate his advices and support for the development and realization of some particularly interesting ideas. His guidance and understanding were very important in developing my research skills.

In addition, I would like to warmly thank my thesis committee members Prof. P. Muralt, Prof. G. J. Vancso, Dr. Y. Simon and Dr. Christine Wandrey for taking the time to review my thesis, for their patience and valuable discussion about my research.

Thanks to all collaboration partners, who significantly enriched this interdisciplinary work: Prof. R. Landmann, Dr. N. Khanna and Dr. J. Nowakowska from Department of Biomedicine, University Hospital Basel as well as Prof. J. McKinney who allowed me to perform my antibacterial experiments in his laboratory and François Signorino-Gelo for all his help during these experiments.

I would like to thank the whole team of the Laboratoire des Polymères, especially my office colleagues Sanhao, Dusko, Nicolas and Justin for the nice time spent together and their useful advices. Many thanks also to the other people in the LP, past and present, for the amazing experience they gave me working together, for their help and interesting talks. Special thanks to Solenne with whom I shared the lab for such a long time and Ana who supported me in my most difficult moments. Also I would like to thank Conor who helped me whenever I needed help and most importantly taught me about Saint Patrick's Day. All these people were and are very important to me, forming a real family, helping me to feel "at home" in Lausanne and at EPFL. I am especially grateful that many of them became good friends and I hope this friendship will last past my doctoral years. I learned a lot of things from them and I am grateful for all moments we shared.

I am truly grateful to my wife Simina for her support, confidence, patience and kindness during our stay here. Last, but not least, all my gratitude for my family for all their support throughout all these years of studies.



---

## Table of contents

<b>Summary</b> .....	<b>1</b>
<b>Résumé</b> .....	<b>3</b>
<b>1. Antibacterial Polymer Brushes via Surface-Initiated Controlled Radical Polymerization</b> .....	<b>7</b>
1.1. Impact of bacteria adhesion on implants and biomedical devices .....	7
1.2. Mechanisms of biofilm formation.....	8
1.3. Strategies to prevent bacteria adhesion .....	11
1.3.1. Biopassive surfaces .....	12
1.3.2. Bioactive surfaces .....	14
1.3.2.1. Bioactive non-leaching surfaces .....	14
1.3.2.2. Bioactive leaching surfaces .....	18
1.4. Polymer brushes .....	19
1.4.1. Introduction.....	19
1.4.2. Synthesis of polymer brushes.....	21
1.4.2.1. Surface-Initiated Atom Transfer Radical Polymerization (SI-ATRP).....	21
1.4.3. Post-modification reactions on hydroxyl-functionalized polymer brushes .....	24
1.4.4. Characterization methods for polymer brushes.....	25
1.5. References .....	28
<b>2. HEMA/OEGMA Polymer Brushes as an Attractive Platform to Prevent Bacteria Adhesion</b> .....	<b>41</b>
2.1. Introduction.....	41
2.2. Experimental Section .....	45
2.2.1. Materials .....	45
2.2.2. Methods.....	45
2.2.3. Procedures.....	46
2.2.3.1. Synthesis of SI-ATRP initiator (1b) .....	46
2.2.3.2. Synthesis of SI-ATRP inactive chlorosilane (2b).....	47
2.2.3.3. Immobilization of the ATRP initiator.....	47
2.2.3.4. HEMA polymer brush synthesis.....	48
2.2.3.5. OEGMA <sub>6</sub> polymer brush synthesis.....	48
2.2.3.6. Bacterial culture preparation.....	48
2.2.3.7. Bacterial adhesion tests .....	49
2.2.3.7.1. Crystal violet staining .....	49
2.2.3.7.2. LIVE/DEAD staining .....	49
2.3. Results and Discussion.....	50
2.3.1. Polymer-brush synthesis .....	50
2.3.2. Bacteria adhesion tests .....	54
2.4. Conclusions.....	59
2.5. References.....	60
2.6. Supporting Information.....	65

---

<b>3. Dual Biopassive-Bioactive Antibacterial Coatings Based on Vancomycin Functionalized Polymer Brushes.....</b>	<b>69</b>
3.1. Introduction.....	69
3.2. Experimental Section.....	72
3.2.1. Materials.....	72
3.2.2. Methods.....	73
3.2.3. Procedures.....	73
3.2.3.1. p-Nitrophenyl chloroformate (NPC) activation of PHEMA and POEGMA <sub>6</sub> brushes.....	73
3.2.3.2. Vancomycin coupling via the amine group.....	73
3.2.3.3. Vancomycin coupling via the carboxylic acid group.....	74
3.2.3.4. ELISA testing.....	74
3.2.3.5. Bacteria culture preparation.....	74
3.2.3.6. LIVE/DEAD staining.....	75
3.3. Results and Discussion.....	75
3.3.1. Synthesis of vancomycin modified polymer brushes.....	75
3.3.2. Characterization of vancomycin modified polymer brushes.....	77
3.3.3. Antibacterial testing of vancomycin modified polymer brushes.....	82
3.4. Conclusions.....	88
3.5. References.....	89
3.6. Supporting Information.....	92
<b>4. Polymer brushes as a platform for bacteria triggered release .....</b>	<b>93</b>
4.1. Introduction.....	93
4.2. Experimental Section.....	95
4.2.1. Materials.....	95
4.2.2. Methods.....	96
4.2.3. Procedures.....	96
4.2.3.1. Peptide functionalization of PHEMA brushes.....	96
4.2.3.2. Autolysin triggered release experiment.....	96
4.2.3.3. $\beta$ -Amino-3-(hydroxymethyl)cephalosporinic acid (7-HACA) synthesis.....	97
4.2.3.4. Coupling of dansylcadaverine to PHEMA.....	97
4.2.3.5. Coupling of dansylcadaverine via 7-HACA linker.....	97
4.2.3.6. Release experiment $\beta$ -lactamase.....	97
4.3. Results and Discussion.....	98
4.3.1. Autolysin triggered release.....	98
4.3.2. $\beta$ lactamase triggered release from PHEMA brushes.....	103
4.4. Conclusions.....	110
4.5. References.....	111
4.6. Supporting Information.....	113
<b>5. Synthesis and characterization of hydrolytically degradable polymer brushes</b>	<b>115</b>
5.1. Introduction.....	115
5.2. Experimental Section.....	118
5.2.1. Materials.....	118



---

5.2.2.	Methods.....	118
5.2.3.	Procedures.....	119
5.2.3.1.	Synthesis of 1,2-benzenedimethanol .....	119
5.2.3.2.	Synthesis of 5,6-Benzo-2-(chloromethyl)-1,3-dioxepane.....	119
5.2.3.3.	Synthesis of 5,6-Benzo-2-methylene-1,3-dioxepane .....	120
5.2.3.4.	Synthesis of Poly(OEGMA <sub>6</sub> -BMDO-DEAEMA) brushes .....	120
5.2.3.5.	Hydrolytic degradation of Poly(OEGMA <sub>6</sub> -BMDO-DEAEMA) brushes .....	120
5.2.3.6.	Synthesis of 2-ethoxy-2-oxo-1,3,2-dioxaphospholane (EEP).....	121
5.2.3.7.	Synthesis of the thiourea (TU) cocatalyst.....	121
5.2.3.8.	Synthesis of undecanol modified substrates .....	121
5.2.3.9.	Synthesis of polyphosphoester brushes .....	122
5.3.	Results and Discussion.....	122
5.3.1.	Hydrolytically degradable P(OEGMA-BMDO-DEAEMA) brushes .....	122
5.3.1.1.	Synthesis of P(OEGMA-BMDO-DEAEMA) brushes .....	122
5.3.1.2.	Degradation kinetics .....	125
5.3.2.	Synthesis and characterization of polyphosphoester polymer brushes.....	128
5.4.	Conclusions.....	134
5.5.	References.....	135
5.6.	Supporting Information.....	137
<b>6.</b>	<b>Conclusions and Perspectives.....</b>	<b>139</b>
	<b>Curriculum vitae.....</b>	<b>a</b>



---

## List of Abbreviations

$^1\text{H}$ NMR	proton nuclear magnetic resonance
7-HACA	7 $\beta$ -amino-3-(hydroxymethyl)cephalosporinic acid
AA	acrylic acid
Abs.	absorbance
AFM	atomic force microscopy
A(R)GET	activators (re)generated by electron transfer
AMPs	antimicrobial peptides
ATRP	atom transfer radical polymerization
BMDO	5,6-benzo-2-methylene-1,3-dioxepane
bipy	2,2'-bipyridine or 2,2'-bipyridyl
CFU	colony-forming unit
CNS	coagulase-negative staphylococcus
$\text{Cu}^{\text{I}}\text{Br}$	copper(I) bromide
$\text{Cu}^{\text{I}}\text{Cl}$	copper(I) chloride
$\text{Cu}^{\text{II}}\text{Br}_2$	copper(II) bromide
$\text{Cu}^{\text{II}}\text{Cl}_2$	copper(II) chloride
CV	crystal violet
DBU	1,8-diazabicyclo[5.4.0]undec-7-ene
DEAEMA	2-(diethylamino)ethyl methacrylate
DLS	dynamic light scattering
DMAP	4-(dimethylamino)pyridine
DMSO	dimethyl sulfoxide
DSC	<i>N,N'</i> -disuccinimidyl carbonate
EDC	<i>N</i> -(3-dimethylaminopropyl)- <i>N</i> -ethylcarbodiimide hydrochloride
EEP	2-ethoxy-2-oxo-1,3,2-dioxaphospholane
ELISA	enzyme-linked immunosorbent assay
FTIR	Fourier transform infrared
GMA	glycidyl methacrylate
GPC	gel permeation chromatography
LCST	lower critical solution temperature
MHA	Mueller-Hinton agar
MMA	methyl methacrylate
$M_n$	number-average molecular weight of the polymer chains
NaCl	sodium chloride
NaOH	sodium hydroxide
NEXAFS	near edge X-ray absorption fine structure analysis
NHS	<i>N</i> -hydroxysuccinimide
NPC	<i>p</i> -nitrophenyl chloroformate
P4VP	poly(4-vinylpyridine)
PAA	poly(acrylic acid)
PAM	polyacrylamide

PBS	phosphate buffered saline
PCBMA	poly(carboxybetaine methacrylate)
PDEAEMA	poly(2-(diethylamino)ethyl methacrylate)
PDMAEMA	poly(2-(dimethylamino)ethyl methacrylate)
PDMS	polydimethylsiloxane
PGMA	poly(glycidyl methacrylate)
PHEMA	poly(2-hydroxyethyl methacrylate)
PI	propidium iodide
PMMA	poly(methyl methacrylate)
POEGMA	poly[oligo(ethylene glycol) methyl ether methacrylate]
PPE	phosphoester
PPEGMA	poly(poly(ethylene glycol) methacrylate)
ROP	ring-opening polymerization
RROP	radical ring-opening polymerization
QCM	quartz crystal microbalance
QCM-D	quartz crystal microbalance with dissipation
SAM	self-assembled monolayer
SE	staphylococcus epidermidis
SI-ATRP	surface-initiated atom transfer radical polymerization
SI-CRP	surface-initiated controlled radical polymerization
SI-NMP	surface-initiated nitroxide-mediated polymerization
SiO <sub>2</sub>	silicon (di)oxide
SI-PIMP	surface-initiated photoiniferter-mediated polymerization
SI-RAFT	surface-initiated reversible-addition fragmentation chain transfer
TBD	1,5,7-triazabicyclo[4.4.0]-undec-5-ene
TEA	triethylamine
TGA	thermogravimetric analysis
THF	tetrahydrofurane
TMB	3,3',5,5'-tetramethylbenzidine
TSB	tryptic soy broth
TU	thiourea
UAME	undecylenic acid methyl ester
UV-Vis	ultraviolet-visible spectroscopy
Vanc	vancomycin
XPS	X-ray photoelectron spectroscopy
WCA	water contact angle

## Summary

The continuous increased number of medical devices necessary to improve and save millions of patient's lives is a challenging task the modern society has to face. Albeit very useful, their use is associated with the increased risk of nosocomial infections. Therefore the need for new and more effective biomaterials able to reduce the vulnerability of implants to bacterial contamination and infection is constantly growing. Various strategies have been proposed and applied to prepare antibacterial materials able to respond to different requirements specific for antibacterial applications. Among diverse strategies the approach based on substrates modification with polymer brushes proved both versatile and reliable. Polymer brushes are thin polymeric films with all chains tethered with one end on a surface and since the development of surface-initiated controlled radical polymerization they can be obtained with good control over conformation, architecture and thickness. Therefore polymer brush coatings can be tailored with desired and fine tuned properties as functional biomaterials for a large variety of biomedical applications. The main objective of this Thesis was to develop versatile platforms for antibacterial applications based on polymer brush surfaces able to prevent bacteria adhesion and/or to kill bacteria on contact or through bacteria triggered controlled release of an antimicrobial compound. Moreover, novel systems based on polymer brushes have been synthesized as hydrolytically degradable platforms for potential biomedical applications as scaffolds for tissue engineering or protein/drug delivery systems.

**Chapter 1** analyses the mechanism of the biofilm formation and different strategies developed to inhibit bacterial adhesion, to prevent biofilm formation and proliferation and to reduce hospital-acquired bacterial infection. Various approaches for surfaces modification with polymer brushes are discussed, emphasizing on the possibilities of tailoring their antibacterial properties. **Chapter 2** explores, for the first time, Staphylococcus Epidermidis adhesion on HEMA or OEGMA polymer brushes on a wide range of grafting densities and film thicknesses. Both PHEMA and POEGMA brushes have antifouling properties comparable with PEG brushes still considered a "gold standard" material for antibacterial applications. Both brushes carry functional groups on each repeating unit and are more appropriate for the development of platforms for novel biomedical applications. In **Chapter 3** the possibility to obtain dual functional coatings combining the bacteria repellent character of the polymer brush with the possibility to

selectively immobilize antibiotics is investigated and the antibacterial activity against *S. Epidermidis* of vancomycin modified surfaces is analyzed. In this case the nature of the brush is remarkably important, as its architecture influences the capability of the immobilized antibiotic to reach the bacteria membrane and to exhibit its bactericidal activity. Moreover, the way in which the antibiotic is connected to the polymer brush has a great influence on the overall activity of the synthesized system. Vancomycin can be successfully connected both via the primary amine and the carboxylic group to the polymer brushes, but only the later keeps the antibiotic bactericidal activity. The aim of **Chapter 4** is to develop systems based on polymer brush able to release an active compound in the presence of selected bacterial signals. A dye is coupled to PHEMA brushes via a specific linker sensitive to autolysins or  $\beta$ -lactamase and its controlled release is monitored as a function of brush architecture. Finally, **Chapter 5** focuses on improving existing hydrolytically degradable polymer brushes by neighboring group participation of a nucleophilic moiety. It is obvious that adding a nucleophilic group to a polymer brush has favorable influence on its degradability in neutral or slightly acidic media. Moreover, the possibility to develop novel hydrolytically degradable polymer brushes based on polyphosphoesters is reported. The two studied systems are suitable as building blocks for platforms with antibacterial applications, as well as devices for controlled drug delivery systems or tissue engineering.

This Thesis work successfully proved the versatility of polymer brushes for antibacterial applications. First, PHEMA and POEGMA brushes with different grafting densities and thicknesses were for the first time tested against clinically relevant *S. Epidermidis* and their applicability as biopassive platforms has been proved. Second, the polymer brushes were modified with vancomycin to obtain dual biopassive-bioactive surfaces able to ensure both anti-adhesive bacterial properties and bactericidal activity. Third, the polymer brushes were used as platforms for bacteria signal triggered release of active compounds and fourth, the possibility to add degradability to these polymers brushes was explored.

**Keywords:** Antibacterial surfaces, implant-related infections, polymer brushes, surface-initiated atom radical polymerization (SI-ATRP), biomaterials, bacteria adhesion, Crystal violet staining, bioactive compounds, dual-functional biopassive-bioactive platforms, vancomycin, ELISA testing, SYTO9/PI staining, bacteria triggered release systems, autolysin,  $\beta$ -lactamase, hydrolytically degradable polymer brushes, nucleophilic moieties, neighboring group participation, polyphosphoester brushes.

## Résumé

La conception de dispositifs médicaux nécessaire à l'amélioration de la vie de millions de patients représente un défi de taille pour notre société moderne. Leur utilisation est cependant souvent associée à une augmentation du risque lié aux infections nosocomiales. Il existe de ce fait une réelle demande pour de nouveaux biomatériaux capables de réduire la vulnérabilité de ce type d'implants médicaux face aux contaminations bactériennes ainsi qu'aux infections. Différentes stratégies ont été proposées et appliquées pour la préparation de matériaux possédant des propriétés antibactériennes et ayant la capacité de répondre à différents critères spécifiques aux applications antibactériennes. Parmi ces différentes stratégies, l'approche basée sur la modification de substrats avec des brosses de polymères se révèle particulièrement versatile et fiable. Les brosses de polymères sont des couches polymériques minces formées par l'attachement des chaînes de polymères de manière covalente par l'une des extrémités à une surface. La polymérisation radicalaire contrôlée, initiée directement par greffage d'un initiateur sur une surface permet d'obtenir des brosses de polymères avec un contrôle sur la conformation, l'architecture et l'épaisseur de la couche greffée. Plus spécifiquement, les brosses de polymères peuvent être spécifiquement modifiées afin d'obtenir des biomatériaux fonctionnels pour une grande variété d'applications biomédicales. L'objectif de cette thèse est le développement de d'une plateforme versatile basée sur le recouvrement d'une surface par des brosses de polymères afin de prévenir l'adhésion de bactéries ou directement en combattant celles-ci par le biais d'une libération contrôlée d'agents antimicrobiens. Des systèmes innovants basés sur les brosses de polymères dégradables ont également été étudiés comme substrat pour l'ingénierie tissulaire ou à des fins de libération contrôlée de protéines thérapeutiques.

**Le chapitre 1** analyse le mécanisme de formation de biofilms ainsi que le développement de différentes stratégies qui permettent d'inhiber l'adhésion bactériennes, prévenant ainsi la formation et prolifération de biofilms et de facto la réduction d'infections nosocomiales. Différentes approches ont été utilisées pour la préparation de brosses de polymères et celles-ci sont discutées en donnant une importance particulière à la possibilité d'adapter leur propriétés antibactériennes de manière spécifique. **Le chapitre 2** explore, pour la première fois, l'adhésion du *Staphylococcus Epidermidis* sur des brosses de polymères de type HEMA et OEGMA en fonction de la densité de greffage ainsi que de l'épaisseur de la couche polymérique. Les brosses PHEMA et

POEGMA ont toutes deux démontrées des propriétés comparables à celles des brosses PEG, considérées alors comme matériau de référence dans les applications antibactériennes. Cependant, dans le cas de HEMA et OEGMA, chaque monomère possède un groupe fonctionnel, ce qui en fait des plateformes particulièrement intéressantes pour le développement de dispositifs biomédicaux. Dans le **chapitre 3**, des matériaux combinant à la fois les propriétés antiadhésives, intrinsèques aux brosses de polymères, ainsi que l'immobilisation sélective d'antibiotiques tel que la vancomycine dans ces même brosses ont été étudiés. Dans le cas de *S. Epidermidis* par exemple, le type de brosses de polymères est très important. En effet l'architecture des brosses influence la capacité de l'antibiotique immobilisé à accéder à la membrane des bactéries et y exercer son activité bactéricide. La façon dont l'antibiotique est lui-même immobilisé sur le polymère revêt également une grande importance et influence l'ensemble de l'activité du système synthétique en question. La vancomycine peut être attachée de manière covalente aux brosses de polymères soit par son amine primaire soit par son acide carboxylique. Seule la connexion via ce dernier retient l'activité bactéricide de l'antibiotique. L'objectif du **chapitre 4** est le développement de systèmes basés sur des brosses de polymères capable de libérer un agent en réponse à certains signaux liés à la présence de bactéries. Un colorant a été conjugué à des brosses PHEMA via une séquence sensible à l'activité des autolysines ou des  $\beta$ -lactamases et sa libération contrôlée a été analysée en fonction de l'architecture des brosses. Finalement, le **chapitre 5** se concentre sur l'optimisation de brosses de polymères dégradables grâce à la participation d'une espèce nucléophile voisine au site d'hydrolyse. Il est évident que la présence d'une espèce nucléophile dans une brosse de polymères influence favorablement sa dégradation en milieu neutre ou faiblement acide. Par ailleurs, la possibilité de développer des brosses de polymères dégradables basées sur les polyphosphoesters a également été étudiée. Les deux systèmes présentés ont été adaptés comme plateforme antibactériennes, mais aussi comme dispositif de libération contrôlé d'agents thérapeutiques ainsi que dans le contexte de l'ingénierie tissulaire.

Ce travail de thèse a prouvé la versatilité des brosses de polymères pour des applications antibactériennes. Premièrement, les brosses PHEMA et POEGMA ayant différentes densités de greffage et différentes épaisseurs ont été pour la première fois testées contre les infections liés à *S. epidermidis* et leur applicabilité en tant que plateforme biopassive a été démontrée. Deuxièmement, les brosses de polymères ont été modifiées avec l'antibiotique vancomycine afin d'obtenir un matériau présentant une



surface à la fois biopassive et bioactive, démontrant aussi bien une activité antiadhésive que bactéricide. Troisièmement, les brosses de polymères ont été utilisées comme plateforme pour la libération de molécules actives en réponse à une infection bactérienne et enfin la possibilité de rendre ces brosses de polymère dégradable a également été explorée.

**Mots-clés :** Surfaces antibactériennes, infections liées à un implant, brosses de polymères, polymérisation atomique radicalaire initiée à partir d'une surface (SI-ATRP), biomatériaux, adhésion bactérienne, coloration Crystal violet, composés bioactifs, biopassive-bioactive plateforme, vancomycine, test ELISA, coloration SYTO9/PI, dispositif de libération contrôlée par une infection bactérienne, autolysine,  $\beta$ -lactamase, brosses de polymères dégradables, espèce nucléophiles, participation du groupe voisin, brosses polyphosphoester.



# 1. Antibacterial Polymer Brushes via Surface-Initiated Controlled Radical Polymerization

## 1.1. Impact of bacteria adhesion on implants and biomedical devices

In modern society, the number of patients necessitating biomaterial-based implants is continuously increasing. The use of sophisticated medical devices increases life expectancy but often is challenging due to the implant-associated infections caused by biofilms. The complex problems arising when implant-related infections are considered involve long-term antibiotics treatments, implant removal or even, major health risks. Bacterial attachment on implant surface has serious consequences on the patient's life and significant impact on medical costs and health care systems<sup>1-4</sup>. A large number of bacteria can attach on implant and medical devices surfaces and form biofilms, but coagulase-negative staphylococci, mainly *Staphylococcus epidermidis* and *Staphylococcus aureus* are responsible for many biomaterial-related infections worldwide<sup>5</sup>. Specificity of implant-related infections caused by coagulase-negative staphylococci (mostly *Staphylococcus epidermidis*), *Staphylococcus aureus*, and other bacteria of lower virulence resides in their ability to overcome innate or acquired immunity of human host and to resist to antimicrobial therapy due to the phenotypic resistance ascribed to the difficulty of antimicrobial agents to penetrate the biofilm, while the architecture of the biofilm ensures communication among individual members of community and access to nutrients<sup>5,6</sup>. Biomaterial-related infections also have the risk to produce chronic affections, often necessitating surgery to save patient's life.

In Germany only more than 2.5 million biomedical devices like central venous catheters, prosthetic joints, knee and hip implants, cardiac pacemakers and heart valves, artificial lenses, and CSF-shunts are used every year<sup>5,6</sup>. In the United States, direct costs for healthcare associated infections were estimated to range from US\$28 billion to \$45 billion in one year with upward of 60% of these being related to medical devices<sup>3</sup>.

According to data reported to the National Health Care Safety Network, coagulase-negative staphylococci today are the most frequent cause of device- or surgery-associated hospital-acquired infection in the USA<sup>7</sup>. Annually, millions of patients are affected by implant associated infection all over the world, 80% of human infection being connected with biofilm formation<sup>1,3,5,6</sup>.

## **1.2. Mechanisms of biofilm formation**

Bacteria can exist and grow as free microorganisms suspended in a fluid medium (water, blood, etc.). This type of population is known as planktonic bacteria and they are the less dangerous for humans, being vulnerable to antibiotics and immune body response. More than 80% of bacteria exist and grow as biofilms – communities of bacterial cells attached to a surface and protected by an extracellular matrix<sup>1-6,8</sup>. The organization of bacteria in biofilms confers access to nutrients, resistance to antimicrobial agents due to the poor diffusion, and possibilities to transgenic mutations beneficial for bacterial survival<sup>9</sup>. Even if the planktonic state was considered dominant, for more than 350 years practical observations evidenced the existence of communities of bacteria on surfaces and their natural tendency to form aggregates. Biofilms were first observed and mentioned by the end of the 17<sup>th</sup> century, when Antonie van Leuwenhoek used his primitive but effective microscope to describe aggregates of “animalcules” that were scraped from human tooth surfaces<sup>8,10,11</sup>.

Numerous theories were elaborated to explain biofilm formation taking into consideration the interference of different physical, chemical and biological processes. Clearly, first of all, the microorganisms approach surfaces and adhere to substrate forming micro-colonies in which cell-to-cell cohesion forces appear and develop<sup>10,11</sup>. To explain the mechanism of biofilm formation firstly, a three stages process was supposed. The first step includes the “exploration” of the surface by bacteria and the reversible attachment on the substrate. The attached bacteria modify their layer of exopolysaccharide (EPS) surrounding each cell, adapting it to the new environment. So, a first layer or deposit of adsorbed bacteria is formed. In the second stage polymer bridges are formed within different bacterial layers and the surface and the third stage involves irreversible adhesion of bacteria on substrate, colonization or growth and division of organisms on the surface<sup>8,10,11</sup>(Figure 1).

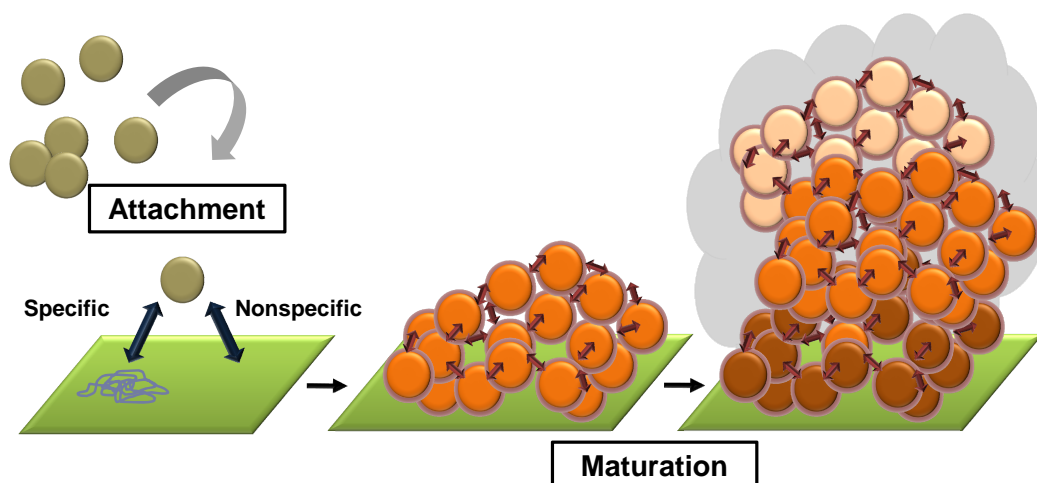


**Figure 1.** Three stage mechanism for biofilm formation

Later on, based on observations considering complex processes involved in cell–substrate and cell–cell interactions more elaborated mechanisms have been proposed<sup>12-29</sup>. Salwiczek et al.<sup>3</sup> proposed a four stage mechanism for biofilm formation by *Staphylococcus epidermidis* including (1) attachment and monolayer formation, (2) formation of microcolonies, (3) maturation and structuring and (4) detachment and return to the planktonic growth model. They explained the role of physiochemical forces (van der Waals forces, hydrophobic interactions, and polar and ionic interactions) in the first stage of reversible attachment of bacteria on substrate and the formation of an “adherent monolayer”. Based on bacteria multiplication and aggregation processes the microcolonies are formed depending on secreted and surface-adsorbed bio-macromolecules, including polysaccharide intercellular adhesin (PIA), surface proteins, teichoic acid, and extracellular DNA<sup>3,19</sup>. The third stage the microcolonies evolve in macrocolonies encapsulated in an exopolysaccharide (EPS) that is highly penetrated by channels<sup>3,20</sup>. The fourth stage, after complete development of biofilm, is highly responsible for infection propagation and subsequent colonization.

T.R. Garrett et al.<sup>8</sup> describe a five step mechanism for biofilm formation explaining the importance of the conditioning layer formation, ensuring, in the first stage, anchorage and nutrients for the first bacterial communities. The second stage refers to the reversible adhesion of bacteria reaching surface either due to physical forces or by bacterial appendages such as flagella. This stage is influenced by different factors such as available energy, surface functionality, bacterial orientation, temperature and pressure conditions. The irreversible adhesion of bacteria appears in the third stage when the surface is

colonized with microorganisms which overcame the repulsive forces, process dependent on the hydrophobic–hydrophilic properties of interacting surfaces<sup>30</sup>. This population develops and strengthens the linkages with the support surface. In the fourth stage the irreversibly absorbed bacteria begin to grow and generate mushroom-like structures, architecture favorable for biofilm development allowing the nutrients to penetrate deep in the biofilm<sup>31</sup>. Depending on the availability of nutrients and all chemical and physical environmental condition, the biofilm exponentially grows, biological processes dominating physical and chemical interactions. Excretion of polysaccharide intercellular adhesin (PIA) polymers and the presence of divalent cations interact to form stronger bonding between cells<sup>32</sup>. The bacteria forming the biofilm modify the gene expression and differences have been evidenced between the two forms of bacteria states (planktonic/sessile). Hall-Stoodley and Stoodley<sup>31</sup> identified the differences in gene expression of planktonic and sessile cells, and as many as biofilm associated proteins were not found in the planktonic profile. The last stage in biofilm formation is characterized by the equality between the rate of cell division and the rate of cell death. This is the moment in which the biofilm consolidates and a part of bacteria are spreading to invade new zones.

The process of biofilm formation is influenced by a series of environmental factors, the most important being pH<sup>33-37</sup>, temperature<sup>38-42</sup>, surface elasticity, availability of nutrients<sup>43,44</sup>. Galanakos et. al<sup>45</sup> analyzing the impact of bacterial biofilms on the viability of orthopedic implants also describe a five-stage process for biofilm formation taking into consideration studies performed for a number of bacterial species, including *Escherichia coli*, *Pseudomonas aeruginosa* and *Vibrio cholera*. The stages they describe are: (1) initial attachment of cells to the surface, (2) production of extracellular polymeric substance, (3) early development of biofilm architecture (colonization), (4) maturation of biofilm architecture, (5) dispersion of single cells from the biofilm. The authors also emphasize that in the final stage few bacteria can leave the surface to find more appropriate location and thus, spreading infection.

In an interesting review Arciola et al.<sup>46</sup> investigate the influence of specific biofilm factors in the pathogenesis of biofilm-associated infections. They underline a four-step process for biofilm formation: 1) Initial attachment of cells to the biomaterial surface: hydrophobic interactions, AtlE, AtlA; 2) Accumulation in multiple bacterial layers; 3) Biofilm maturation: production of exopolysaccharide (EPS), proteins (Bap, Aap, SasG, SasC, Embp, FnbpA and FnbpB), eDNA; 4) Detachment of cells from the biofilm into a

planktonic state: environmental signals, signal transduction pathways and effectors. Different factors influencing the mechanism that regulates the on/off switch of the biofilm production are discussed. The biofilm functions as a complex living organism build up by microbial cells, embedded in a matrix material. Existing channels form a complex circulatory system available for liquids carrying nutrients to the cells at the bottom of the construction. As a living organism the biofilm possess a signaling and communication system. The organization of biofilms is regulated by signals analogous to the hormones and pheromones typical of multicellular communities of eukaryotic cells<sup>46</sup>. Analyzing the vast literature including *in vivo* and *in vitro* studies on various bacteria species they concluded that the identification of the biofilm components PIA, extracellular DNA and proteins, the possibility to manipulate the accessory gene regulator (*agr*) system and thus to modulate biofilm expression are the bases for novel antibiofilm strategies. In a paper published in 2012, quorum sensing was indicated as a cell-to-cell communication system capable of regulating motility, adhesion, cell aggregation and biofilm formation, as well as virulence and metabolic activity in several bacterial species<sup>47,48</sup>.

### 1.3. Strategies to prevent bacteria adhesion

There are diverse strategies developed to inhibit/diminish bacterial adhesion, to prevent biofilm formation and proliferation, thus responding to continuously increasing demand for reducing the incidence of biomaterial and hospital-related infections and making implants and, generally, medical devices safer. Beside sterilization and aseptic procedures, antimicrobial agents have a long history of usage for avoiding bacterial/hospital acquired infections but their efficiency is limited. It is known that the most common disinfectant, chlorine, which is moderately oxidative, can act on different components of bacterial cells<sup>49</sup>. Nevertheless, the effectiveness of chlorine against biofilms is about 4 orders of magnitude lower than against planktonic cells<sup>49,50</sup>. Long-term antibiotic therapies are often used for the treatment of implant-related infections but the main disadvantage lies in developing increased antibiotic resistance, frequently surgical revision and implant removal being also necessary<sup>3,11</sup>.

The high resistance of sessile bacteria in biofilm to conventional antibiotic therapy determined intense research focused on creating and developing antimicrobial/

antibacterial surfaces able to reduce or even suppress bacteria adhesion on implant surfaces and, in many cases to release active principles capable to fight and kill bacteria<sup>2-6,45,46,50,51</sup>.

Bacterial infection at the site of implanted materials can be prevented by appropriate surface modification of the implanted device. The surface modification strategies that have been developed so far can be divided in two main classes:

- **Biopassive (anti-adhesion) approaches** intended to inhibit/reduce bacterial adhesion and to ensure protection of surfaces from colonization
- **Bioactive approaches** (active compounds are incorporated in biomaterials or covalent tethered to material surfaces):
  - *Non-leaching bioactive surfaces*
  - *Leaching bioactive surfaces*

### 1.3.1. Biopassive surfaces

As mentioned in the comments referring to the mechanism of biofilm formation the biological response of human body in contact with a foreign entity (implant, other device) strongly depends on the nature and amount of surface-adsorbed proteins<sup>52-54</sup>. The concept of passive protection relies on disabling any interaction with proteins, host cells or microorganisms. The biopassive base layer thereby ensures minimal protein adsorption occurs for bacteria to use as an attachment platform, which further prevents biofilm formation on the implant surface. Biopassive surfaces prevent/reduce the adhesion of bacteria usually through the use of hydrophilic or charged polymers. These kinds of polymers are either physisorbed or covalently linked on the surface<sup>54</sup>. Researchers appealed to various chemical approaches to create *low-fouling* or *antifouling* coatings including self-assembled monolayers (SAMs)<sup>55,56</sup>, different polymer-based systems<sup>2-4,45,46,54,57</sup>, liquid-infused nanostructured surfaces with a dynamic surface structure<sup>58</sup>. Even if SAMs have been used for a while, they are less stable, more difficult to control and less versatile. Meanwhile, polymer coatings have multiple advantages being suited for protection of various types of surfaces (metallic, polymer-based, glass, silicon, etc.); their properties and architectures can be tailored and tuned to meet requirements for functionality and applicability for various microbial/bacterial strains. It can be stated that the best antifouling surface should be hydrophilic, have functional groups with hydrogen bond acceptors but without hydrogen bond donors, and be electrostatically neutral<sup>59</sup>.



In a very recent review, Mario Salwiczek et al.<sup>3</sup> emphasized the main techniques used to synthesize polymer-based low-fouling coatings and the most important classes of polymers that are suitable for this purpose. As mentioned in a series of very good reviews<sup>2-4,45,46,48,50,54-61</sup> antifouling polymer coatings may be obtained using physical or chemical techniques of deposition on surfaces. Using conventional, classical methods or grafting techniques a large variety of polymers were produced and studied as biopassive coatings: poly(ethylene glycol) (PEG)<sup>3,54,57,59-64</sup>, polyacrylamide (PAM)<sup>65</sup>, poly(2-methyl-2-oxazoline) (PMOXA)<sup>54,62,66-69</sup>, zwitterionic structures, such as poly(*N*-sulfobetaine methacrylamide) (PSBMA)<sup>3,59-64,70,71</sup>, phosphobetaine, sulfobetaine, phospholipid polymers having a phosphorylcholine group<sup>70-72</sup>, poly(*N*-hydroxy-propyl methacrylamide) (PHPMA)<sup>73</sup>, polysaccharides such as dextrane<sup>54,74</sup> and hydrophilic polyurethanes<sup>75</sup>.

To increase suitability and efficiency on various surfaces and microbial/bacterial strains the biopassive coatings can be designed in different manners varying the main polymeric chain, the molecular weight and the nature and distribution of functional groups. The surface functionalization of numerous materials with non-biofouling molecules has been successfully exploited to reduce bacterial adhesion *in vitro*. Titanium oxide surfaces coated with PLL-g-PEG present a >80% reduction in adhesion of *S. aureus*; moreover any remaining bacteria formed aggregates which is envisioned to aid removal by the host's immune system<sup>52</sup>.

One of the most studied antifouling polymeric coatings is poly(ethylene glycol). Poly(ethylene glycol) (PEG) [H(OCH<sub>2</sub>CH<sub>2</sub>)<sub>n</sub>OH], also known as poly(ethylene oxide) (PEO), polyoxyethylene (POE) or polyoxirane, depending on its molecular mass (PEG refers to oligomers and polymers with a molecular mass below 20,000 g/mol, PEO to polymers with a molecular mass above 20,000 g/mol, and POE to a polymer of any molecular mass), is a macromolecular compound characterized by unique properties making it suitable for applications involving high resistance to protein absorption<sup>61-64</sup>. (PEG)-based polymers and their low-fouling properties have been intensively studied during the last decade<sup>3,54,57,59-64</sup> and they are still considered "gold standard material in the preparation of biomedical devices"<sup>2,76</sup>. The non-specific behavior of PEG, still not completely clarified against proteins, differentiating it of poly(butylene oxide), and poly(methylene oxide) or poly(propylene glycol), makes this polymer very interesting for low-fouling and other specific biological applications<sup>76</sup>. Explanations reside in its peculiar interaction with water. PEG, possessing unexpected water solubility or "hydrophilicity"<sup>76</sup> is able to alter the interactions of cells and proteins with water and with

each other. On the other hand, PEG does not hold a formal electrostatic charge so protein attraction is not favored. In its most favorable energetic configuration PEG has a large dipole moment and is surrounded by a strongly bonded water layer due to the ability of oxygens on PEG polar chain to act as hydrogen bond acceptors. Steric effects also play an important role in the special behavior of PEG chains against proteins and thus, the molecular weight of the polymer was found as an important factor of influence<sup>2,3,57,59-64</sup>. Linear, star-shaped as well as “bottle-brush” architectures have been ascribed to PEG chains. PEG utilization in antifouling coatings is limited by its relatively low stability toward oxidation and the instability of the coating layer which can be disrupted over longer periods of time due to degradation reactions<sup>78-82</sup>. Although PEG-brush covered surfaces exhibited excellent peptide/protein repellent properties, still its efficiency against bacteria attachment on surfaces is an open field of research.

### **1.3.2. Bioactive surfaces**

Even if extensively used, the efficiency of the biopassive coatings in preventing protein absorption and thus reducing bacteria adhesion has limitations due to improbability of obtaining defect-free surfaces<sup>54</sup>, their specificity to different bacterial strains<sup>51</sup> and substrates<sup>4</sup>. An alternative method to reduce bacterial adhesion and avoid biofilm formation focuses on bioactive surfaces able not only to prevent bacterial adhesion but to actively kill bacteria on contact or by releasing an antimicrobial agent<sup>4,54</sup>. Non-leaching bioactive surfaces suppose the physical or covalent immobilization of an antibacterial agent on surface, able to effectively kill bacteria on contact<sup>4</sup>, while the leaching bioactive surfaces involve the controlled release of the antimicrobial agents from coatings<sup>51</sup>.

#### **1.3.2.1. Bioactive non-leaching surfaces**

Trying to solve complex problems connected with the reduction in the bacteria repellent properties of the biopassive coatings due to the formation of an adsorbed conditioning film hindering the anti-adhesive surface, researchers concentrated on solutions able not only to prevent bacteria adhesion but to actively kill bacteria. The approach involved the immobilization of a bactericidal compound in the coating able to act mainly on the bacterial cellular membrane, disrupting it and thus provoking the death of bacteria. Different methods have been reported to include bactericidal agents in polymer coatings<sup>4,54,62,83</sup> including physical incorporation by mixing, layer by layer deposition, chemical grafting or plasma polymerization<sup>57</sup>. The most representative

bioactive non-leaching coatings are polymers functionalized with different bactericidal agents such as low molecular weight antibiotics (penicillin, ampicillin and gentamycin), bacteriophages, quaternary ammonium compounds, antimicrobial peptides, lysozyme, and chitosan<sup>4,54,57</sup>. Coatings containing antibiotics proved their effectiveness but also the disadvantage of inducing bacterial strain resistance<sup>84-86</sup>. Penicillin<sup>90</sup> and ampicillin<sup>85</sup> were attached to microwave plasma modified poly(tetrafluoroethylene) (subsequently hydrolyzed and esterified with PEG) and the resulted surfaces were effective against *S. Aureus* and a series of other microorganisms. Even if such coatings proved antibacterial properties, the antibiotic efficiency was reduced due to the steric effects, impeding their contact with bacterial cell membrane. Also, debris of the dead bacteria accumulated on surface can reduce antibiotics activity. Bacteriophages were efficient but with limited applicability due to their specificity for only few bacterial strains, potential toxicity and development of bacterial resistance<sup>87-89</sup>.

Antimicrobial peptides (AMPs) are natural products consisting of less than 50 amino acids, secreted by living organisms for protection against pathogens. Usually they are positively charged and interact with bacteria cell membrane, rip it apart and consequently cause the death of the microorganism<sup>4,54,83</sup>. The advantages of using AMPs as antibacterial agents reside in their broad spectrum, reduced potential of inducing bacterial resistance, as well as fast bacteria killing action, while the disadvantages refer mainly to high costs involved in their synthesis, the susceptibility to proteolysis, and unknown yet level of local toxicity as the clinical trials are still ongoing<sup>83</sup>. Different physical and chemical methods have been tried to efficiently immobilize the AMPs on surfaces without losing their accessibility and ensuring long-term durability of the bactericidal activity<sup>91</sup>. AMPs were firstly tethered on different surfaces (cellulose, PEGylated gels, polyamides) using short linkers and it was proved they partially retain the antibacterial efficiency but their activity is conditioned by various factors including the position on the amino acid sequence, orientation of the peptide sequence, the distribution of charges, as well as the nature of the group used (C or N termini) for binding on the substrate. In an excellent review, Glinel and coworkers<sup>83</sup> followed the development of the antibacterial materials based on the immobilization of antimicrobial peptides, underlining advantages and disadvantages of each technique. Layer-by-layer method was extensively used to obtain antibacterial surfaces embedding AMPs into polyelectrolyte multilayers<sup>92-97</sup> and the obtained surfaces proved efficient against *Escherichia coli* and *Enterococcus faecalis*. Other strategies involved the bulk inclusion of AMPs into an acrylate resin<sup>98</sup> obtaining

antibacterial materials efficient against *E. coli* and *S. aureus*. The main disadvantage of these methods resides in the diffusion of the embedded AMP in the surrounding environment with potential negative implications in biomedical applications. To overcome this inconvenience, covalent immobilization of AMPs on surfaces was realized, firstly by using standard methods to bind magainin II to water-insoluble polyamide resin<sup>99, 100</sup>, sol-gel technology for silane coating with covalently bound polymyxin B<sup>101</sup> or by combining the layer-by-layer method with chemical cross-linking<sup>102</sup> obtaining materials effective against *E. coli* and *Bacillus subtilis* without leaching of the peptide. Another approach explored for obtaining antibacterial surfaces with immobilized AMPs was grafting on self-assembled monolayers (SAMs). AMPs were grafted on amine- or epoxy-silanized titanium surfaces using a flexible oligo(ethylene glycol) spacer<sup>103</sup> ensuring the protection against *E. coli*. Tethering magainin I peptide on gold surfaces<sup>104,105</sup> increased efficiency against *Listeria ivanovii*, *E. faecalis* and *S. aureus*. All studies evidenced the importance of the AMPs mobility, length of the spacer and peptide orientation on the antibacterial efficiency, noticing that in many cases the AMPs activity is decreased after connecting to a surface. To offer the best solutions to these problems approaches using polymer brushes to immobilize AMPs on surfaces have been reported. In 2009, Glinel and coworkers reports the use of a surface-initiated ATRP from silicon wafers<sup>106</sup> or silica and paramagnetic silica microparticles<sup>107</sup> to copolymerize 2-(2-methoxyethoxy)ethyl methacrylate (MEO<sub>2</sub>MA) and hydroxyl-terminated oligo(ethylene glycol) methacrylate (HOEGMA) and then coupled the AMP, magainin I, to the hydroxyl groups. The surfaces exhibited antibacterial activity against *Listeria ivanovii* and *Bacillus cereus*. Moreover, the polymer brushes kept their antifouling properties and the AMP did not lose its activity. After establishing the principles for obtaining antibacterial surfaces by immobilizing AMPs on polymer brushes, Glinel et al.<sup>108</sup> performed in depth studies to clarify the influence of various factors on bactericidal activity of AMPs immobilized on surfaces via polymer brushes, as well as the influence of the immobilized peptide on the antifouling properties of surfaces. They developed thermosensitive surfaces with a LCST close to the physiological temperature, able to switch from bactericidal to bacteria repellent. A general method for AMPs immobilization on surfaces has been developed by Basu et al. by conjugation of self-polymerized allyl glycidyl ether with Polybia-MPI, which proved effective against *E. coli*<sup>109</sup>. *N*-substituted polyacrylamide brushes conjugated with a series of short synthetic AMPs were reported by Gao et al<sup>1,110,111</sup> to be antibacterial against *P. Aeruginosa* and *S. Aureus* on titanium implants. Even if AMPs

immobilized on surfaces proved to be highly effective against many bacterial strains, they cannot be extensively used due to still ongoing clinical trials meant to clarify toxicological aspects, as well as to high cost involved in peptides synthesis<sup>83</sup>. Furthermore, research has to be carried out to find the optimum balance between the maximum bactericidal activity ensured for the immobilized AMP and the antifouling properties of the polymer brush coated surfaces. It was noticed that for high densities of AMPs on surfaces, good bactericidal activity is obtained but the antifouling character of the surface is somewhat compromised due to the layer of dead bacteria or dead bacteria debris accumulated on surface<sup>4,54</sup>.

Another type of efficient bioactive non-leaching surfaces is based on quaternary ammonium compounds (QAC). As mentioned by Textor et al.<sup>54</sup>, for a true efficiency, such compounds need a cationic group and an apolar alkyl chain. To interact with bacteria the cationic group fixed on the surface has to keep its mobility. This is ensured by binding it to the surface through a spacer (usually PEG or PMOXA spacers). Waschinski et al.<sup>112</sup> used long PMOX polymeric spacer to immobilize the biocidal compound, *N,N*-dimethyldodecylammonium (DDA), and proved it to be efficient against *S. Aureus*. Matyjaszewski and his team<sup>113</sup> tethered cationic polyacrylates to surfaces using ATRP of *N,N*-dimethyl-2-aminoethylacrylamide followed by quaternization. Klibanov et al.<sup>114</sup> reported quaternized surface grafted polyethyleneimine efficient against bacterial strains and also inactivating specific viruses<sup>115</sup>. The authors<sup>116</sup> proved such surfaces kill bacteria by rupturing cell membranes and without developing resistance in *S. aureus* or *E. coli* strains. The researchers pointed out the importance of the spacer in conferring enough mobility to the active group to reach and disrupt bacterial membrane. Surfaces with immobilized quaternized poly(2-vinyl pyridine)<sup>117</sup> proved antibacterial against *S. aureus*. Permanent non-leaching antibacterial surfaces effective against *E. coli* were obtained in the Matyjaszewski group<sup>118,119</sup> by SI-ATRP of 2-(dimethylamino)ethyl methacrylate (DMAEMA) and subsequent quaternization with alkyl bromides. Although, with good bactericidal efficiency, coatings based on quaternary ammonium compounds have the disadvantage of increased toxicity and low biocompatibility<sup>4,54</sup>.

Antibacterial surfaces have been obtained using polymer brushes incorporating lysozyme, enzymes able to damage the bacterial cell wall by catalyzing the hydrolysis of 1,4-beta-linkages in peptidoglycan. Yuan et al.<sup>120</sup> immobilized lysozyme on poly(oligo(ethylene glycol) monomethacrylate) (POEGMA) brushes to confer antibacterial protection for stainless steel surfaces and the obtained coatings proved their

efficiency against *S. aureus* and *E. coli*. Lysozyme was also coupled to PEO polypropylene oxide-PEO tri-block copolymer (Pluronic F-127) and obtained reduced *Bacillus subtilis* adhesion on modified silicon rubber surfaces<sup>121</sup>. The enzyme was bound through a glutaraldehyde cross-linker on stainless steel surfaces prefunctionalized with an amino(propyl)triethoxysilane (APTES) SAM<sup>122</sup> or through PEG spacer with terminal aldehyde groups on an amino-enriched poly(ethylene imine) (PEI) layer physisorbed on the stainless steel<sup>63,123</sup>. Chitosan was also immobilized on surfaces via PHEMA brushes conferring antibacterial protection to stainless steel surfaces. Through its positively charged amino groups chitosan interacts with the bacterial cell wall usually carrying a negative charge determining the death of bacteria<sup>124</sup>.

### 1.3.2.2. Bioactive leaching surfaces

The application of bioactive approaches is somewhat limited by the reduction in the nonfouling character of coatings due to the accumulation of dead cells on the surface. Therefore new strategies are needed to overcome the limitations of bioactive non-leaching surfaces, based on controlled release of antimicrobial agents. Such coatings have been developed to release high amounts of antimicrobials immediately after implantation thus avoiding bacteria adhesion and biofilm formation, and then a reduced amount to ensure proper healing<sup>51</sup>. The history of using silver as antimicrobial agent is very old and its roots are lost in time. The ancient Egyptians, Greeks and Romans used silver for various medical applications, especially preventing or treating infections, and for food and water preservation<sup>125</sup>. Coatings able to release silver ions at the implantation site have been developed and successfully applied<sup>4,51,54,125</sup> and they proved effective for different bacterial strains *P. aeruginosa*, *E. coli*, *S. aureus*, and *S. epidermidis*. Silver was used in metallic form as coating for catheters<sup>126</sup> and orthopedic devices<sup>127</sup> but their efficiency was low due to the fact that the active bactericidal form is  $\text{Ag}^+$ , and not all metallic coatings have the ability to release silver ions. Therefore silver was incorporated in polymers able to function as silver ions reservoirs and to ensure effective and prolonged antibacterial activity<sup>51,125</sup>. Such coatings have limitations due to poor diffusivity of silver ions through polymers and low biocompatibility of  $\text{Ag}^+$ . Recently, silver nanoparticles have been used as bactericidal agents and their applicability seems promising but studies are still ongoing to clarify all aspects related to their biocompatibility, cytotoxicity and effectiveness<sup>125,128</sup>.

Antibiotics are bactericidal agents, but their dosage should be accurately established and the period of treatment limited to avoid the development of specific resistance in

bacteria. To prolong their period of activity, to extended effectiveness and reduce toxicity, the antibiotics can be incorporated in biomaterials and released in a controlled manner directly to the implantation site<sup>4,51,54</sup>. Controlled release of AMPs was reported by Shukla et al.<sup>129</sup> and the obtained surface was efficient against *Staphylococcus aureus*. Different types of coatings have been used for the controlled release of antibiotics: biocompatible polymers (polyurethane, silicone rubber, polyhydroxyalkanoates)<sup>130-132</sup>, biodegradable polymers including poly(propylenefumarate/methylmethacrylate), collagen, polyanhydrides, polyorthoesters, polylactide-co-glycolide (PLGA), and poly(D,L-lactide) (PDLLA)<sup>51,125,133,134</sup>, and hydroxyapatite<sup>135-137</sup>. These types of coatings proved their efficiency in combating implant related infections but their use is still controversial due to the possibility of developing specific resistance in the bacterial strains<sup>125</sup>. Bioactive leaching approaches based on polymer brushes are relatively less studied due to the low number of antimicrobial agents suitable for immobilization and controlled release from this type of coatings. Approaches based on bioactive surfaces proved efficient in preventing bacteria adhesion and biofilm formation for a broad range of bacterial strains<sup>4,51,54</sup>.

## 1.4. Polymer brushes

### 1.4.1. Introduction

The interest for the surfaces quality and functionality is as old as mankind is, but in the last century and mainly after '70s a great attention was paid to tailoring special designed surfaces for specific biomedical applications. The researchers' great interest in the study of surfaces and interfaces was manifested in a huge number of publications dealing with surface modification, proposing various solutions with deep implications in biology, medicine, electronics, aeronautics, food and many other "high-end" fields with impact in humanity daily life. Surface and interface science is strongly interdisciplinary requiring knowledge of chemistry, physics, biology, mathematics, computer assisted design and modeling. Considering surface-modification area, polymer-based coatings proved successful and versatile alternative to self-assembled low molecular weight compounds, developing three-dimensional arrangements of functionalities.

Polymer brushes, able to be produced in a large variety of architectures and chemical compositions, have been intensively studied and are considered the most promising coatings especially for protection of diverse surfaces in contact with natural products<sup>1-4,54-57,59-64,68,81-83</sup>. In an interesting article published in 2007, Brittain and Minko<sup>138</sup> attempted a clarification of the structural definition of polymer brushes. As mentioned in their paper the denomination “polymer brushes” is often considered synonym with “tethered polymer chain”, being related with a thin layer of polymeric chains linked with one end to a surface in special energetic conditions determined by high grafting density forcing the chains to stretch and adopt a straight configuration. In the extensive review published in 2009, Klok and his team<sup>60</sup> define polymer brushes as ultra-thin layers of polymer chains tethered with one end to a specific interface (often a solid substrate). Polymer brushes can adopt different conformations depending on the grafting density - for high grafting densities repulsive forces stretch the chains, while for low grafting densities mushroom or pancake type conformations are specific<sup>60,138</sup>. There are two main strategies that can be adopted for obtaining polymer brushes: “grafting from” and “grafting to” methods (Figure 2). The “grafting to” strategy involves the use of a preformed polymers with reactive end-groups subsequently attached onto surfaces either by physical bounds (*physisorption*), or through covalent linkages (*chemisorption*). Even if intensively studied and applied the “grafting to” strategy has limitations regarding the possibility to obtain thick and dense polymer brushes. Due to steric repulsions it is difficult for approaching macromolecular units to pass through the already formed tethered polymer chains and to reach the surface. The “grafting from” approach supposes the growth of polymer brushes from initiator-functionalized surfaces and this versatile and reliable technique allows obtaining of very robust, dense and thick polymer brushes<sup>60</sup> and can be performed using almost all polymerization methods: atom transfer radical polymerization (ATRP)<sup>139</sup>, single-electron transfer living radical polymerization (SET-LRP)<sup>140</sup>, ring opening metathesis polymerization (ROMP)<sup>141</sup>, nitroxide-mediated polymerization (NMP)<sup>142</sup>, or reversible addition fragmentation chain transfer (RAFT) polymerization<sup>143</sup>, to mention only few examples<sup>144</sup>. One of the most attractive aspects of polymer brushes is their ability to be tethered on a large variety of substrates such as polymeric materials including chitosan<sup>145</sup>, cellulose<sup>146</sup>, polyurethane<sup>147</sup>, polypropylene<sup>148</sup>, polyimide<sup>149</sup>, poly(ethyleneterephthalate)<sup>150</sup>, poly(methylmethacrylate)<sup>151</sup>, nylon<sup>152</sup>, poly(dimethylsiloxane)<sup>153</sup>, poly(vinyl chloride)<sup>154</sup>, polystyrene<sup>155</sup>, as well as inorganic and organic surfaces: zirconium phosphonate<sup>156</sup>, mica<sup>157</sup>, steel<sup>158</sup>, diamond<sup>159</sup>, singlewalled<sup>160</sup>



and multiwalled<sup>161</sup> carbon nanotubes. The schematic representation of the “grafting to” and “grafting from” approaches is presented in Figure 2.

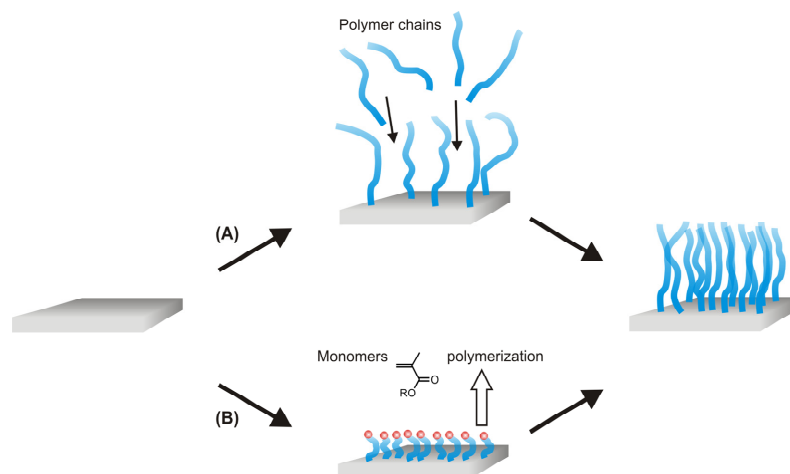


**Figure 2.** “Grafting to” (A) and “grafting from” (B) strategies for the preparation of polymer brushes modified surfaces<sup>60</sup>

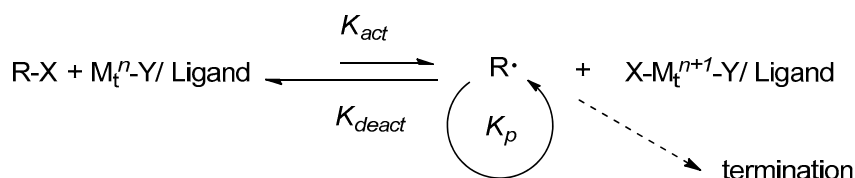
The application of controlled “living” polymerization methods and among them radical-based strategies allowed a very good control over molecular mass, molecular mass distribution, architecture of the synthesized polymer brushes. As surface-initiated atom transfer radical polymerization is the method adopted in this Thesis for the synthesis of polymer brushes the following sections will highlight the main characteristics of this technique. Moreover, the methods available for the characterization of polymer brushes and the potential antibacterial applications will be analyzed.

## 1.4.2. Synthesis of polymer brushes

### 1.4.2.1. Surface-Initiated Atom Transfer Radical Polymerization (SI-ATRP)

Surface-initiated atom transfer radical polymerization (SI-ATRP) is the method most widely used to obtain polymer brushes through the “grafting-from” approach. Reported for the first time in 1995<sup>162,163</sup>, ATRP method proved to be extremely versatile, reliable and robust and was since then extensively used and reviewed<sup>56,60,62,113,164-174</sup>. The main characteristic of ATRP is the balance between a reduced concentration of active species and the high number of dormant chains via an inner sphere electron transfer process

promoted by a transition metal complex<sup>172</sup>. The mechanism of an ATRP reaction catalyzed by transition metals, as proposed by Matyjaszewski is presented in Scheme 1.



**Scheme 1.** Schematic representation of the mechanism of ATRP catalyzed by transition metals ATRP<sup>172</sup>

ATRP allows the termination reaction to be controlled with high precision since in an ATRP system the majority of the macromolecular chains are “living”, even if “dormant”. Thus polymers with low polydispersity and high molecular mass can be obtained with good control over architecture and composition. As for all classical free radical polymerization reactions, ATRP supposes generation of the radicals, propagation and termination, but the generation of radicals proceeds through a reversible redox process using a transition metal complex ( $\text{M}_t^n\text{-Y/Ligand}$ )<sup>172</sup>. Most frequently copper is used as transition metal but the use of iron was also reported<sup>175,176</sup>. The dormant alkyl halide-terminated polymer chain end can be activated by the halogen transfer to the transition metal complex, determining the homolytic cleavage of the carbon-halogen bond and thus generating active, free radical species. The catalyst, which now is in an oxidized form, reconverts the growing radical to the corresponding dormant species very quickly. Maintaining the concentration of propagating radicals very low significantly reduces the probability of termination reactions through radical-radical coupling and the time for manipulating the “living” polymers is increased.

In 1997, Huang and Wirth, reported for the first time the use of SI-ATRP for growing poly(acrylamide) brushes from silica particles<sup>177</sup> and 1998 Fukuda and coworkers<sup>178</sup> succeeded to obtain PMMA polymer brushes on silicon surfaces prepared the Langmuir–Blodgett (LB) technique and they found a correlation between the thickness of the polymer brushes and the concentration of the free initiator observing an inverse dependency. Due to good control over the composition, conformation, grafting density and film thickness SI-ATRP has imposed as a versatile method for obtaining polymer brushes for a wide range of applications and was extensively used in the last decades.

Moreover, this method is robust and less sensitive to the presence of impurities or oxygen and the preparation of the initiator layer on substrates is not complicated using commercially available *α*-haloesters or benzyl halides<sup>60,62</sup>. The very low concentration of the initiator immobilized on the surface differentiates the surface-initiated ATRP from ATRP in solution, and also it is possible that after the halogen transfer to the transition metal catalyst the chains grow uncontrollably, due to a very low concentration of persistent radical (deactivator). To overcome this problem the addition of a free, sacrificial, initiator maybe indispensable for establishing the necessary equilibrium between active species and dormant chains, or as an alternative an excess deactivating Cu(II) complex (CuCl<sub>2</sub> or CuBr<sub>2</sub>)<sup>62,139</sup>. SI-ATRP allowed polymer brushes of different compositions to be grown from various substrates (silicon, silicon wafers, titanium, stainless steel, Au, carbon, and different polymers)<sup>60,62</sup>. Studies have been performed to modify the composition of the brushes thus obtaining diblock and triblock copolymer brushes with tunable properties<sup>139,179-181</sup> as well as hyperbranched, comb-shaped and/or cross-linked polymer brushes<sup>60</sup>. The reaction rate of SI-ATRP was substantially increased for reactions performed in non-polar solvents and preferentially in aqueous media, and the reactions can be carried out at room temperature. In these conditions, SI-ATRP can be applied also for temperature sensitive surfaces and side reaction can be avoided<sup>182</sup>. Huck reported 30 nm thick PMMA brushes grown in aqueous media in only 35 min using CuBr/2,2'-bipyridine (bpy) catalyst system in water/methanol mixture<sup>183</sup>, and Huang *et al.* succeeded to obtain 700 nm thick PHEMA films in 12 hours grown from SAMs on gold using a mixed halide CuCl/CuBr<sub>2</sub>/bpy catalyst system<sup>184</sup>. Bruening *et al.*<sup>185</sup> used a “water accelerated” SI-ATRP to obtain PHEMA brushes and they also studied the effect of mixed halide catalyst/deactivator systems. It was noticed a better control of the reaction when CuCl/CuBr<sub>2</sub> system was used instead of CuBr/CuBr<sub>2</sub>. As stated also by Matyjaszewski and his coworkers<sup>186</sup>, this is due to the higher strength of the C-Cl bond as compared with the C-Br and represents a good modality to obtain a good reaction control by establishing the desired equilibrium between dormant and propagating radical species. As mentioned in the previous section, SI-ATRP was extensively used to prepare polymer brushes for biomedical applications and in these situations, a factor of concern is the traces of copper catalyst. To overcome this problem, solutions have been proposed to use less cytotoxic iron catalyst<sup>175,176</sup> or to decrease copper content<sup>187</sup>. Moreover, Matyjaszewski and his team<sup>187-191</sup> proposed a new variant of ATRP, named Activator (Re)Generated by Electron Transfer ATRP or A(R)GET ATRP, which allows the

diminution of copper catalyst concentration to several ppm and enhances the tolerance of the reaction system towards radical traps. This new variant was also used for surface-initiated polymerization reactions and has to be underlined that it employs reducing agents, for continuous restoration of Cu<sup>I</sup> from Cu<sup>II</sup>.

SI-ATRP was extensively used to generate polymer brushes with antibacterial applications, based on OEGMA<sup>192-200</sup>, HEMA<sup>197,199,201-206</sup>, DMAEMA<sup>207-209</sup> (co)polymer brushes, just to mention few examples in the last years. Moreover, applications using SI-ATRP to obtain degradable polymer brushes have begun to gain more attention in the last years and the proposed approach involves the combination of ATRP with radical ring-opening polymerization (RROP) but still there are not many references regarding the successful synthesis of polymer brushes<sup>172</sup>.

In conclusion, SI-ATRP is a versatile, robust and reliable method for the synthesis of polymer brushes offering good control over brush composition and architecture. This method has reduced sensitivity to impurities and oxygen and can be applied for a large variety of monomers. Furthermore, the most catalyst systems and initiators are commercially available or easy to synthesize and the reaction conditions can be easily tailored. SI-ATRP has limitations regarding the polymerization of monomers that can complex or react with the metal catalyst but, partially, these situations have been solved using specific ligands<sup>179,210</sup>, temporarily protecting the reactive groups<sup>211,212</sup> or by modified synthesis protocols<sup>213</sup>.

### **1.4.3. Post-modification reactions on hydroxyl-functionalized polymer brushes**

This section is intended to give a brief overview of the most important post-modification reactions that can be performed on hydroxyl-functionalized polymer brushes as PHEMA or POEGMA. There are a variety of reactions that can be used to modify the hydroxyl groups present on the side-chains of such polymer brushes and they were extensively presented in an excellent review<sup>60</sup>. Herein we will only underline some of the most used reactions valuable for introducing bioactive moieties on the brush. Generally, the hydroxyl groups on the side chain can be modified with halogen functionalities, carboxylic acid or hydrophobic groups regarding the final destination of the surface. Until now, the hydroxyl groups have been modified with carboxylic acid groups mainly to produce double responsive polymer brushes or for obtaining templates for the synthesis

of polymer/metal hybrids. Moreover, carboxylic acid modified polymer brushes can support further modifications to ensure the tethering of different active compounds. Usually such a modification supposes the reaction of hydroxyl group on the polymer brush with an excess of succinic anhydride in alkaline conditions, using for example pyridine<sup>214-218</sup>. The modification with halogen functionalities is important for facilitating the formation of comb-shaped polymer brushes or for other further modifications and involves the esterification of hydroxyl groups with 2-bromoisobutryl bromide to introduce ATRP initiating side-chain functional groups<sup>219,220</sup> or the use of SOCl<sub>2</sub> for introducing chloroalkyl functional groups available for additional nucleophilic substitution reactions<sup>215,221,222</sup>. The hydrophobic groups were used for the modification of the hydroxyl groups on the polymer brushes for tuning the barrier properties, etch resistance or wettability and were performed, for example, by the acylation of PHEMA<sup>223-225</sup>.

PHEMA and POEGMA based brushes are suitable for a broad variety of antibacterial applications and this is due also to the high density of hydroxyl groups they carry on the side-chains allowing post-modification reactions very useful for temporary or permanent immobilization of antibacterial agents. The most popular method used for the modification of their hydroxyl groups relies on the activation of the hydroxyl groups with *p*-nitrophenyl chloroformate (NPC), resulting a carbonate intermediate that can be reacted with the N terminal amine group of short peptides<sup>226-229</sup>, or other amine-functionalized moieties<sup>230</sup>. Other reported options for the modification of hydroxyl groups include 1,1'-carbonyldiimidazole (CDI)<sup>231</sup> and *N,N'*-disuccinimidyl carbonate (DSC)<sup>232,233</sup> which can be used for the attachment of proteins on polymer brush surfaces. Hydroxyl groups on the side chains of POEGMA brushes can be also converted into aldehyde groups by exposing the brushes to a mixture of acetic anhydride and DMSO at room temperature for 8 h<sup>215</sup> which can be further used for the immobilization of peptides or proteins. Moreover, to obtain surfaces suitable for peptide coupling, hydroxyl groups on PHEMA can be reacted with succinic anhydride to generate carboxylic acid groups<sup>234-237</sup>.

#### 1.4.4. Characterization methods for polymer brushes

Without very sensitive and accurate characterization techniques, all efforts to obtain well-defined polymer brushes for high-end application would be futile. It is not an easy task to characterize ultrathin films of polymers tethered on surfaces as long as the majority of available equipment for polymer characterization has been developed for

systems in solution. However, the equipment modification as well as adaptations allowed establishing precise methods for the evaluation of the most important properties of polymer brushes. The interpretation of the experimental data is more accurate if results from several complementary methods are analyzed together.

Chemical composition and structure of polymer brushes synthesized by various methods can be assessed using IR spectroscopy which confirms the presence of different functional groups<sup>1,220,229,238</sup>. Grazing angle reflection-absorption infrared spectroscopy is used for increasing sensitivity in the case of very thin films<sup>239,240</sup>. X-ray photoelectron spectroscopy (XPS) is often employed for quantitative evaluation of the composition on pristine and coated surfaces<sup>1,108,220,229,238</sup> also offering information about the structure of the polymer brushes as well as the possibility of depth profiling<sup>241</sup> and mapping analysis<sup>242</sup>, the depth of X-ray penetration ranging between 2 and 10 nm. Surface elemental stoichiometry was determined from peak-area ratios<sup>220</sup>. Other methods able to offer information about the chemical composition and structure of polymer brushes are: time-of-flight secondary ion mass spectroscopy (TOF-SIMS)<sup>243-245</sup>, Auger electron spectroscopy (AES)<sup>246</sup>, near-edge X-ray absorption fine structure (NEXAFS) giving supplementary data about the bond-type and molecular orientation of the chemical groups on the top 3 nm of a polymer brush-covered substrate<sup>247</sup>.

The thickness of the initiator monolayer and the polymer brush can be assessed using ellipsometry<sup>1,81,199,226,229,230,238</sup> as well as atomic force microscopy (AFM), the latter involving the use of either patterned brushes or removing (scratching) part of the polymer brush coating prior to the analysis<sup>1,226, 229,230,248</sup>. Other available methods that can be employed in specific situations for determining the brush thickness are X-ray reflectivity (XRR)<sup>249,250</sup> as well as transmission electron microscopy (TEM)<sup>220,251</sup>, dynamic light scattering (DLS)<sup>252</sup>, and thermogravimetric analysis (TGA)<sup>253</sup> for brushes grafted on particles. The polymer brush modified surfaces topography and structure can be analyzed by scanning electron microscopy (SEM)<sup>248</sup>, fluorescence microscopy<sup>220</sup>, AFM<sup>238</sup>, XPS<sup>248</sup> and X-ray reflectivity<sup>249,250</sup>. The grafting density can be estimated using the weight loss observed in thermogravimetric analysis, especially when polymer brushes grown from particles are of concern<sup>254</sup>. Removing the polymer brush from surface allows also the use of gas permeation chromatography (GPC) for evaluation of the molecular mass of the polymer chains<sup>185,255</sup>. For SI-ATRP reactions the concentration of the initiators on surface can be evaluated using XPS<sup>211</sup>, elemental analysis<sup>256</sup> or TGA<sup>257</sup>. QCM (quartz crystal microbalance) and QCM-D (quartz crystal microbalance with dissipation monitoring) can

be used to assess viscoelastic and mechanical properties of polymer brush surfaces<sup>258,259</sup> and different specific processes on surface (collapse, swelling), while conformational modifications of polymer brushes can be observed using ellipsometry<sup>1,108,220,226,229,238</sup> scanning probe microscopy<sup>260-262</sup>, or neutron reflectivity<sup>263,264</sup>. Employing ellipsometry or AFM to determine the brush thickness at different polymerization times useful information about the kinetics of SI-ATRP reactions can be obtained<sup>265</sup>. If electrical properties are of interest they can be determined using electrochemical impedance spectroscopy (EIS)<sup>266</sup>, chronoamperometry<sup>267</sup>, and cyclic voltammetry (CV)<sup>268</sup>. Collapse temperature for thermosensitive brushes can be determined using Quartz Crystal Microbalance with Dissipation Monitoring (QCM-D) and the presence of different active compounds or bacteria on surfaces by optical fluorescence microscopy or Confocal Laser Scanning Fluorescence Microscopy (CFLM)<sup>108</sup>.

## 1.5. References

- (1) Gao, G.; Yu, K.; Kindrachuk, J., Brooks, D. E.; Hancock, R. E. W.; Kizhakkedathu, J. N. *Biomacromolecules* **2011**, *12*, 3715
- (2) Harding, J. L.; Reynolds, M. M.; *Trends in Biotechnology* **2014**, *32*, 140
- (3) Salwiczek, M.; Qu, Y; Gardiner, J.; Strugnell, R. A.; Lithgow, T.; McLean, K. M.; Thissen, H. *Trends in Biotechnology* **2014**, *32*, 82
- (4) Hadjesfandiari, N.; Yu, K.; Meiac, Y.; Kizhakkedathu, J. N. *J. Mater. Chem. B* **2014**, *2*, 4968
- (5) Mack, D.; Davies, A. P.; Harris, L. G.; Jeeves, R.; Pascoe, B.; Knobloch, J. K.-M.; Rohde, H.; Wilkinson, T. S *Springer Science+Business Media New York* **2013**
- (6) Mack, D.; Becker, P.; Chatterjee, I.; Dobinsky, S.; Knobloch, J. K.-M.; Peters, G.; Rohde, H.; Herrmann, M. *Int. J. Med. Microbiol.* **2004**, *294*, 203
- (7) Hidron, A. I.; Edwards, J. R.; Patel, J., Horan, T. C.; Sievert, D. M.; Pollock, D. A.; Fridkin, S. K *Infect. Control. Hosp. Epidemiol.* **2008**, *29*, 996
- (8) Garrett, T. R.; Bhakoo, M.; Zhang, Z. *Prog. Nat. Sci.* **2008**, *18*, 1049
- (9) Davies, D. *Nat. Rev. Drug Discovery* **2003**, *2*, 114
- (10) Costerton, J. W. *Int. J. Antimicrob. Agents* **1999**, *11*, 217
- (11) Costerton, J. W.; Stewart, P. S.; Greenberg, E. P. *Science* **1999**, *284*, 1318
- (12) Peters, G.; Locci, R.; Pulverer G. *J. Infect. Dis.* **1982**, *146*, 479
- (13) Donlan, R. M. *Clin. Infect. Dis.* **2001**, *33*, 1387
- (14) von Eiff, C.; Peters, G.; Heilmann, C. *Lancet Infect. Dis.* **2002**, *2*, 677
- (15) Peters, G. *Br. J. Clin. Pract. Suppl.* **1988**, *57*, 62
- (16) Gottenbos, B.; Busscher, H. J.; Van Der Mei, H. C., Nieuwenhuis P. *J. Mater. Sci. Mater. Med.* **2002**, *13*, 717
- (17) Herrmann, M.; Vaudaux, P. E.; Pittet D.; Auckenthaler R.; Lew, P. D.; Schunacher-Perdreau, F.; Peters, G.; Waldvogel, F. A. *J. Infect. Dis.* **1988**, *158*, 693
- (18) Espersen, F.; Wilkinson, B. J.; Gahrn-Hansen, B.; Thandrup Rosdahl, V.; Clemmensen, I. *APMIS* **1990**, *98*, 471
- (19) Otto, M. *Nat. Rev. Microbiol.* **2009**, *7*, 555
- (20) Sauer, K.; Camper, A. K.; Ehrlich, G. D.; Costerton, J. W.; Davies, D. G. *J. Bacteriol.* **2002**, *184*, 1140
- (21) Tormo, M. A.; Marti, M.; Manna, A. C.; Cheung, A. L.; Lasa, I.; Penades, J. R. *J. Bacteriol.* **2005**, *187*, 2348



- (22) Xu, L.; Li, H.; Vuong, C.; Vadyvaloo V.; Wang, J.; Yao, Y.; Otto, M.; Gao, Q. *Infect. Immun.* **2006**, *74*, 488
- (23) Tao, J. H.; Fan, C. S.; Gao, S. E.; Wang, H. J.; Liang, G. X.; Zhang, Q. *World J. Gastroenterol.* **2006**, *12*, 4009
- (24) Goller, C. C.; Romeo, T. *Springer* **2008**, 37
- (25) Pintens, V.; Massonet, C.; Merckx, R.; Vandecasteele, S.; Peetermans, W. E.; Knobloch, J. K.-M.; Eldere, J. V. *Microbiology* **2008**, *154*, 2827
- (26) Rupp, C. J.; Fux, C. A.; Stoodley, P. *Appl. Environ. Microbiol.* **2005**, *71*, 2175
- (27) Otto, M. *Springer* **2008**, 207
- (28) Lee, J.-H.; Kaplan, J. B.; Lee, W. Y. *Biomed. Microdevices* **2008**, *10*, 489
- (29) Stoodley, P.; Kathju S.; Hu, F. Z.; Erdos, G.; Levenson, J. E.; Mehta, N.; Dice, B.; Johnson, S.; Hall-Stoodley, L.; Nistico, L.; Sotereanos, N.; Sewecke, J.; Post, J. C.; Ehrlich, G. D. *Clin. Orthop. Relat. Res.* **2005**, *437*, 31
- (30) Liu, Y.; Yang, S. F.; Xu, H.; Qin, L.; Tay, J. H. *J. Biotechnol.* **2004**, *110*, 251
- (31) Hall-Stoodley, L.; Stoodley, P. *Curr. Opin. Biotechnol.* **2002**, *13*, 228
- (32) Dunne, W. M. *Clin. Microbiol. Rev.* **2002**, *15*, 155
- (33) Rowland, B. M. *Clin. Microbiol. Newslett.* **2003**, *25*, 73
- (34) Booth, I.R. *Microbiol Rev* **1985**, *49*, 359
- (35) Olsen, E. R. *Mol Microbiol* **1993**, *8*, 5
- (36) Li, Y. *J Bacteriol* **2001**, *183*, 6875
- (37) Oliveira, R.; Melo, L.; Oliveira, A.; Salgueiro, R. *Colloids Surf. B: Biointerf.* **1994**, *2*, 41
- (38) Stepanovic, S.; Cirkovic, I.; Mijac, V.; Svabic-Vlahovic, M. *Food Microbiol.* **2003**, *20*, 339
- (39) Fletcher, M. *Can. J. Microbiol.* **1977**, *23*, 1
- (40) Herald, P. J.; Zottola, E. A. *J. Food Sci.* **1988**, *53*, 1549
- (41) Nisbet, B.A.; Sutherland, I. W.; Bradshaw, I. J.; Kerr, M. *Carbohydr Polym* **1984**, *4*, 377
- (42) Marion-Ferey, K.; Pasmore, M.; Stoodley, P.; Wilson, S.; Costerton, J. W. *J. Hospital Infect.* **2002**, *53*, 64
- (43) Stoodley, P.; Cargo, R.; Rupp, C. J.; Wilson, S.; Klapper, I. *J. Ind. Microbiol. Biotechnol.* **2002**, *29*, 361
- (44) Klapper, I.; Rupp, C. J.; Cargo, R.; Purvedorj, B.; Stoodley, P. *Biotechnol Bioeng* **2002**, *80*, 289

- (45) Galanakos, S. P.; Papadakis, S. A.; Kateros, K.; Papakostas, I.; Macheras, G. *Orthopaedics and Trauma* **2009**, *23*, 175
- (46) Arciola, C. R.; Campoccia, D.; Speziale, P.; Montanaro, L.; Costerton, J. W. *Biomaterials* **2012**, *33*, 5967
- (47) Bjelland, A. M.; Sørum, H.; Tegegne, D. A.; Winther-Larsen, H. C.; Willassen, N. P.; Hansen, H. *Infection and Immunity* **2012**, *80*, 1681
- (48) Ivanova, E. P.; Bazaka, K.; Crawford, R. J. *Woodhead Publishing* **2014**, 1
- (49) Kim, J.; Pitts, B.; Stewart, P. S.; Camper, A.; Yoon, J. *Antimicrob. Agents Chemother.* **2008**, *52*, 1446
- (50) Hori, K.; Matsumoto, S. *Biochemical Engineering Journal* **2010**, *48*, 424
- (51) Hetrick, E. M.; Schoenfisch, M. H. *Chem. Soc. Rev.* **2006**, *35*, 780
- (52) Harris, L. G.; Tosatti, S.; Wieland, M.; Textor, M.; Richards, R. G. *Biomaterials* **2004**, *25*, 4135
- (53) Skoda, M. W. A.; Schreiber, F.; Jacobs, R. M. J.; Webster, J. R. P.; Wolff, M.; Dahint, R.; Schwendel D.; Grunze, M. *Langmuir* **2009**, *25*, 4056
- (54) Charnley, M.; Textor, M.; Acikgoz, C. *Reactive and Functional Polymers* **2011**, *71*, 329
- (55) Senaratne, W.; Andruzzi, L.; Ober C. K. *Biomacromolecules* **2005**, *6*, 2427
- (56) Raynor, J. E.; Capadona, J. R.; Collard, D. M.; Petrie, T. A.; Garcia, A. J. *Biointerphases* **2009**, *4*, FA3
- (57) Siedenbiedel, F.; Tiller, J. C. *Polymers* **2012**, *4*, 46
- (58) Epstein, A.K.; Wong, T. S.; Belisle, R. A.; Boqqq, E. M.; Aizenberg, J. *Proc. Natl. Acad. Sci. U.S.A.* **2012**, *109*, 13182
- (59) Ostuni, E.; Chapman, R. G.; Holmlin, R. E.; Takayama S.; Whitesides, G. M. *Langmuir* **2001**, *17*, 5605
- (60) Barbey, R.; Lavanant, L.; Paripovic, D.; Schuwer, N.; Sugnaux, C.; Stefano Tugulu, S.; Klok, H.-A. *Chem. Rev.* **2009**, *109*, 5437
- (61) Timofeeva, L.; Kleshcheva, N. *Appl. Microbiol. Biotechnol.* **2011**, *89*, 475
- (62) Xua, F. J.; Neoh, K. G.; Kang, E. T. *Prog. Polym. Sci.* **2009**, *34*, 719
- (63) Caro, A.; Humblot, V.; Méthivier, C.; Minier, M.; Salmain, M.; Pradier, C.-M. *J. Phys. Chem. B* **2009**, *113*, 2101
- (64) Magin, C. M.; Cooper, S. P.; Brennan, A. B. *Mater. Today* **2010**, *13*, 36
- (65) Li, W.; Zhou, J.; Gu, J.-S.; Yu, H.-Y. *J. Appl. Polym. Sci.* **2010**, *115*, 2302
- (66) Konradi, R.; Pidhatika, B.; Mühlebach, A.; Textor, M. *Langmuir* **2008**, *24*, 613

- (67) Pidhatika, B.; Rodenstein, M.; Chen, Y.; Rakhmatullina, E.; Mühlebach, A.; Acikgöz, C.; Textor, M.; Konradi, R. *Biointerphases* **2012**, *7*, 1,
- (68) Krishnan, S.; Weinman, C. J.; Ober, C. K. *J. Mater. Chem.* **2008**, *18*, 3405
- (69) Bai, L.; Tan, L.; Chen, L.; Liu, S.; Wang, Y. *J. Mater. Chem. B* **2014**, *2*, 7785
- (70) Feng, W.; Gao, X.; McClung, G.; Zhu, S.; Ishihara, K.; Brash, J. L. *Acta Biomater.* **2011**, *7*, 3692
- (71) Smith, R. S.; Zhang, Z.; Bouchard, M.; Li, J.; Lapp, H. S.; Brotske, G. R.; Lucchino, D. L.; Weaver, D.; Roth, L. A.; Coury, A.; Biggerstaff, J.; Sukavaneshvar, S.; Langer, R.; Loose, C. *Sci. Transl. Med.* **2012**, *4*, 153ra132
- (72) Yoshimoto, K.; Hirase, T.; Madsen, J.; Armes, S. P.; Nagasaki, Y. *Macromol. Rapid Commun.* **2009**, *30*, 2136
- (73) Rodriguez-Emmenegger, C.; Brynda, E.; Riedel, T.; Houska, M.; Subr, V.; Alles, A. B.; Hasan, E.; Gautrot, J. E.; Huck W. T. *Macromol. Rapid Commun.* **2011**, *32*, 952
- (74) McArthur, S.L.; McLean, K. M.; Kingshoot, P.; St. John, H. A. W.; Chateler, R. C.; Griesser, H. J. *Colloid. Surf. B: Biointerfaces* **2000**, *17*, 37
- (75) Francolini, I.; Donelli, G.; Vuotto, C.; Baroncini, F. A.; Stoodley, P.; Taresco, V.; Martinelli, A.; D'Ilario, L.; Piozzi, A. *Pathogens and Disease* **2014**, *70*, 401
- (76) Li, J.; Kao, W. J. *Biomacromolecules* **2003**, *4*, 1055
- (77) Israelachvili, J. *Proc. Natl. Acad. Sci. U.S. A.* **1997**, *94*, 8378
- (78) Branch, D. W.; Wheeler, B. C.; Brewer, G. J.; Leckband, D. E. *Biomaterials* **2001**, *22*, 1035
- (79) Fan, X.; Lin, L.; Messersmith, P. B. *Biomacromolecules* **2006**, *7*, 2443
- (80) Sharma, S.; Johnson, R. W.; Desai, T. A. *Langmuir* **2004**, *20*, 348
- (81) Tugulu, S.; Klok, H. A.; *Biomacromolecules* **2008**, *9*, 906
- (82) Roosjen, A.; De Vries, J.; Van Der Mei, H. C.; Norde, W.; Busscher, H. J. *Journal of Biomedical Materials Research - Part B Applied Biomaterials* **2005**, *73*, 347
- (83) Glinel, K.; Thebault, P.; Humblot, V.; Pradier, C. M.; Jouenne, T. *Acta Biomaterialia* **2012**, *8*, 1670
- (84) Costa, F.; Carvalho, I. F.; Montelaro, R. C.; Gomes, P.; Martins, M. C. L. *Acta Biomater.* **2011**, *7*, 1431
- (85) Aumsuwan, N.; Danyus, R. C.; Heinhorst, S.; Urban, M. W. *Biomacromolecules* **2008**, *9*, 1712

- (86) Campoccia, D.; Montanaro, L.; Speziale, P.; Arciola, C. R. *Biomaterials* **2010**, *31*, 6363
- (87) Cademartiri, R.; Anany, H.; Gross, I.; Bhayani, R.; Griffiths, M.; Brook, M. A. *Biomaterials* **2010**, *31*, 1904
- (88) Hosseinidou, Z.; Van de Ven, T. G. M.; Tufenkji, N. *Langmuir* **2011**, *27*, 5472
- (89) Page, K.; Wilson, M.; Parkin, I. P. *J. Mater. Chem.* **2009**, *19*, 3819
- (90) Aumswan, N.; Heinhorst, S.; Urban, M.W. *Biomacromolecules* **2007**, *8*, 713
- (91) Onaizi, A. A.; Leong, S. S. J. *Biotechnol Adv* **2011**, *29*, 67
- (92) Duval-Terrie, C.; Cosette, P.; Molle, G.; Muller, G.; De, E. *Protein Sci* **2003**, *12*, 681
- (93) Picard, M.; Duval-Terrie, C.; De, E.; Champeil, P. *Protein Sci* **2004**, *13*, 3056
- (94) Etienne, O.; Picart, C.; Taddei, C.; Haikel, Y.; Dimarcq, J. L.; Schaaf, P.; Voegel, J.-C.; Ogier, J.; Egles, C. *Antimicrob Agents Chemother* **2004**, *48*, 3662
- (95) Guyomard, A.; Muller, G.; Glinel, K. *Macromolecules* **2005**, *38*, 5737
- (96) Guyomard, A.; Nysten, B.; Muller, G.; Glinel, K. *Langmuir* **2006**, *22*, 2281
- (97) Guyomard, A.; De, E.; Jouenne, T.; Malandain, J. J.; Muller, G.; Glinel, K. *Adv Funct Mater* **2008**, *18*, 758
- (98) Guyomard, A.; Muller, G.; Glinel, K. *Macromolecules* **2005**, *38*, 5737
- (99) Haynie, S. L.; Crum, G. A.; Doele, B. A. *Antimicrob Agents Chemother* **1995**, *39*, 301
- (100) Bagheri, M.; Beyermann, M.; Dathe, M. *Antimicrob Agents Chemother* **2009**, *53*, 1132
- (101) Mohorcic, M.; Jerman, I.; Zorko, M.; Butinar, L.; Orel, B.; Jerala, R.; Friedrich, J. *J Mater Sci Mater Med* **2010**, *21*, 2775
- (102) Faure, E.; Lecomte, P.; Lenoir, S.; Vreuls, C.; Van De Weerd, C.; Archambeau, C.; Martial, J.; Jerome, C.; Duwez, A.-S.; Detrembleur, C. *J Mater Chem* **2011**, *21*, 7901
- (103) Gabriel, M.; Nazmi, K.; Veerman, E. C.; Amerongen, A. V. N.; Zentner, A. *Bioconjug Chem* **2006**, *17*, 548
- (104) Humblot, V.; Yala, J. F.; Thébault, P.; Boukerna, K.; Héquet, A.; Berjeaud, J. M.; Pradier, C. *Biomaterials* **2009**, *30*, 3503
- (105) Yala, J. F.; Thébault, P.; Héquet, A.; Humblot, V.; Pradier, C. M.; Berjeaud, J. M. *Appl Microbiol Biotechnol* **2011**, *89*, 623

- (106) Glinel, K.; Jonas, A. M.; Jouenne, T.; Leprince, J.; Galas, L.; Huck, W. T. S. *Bioconjugate Chem.* **2009**, *20*, 71
- (107) Blin, T.; Purohit, V.; Leprince, J.; Jouenne, T.; Glinel, K. *Biomacromolecules* **2011**, *12*, 1259
- (108) Laloyaux, X.; Fautré, E.; Blin, T.; Purohit, V.; Leprince, J.; Jouenne, T.; Jonas, A. M.; Glinel, K. *Adv. Mater.* **2010**, *22*, 5024
- (109) Basu, A.; Mishra, B.; Leong, S. S. J. *J. Mater. Chem. B* **2013**, *1*, 4746
- (110) Gao, G.; Lange, D.; Hilpert, K.; Kindrachuk, J.; Zou, Y.; Cheng, J. T. J.; Kazemzadeh-Narbat, M.; Yu, K.; Wang, R.; Straus, S. K.; Brooks, D. E.; Chew, B. H.; Hancock, R. E. W.; Kizhakkedathu, J. N. *Biomaterials* **2011**, *32*, 3899
- (111) Gao, G.; Cheng, J. T. J.; Kindrachuk, J.; Hancock, R. E. W.; Straus, S. K.; Kizhakkedathu, J. N. *Chem. Biol.* **2012**, *19*, 199
- (112) Waschinski, C. J.; Zimmermann, J.; Salz, U.; Hutzler, R.; Sadowski, G.; Tiller, J. C. *Adv. Mater.* **2008**, *20*, 104
- (113) Lee, S. B.; Koepsel, R. R.; Morley, S. W.; Matyjaszewski, K.; Sun, Y. J.; Russell, A. J. *Biomacromolecules* **2004**, *5*, 877
- (114) Lin, J.; Qiu, S. Y.; Lewis, K.; Klibanov, A. M. *Biotechnol. Prog.* **2002**, *18*, 1082
- (115) Haldar, J.; An, D. Q.; de Cienfuegos, L. A.; Chen, J. Z.; Klibanov, A. M. *Proc. Natl. Acad. Sci. USA* **2006**, *103*, 17667
- (116) Milovic, N. M.; Wang, J.; Lewis, K.; Klibanov, A. M. *Biotechnol. Bioeng.* **2005**, *90*, 715
- (117) Zdyrko, B.; Klep, V.; Li, X.; Kang, Q.; Minko, S.; Wen, X.; Luzinov, I. *Materials Science and Engineering C* **2009**, *29*, 680
- (118) Huang, J.; Murata, H.; Koepsel, R. R.; Russell, A. J.; Matyjaszewski, K. *Biomacromolecules* **2007**, *8*, 1396
- (119) Murata, H.; Koepsel, R. R.; Matyjaszewski, K.; Russell, A. J., *Biomaterials* **2007**, *28*, 4870
- (120) Yuan, S.; Wan, D.; Liang, B.; Pehkonen, S. O.; Ting, Y. P.; Neoh, K. G.; Kang, E. T. *Langmuir* **2011**, *27*, 2761
- (121) Muszanska, A. K.; Busscher, H. J.; Herrmann, A.; Van der Mei, H. C.; Norde, W. *Biomaterials* **2011**, *32*, 6333
- (122) Minier, M.; Salmain, M.; Yacoubi, N.; Barbes, L.; Methivier, C.; Zanna, S.; Pradier, C. M. *Langmuir* **2005**, *21*, 5957

- (123) Caro, A.; Humblot, V.; Minier, M.; Barbes, L.; Li, J.; Salmain, M.; Pradier, C. M. *J Coll Interf Sci* **2010**, *349*, 13
- (124) Yang, W. J.; Cai, T.; Neoh, K. G.; Kang, E. T.; Dickinson, G. H.; Teo, S. L.-M.; Rittschof, D. *Langmuir* **2011**, *27*, 7065
- (125) Menno, L. W.; Knetsch, L.; Koole, H. *Polymers* **2011**, *3*, 340
- (126) Bologna, R. A.; Tu, L. M.; Polansky, M.; Fraimow, H. D.; Gordon, D. A.; Whitmore, K. E. *Urology* **1999**, *54*, 982
- (127) Masse, A.; Bruno, A.; Bosetti, M.; Biasibetti, A.; Cannas, M.; Gallinaro, P.; *J. Biomed. Mater. Res.* **2000**, *53*, 600
- (128) Rai, M.; Yadav, A.; Gade, A. *Biotechnology Advances* **2009**, *27*, 76
- (129) Shukla, A.; Fleming, K. E.; Chuang, H. F.; Chau, T. M.; Loose, C. R.; Stephanopoulos, G. N.; Hammond, P. T. *Biomaterials* **2010**, *31*, 2348
- (130) Schierholz, J. M.; Steinhäuser, H.; Rump, A. F. E.; Berkels, R.; Pulverer, G. *Biomaterials* **1997**, *18*, 839
- (131) Rossi, S.; Azghani, A. O.; Omri, A. *J. Antimicrob. Chemother.* **2004**, *54*, 1013
- (132) Kwok, C. S.; Horbett, T. A.; Ratner, B. D. *J. Controlled Release* **1999**, *62*, 301
- (133) Norowski, P. A.; Bumgardner, J. D. *J. Biomed. Mater. Res. B Appl. Biomater.* **2009**, *88B*, 530
- (134) Zhao, L.; Chu, P. K.; Zhang, Y.; Wu, Z. *J. Biomed. Mater. Res. B Appl. Biomater.* **2009**, *91B*, 470
- (135) Oosterbos, G. J.; Vogely, H. C.; Nijhof, M. W.; Flier, A.; Verbout, A. J.; Tonino, A. J.; Dhert, W. J. *J. Biomed. Mater. Res.* **2002**, *60*, 339
- (136) Stigter, M.; de Groot, K.; Layrolle, P. *Biomaterials* **2002**, *23*, 4143
- (137) Stigter, M.; Bezemer, J.; de Groot, K.; Layrolle, P. *J. Contr. Rel.* **2004**, *99*, 127
- (138) Brittain, W. J.; Minko, S. *Journal of Polymer Science: Part A: Polymer Chemistry* **2007**, *45*, 3505
- (139) Matyjaszewski, K.; Miller, P. J.; Shukla, N.; Immaraporn, B.; Gelman, A.; Luokkala, B. B.; Siclovan, T. M.; Kickelbick, G.; Vallant, T.; Hoffmann, H.; Pakula, T. *Macromolecules* **1999**, *32*, 8716
- (140) Ding, S.; Floyd, J. A.; Walters, K. B. *J. Polym. Sci.: Part A: Polym. Chem.* **2009**, *47*, 6552
- (141) Jeon, N. L.; Choi, I. S.; Whitesides, G. M.; Kim, N. Y.; Laibinis, P. E.; Harada, Y.; Finnie, K. R.; Girolami, G. S.; Nuzzo, R. G. *Appl. Phys. Lett.* **1999**, *75*, 4201

- (142) Husseman, M.; Malmström, E. E.; McNamara, M.; Mate, M.; Mecerreyes, D.; Benoit, D. G.; Hedrick, J. L.; Mansky, P.; Huang, E.; Russell, T. P.; Hawker, C. J. *Macromolecules* **1999**, *32*, 1424
- (143) Baum, M.; Brittain, W. J. *Macromolecules* **2002**, *35*, 610
- (144) Azzaroni, O. *J Polym Sci Part A: Polym Chem* **2012**, *50*, 3225
- (145) Liu, P.; Su, Z. X. *Mater. Lett.* **2006**, *60*, 1137
- (146) Lindqvist, J.; Nyström, D.; Östmark, E.; Antoni, P.; Carlmark, A.; Johansson, M.; Hult, A.; Malmström, E. *Biomacromolecules* **2008**, *9*, 2139
- (147) Lee, H. J.; Matsuda, T. J. *Biomed. Mater. Res.* **1999**, *47*, 564
- (148) Yao, F.; Fu, G.-D.; Zhao, J. P.; Kang, E.-T.; Neoh, K. G. *J. Membr. Sci.* **2008**, *319*, 149
- (149) Xu, F. J.; Zhao, J. P.; Kang, E. T.; Neoh, K. G. *Ind. Eng. Chem. Res.* **2007**, *46*, 4866
- (150) Bech, L.; Elzein, T.; Meylheuc, T.; Ponche, A.; Brogly, M.; Lepoittevin, B.; Roger, P. *Eur. Polym. J.* **2009**, *45*, 246
- (151) Liu, J.; Pan, T.; Woolley, A. T.; Lee, M. L. *Anal. Chem.* **2004**, *76*, 6948
- (152) Xu, F. J.; Zhao, J. P.; Kang, E. T.; Neoh, K. G.; Li, J. *Langmuir* **2007**, *23*, 8585
- (153) Azzaroni, O.; Moya, S. E.; Brown, A. A.; Zheng, Z.; Donath, E.; Huck, W. T. S. *Adv. Funct. Mater.* **2006**, *16*, 1037
- (154) Zou, Y. Q.; Kizhakkedathu, J. N.; Brooks, D. E. *Macromolecules* **2009**, *42*, 3258
- (155) Bontempo, D.; Tirelli, N.; Masci, G.; Crescenzi, V.; Hubbell, J. A. *Macromol. Rapid Commun.* **2002**, *23*, 418
- (156) Burkett, S. L.; Ko, N.; Stern, N. D.; Caissie, J. A.; Sengupta, D. *Chem. Mater.* **2006**, *18*, 5137
- (157) Chen, M.; Briscoe, W. H.; Armes, S. P.; Cohen, H.; Klein, J. *Eur. Polym. J.* **2011**, *47*, 511
- (158) Yang, W. J.; Cai, T.; Neoh, K.-G.; Kang, E.-T.; Dickinson, G. H.; Teo, S. L.-M.; Rittschof, D. *Langmuir* **2011**, *27*, 7065
- (159) Hutter, N. A.; Steenackers, M.; Reiting, A.; Williams, O. A.; Garrido, J. A.; Jordan, R. *Soft Matter* **2011**, *7*, 4861
- (160) Wu, W.; Tsarevsky, N. V.; Hudson, J. L.; Tour, J. M.; Matyjaszewski, K.; Kowalewski, T. *Small* **2007**, *3*, 1803
- (161) Kong, H.; Li, W. W.; Gao, C.; Yan, D. Y.; Jin, Y. Z.; Walton, D. R. M.; Kroto, H. W. *Macromolecules* **2004**, *37*, 6683

- (162) Wang, J.-S.; Matyjaszewski, K. *J. Am. Chem. Soc.* **1995**, *117*, 5614
- (163) Kato, M.; Kamigaito, M.; Sawamoto, M.; Higashimura, T. *Macromolecules* **1995**, *28*, 1721
- (164) Patten, T. E.; Matyjaszewski, K. *Adv. Mater.* **1998**, *10*, 901
- (165) Patten, T. E.; Matyjaszewski, K. *Acc. Chem. Res.* **1999**, *32*, 895
- (166) Matyjaszewski, K.; Xia, J. H. *Chem. Rev.* **2001**, *101*, 2921
- (167) Coessens, V.; Pintauer, T.; Matyjaszewski, K. *Prog. Polym. Sci.* **2001**, *26*, 337
- (168) Kamigaito, M.; Ando, T.; Sawamoto, M. *Chem. Rev.* **2001**, *101*, 3689
- (169) Tsarevsky, N. V.; Matyjaszewski, K. *Chem. Rev.* **2007**, *107*, 2270
- (170) di Lena, F.; Matyjaszewski, K. *Progress in Polymer Science* **2010**, *35*, 959
- (171) Matyjaszewski, K. *Macromolecules* **2012**, *45*, 4015
- (172) Siegwart, D. J.; Oh, J. K.; Matyjaszewski, K. *Prog. Polym. Sci.* **2012**, *37*, 18
- (173) Król, P.; Chmielarz, P. *Progress in Organic Coatings* **2014**, *77*, 913
- (174) Ran, J.; Wu, L.; Zhang, Z.; Xu, T. *Prog. Polym. Sci.* **2014**, *39*, 124
- (175) Wang, Y.; Matyjaszewski, K. *Macromolecules* **2010**, *43*, 4003
- (176) Wang, Y.; Matyjaszewski, K. *Macromolecules* **2011**, *44*, 1226
- (177) Huang, X.; Wirth, M. J. *Anal. Chem.* **1997**, *69*, 4577
- (178) Ejaz, M.; Yamamoto, S.; Ohno, K.; Tsujii, Y.; Fukuda, T. *Macromolecules* **1998**, *31*, 5934
- (179) Ayres, N.; Cyrus, C. D.; Brittain, W. J. *Langmuir* **2007**, *23*, 3744
- (180) Boyes, S. G.; Akgun, B.; Brittain, W. J.; Foster, M. D. *Macromolecules* **2003**, *36*, 9539
- (181) Boyes, S. G.; Brittain, W. J.; Weng, X.; Cheng, S. Z. D. *Macromolecules* **2002**, *35*, 4960
- (182) Steve Edmondson, S.; Vicky L. Osborne, V. L.; Huck, W. T. S. *Chem. Soc. Rev.* **2004**, *33*, 14
- (183) Jones, D. M.; Huck, W. T. S. *Adv. Mater.* **2001**, *13*, 1256
- (184) Huang, W.; Kim, J.-B.; Bruening, M. L.; Baker, G. L. *Macromolecules* **2002**, *35*, 1175
- (185) Kim, J. B.; Huang, W. X.; Bruening, M. L.; Baker, G. L. *Macromolecules* **2002**, *35*, 5410
- (186) Matyjaszewski, K.; Shipp, D. A.; Wang, J.-L.; Grimaud, T.; Patten, T. E. *Macromolecules* **1998**, *31*, 6836
- (187) Jakubowski, W.; Min, K.; Matyjaszewski, K. *Macromolecules* **2006**, *39*, 39



- (188) Jakubowski, W.; Matyjaszewski, K. *Macromolecules* **2005**, *38*, 4139
- (189) Min, K.; Gao, H. F.; Matyjaszewski, K. *J. Am. Chem. Soc.* **2005**, *127*, 3825
- (190) Jakubowski, W.; Matyjaszewski, K. *Angew. Chem. Int. Ed.* **2006**, *45*, 4482
- (191) Matyjaszewski, K.; Jakubowski, W.; Min, K.; Tang, W.; Huang, J. Y.; Braunecker, W. A.; Tsarevsky, N. V. *Proc. Nat. Acad. U SA* **2006**, *103*, 15309
- (192) Rodriguez-Emmenegger, C.; Hasan, E.; Pop-Georgievski, O.; Houska, M.; Brynda, E.; Bologna Alles, A. *Macromol. Biosci.* **2012**, *12*, 525
- (193) Teixeira Jr., F.; Popa, A. M.; Guimond, S.; Hegemann, D.; Rossi, R. M. *J. Appl. Polym. Sci.* **2013**, *129*, 636
- (194) Shao, X.-S.; Li, J.-H.; Zhou, Q.; Miao, J.; Zhang, Q.-Q. *J. Appl. Polym. Sci.* **2013**, *129*, 2472
- (195) Wang, Y.; Zhou, F.; Liu, X.; Yuan, L.; Li, D.; Wang, Y.; Chen, H. *ACS Appl. Mater. Interfaces* **2013**, *5*, 3816
- (196) Li, X.; Wang, M.; Wang, L.; Shi, X.; Xu, Y.; Song, B.; Chen, H. *Langmuir* **2013**, *29*, 1122
- (197) Gunkel, G.; Huck, W. T. S. *J. Am. Chem. Soc.* **2013**, *135*, 7047
- (198) Riedel, T.; Riedelova-Reicheltova, Z.; Majek, P.; Rodriguez-Emmenegger, C.; Houska, M.; Dyr, J. E.; Brynda, E. *Langmuir* **2013**, *29*, 3388
- (199) Sugnaux, C.; Lavanant, L.; Klok, H.-A. *Langmuir* **2013**, *29*, 7325
- (200) Lin, N.-J.; Yang, H.-S.; Chang, Y.; Tung, K.-L.; Chen, W.-H.; Cheng, H.-W.; Hsiao, S. W.; Aimar, P.; Yamamoto, K.; Lai, J. Y. *Langmuir* **2013**, *29*, 10183
- (201) Sui, Y.; Wang, Z.; Gao, X.; Gao, C. *J. Membr. Sci.* **2012**, *413–414*, 38
- (202) Li, Y.; Zhang, J.; Liu, W.; Li, D.; Fang, L.; Sun, H.; Yang, B. *ACS Appl. Mater. Interfaces* **2013**, *5*, 2126
- (203) Zhang, Y.; Carbonell, R. G.; Rojas, O. J. *Biomacromolecules* **2013**, *14*, 4161
- (204) Li, Y.; Peterson, J. J.; Jhaveri, S. B.; Carter, K. R. *Langmuir* **2013**, *29*, 4632
- (205) Ren, T.; Mao, Z.; Guo, J.; Gao, C. *Langmuir* **2013**, *29*, 6386
- (206) Zhang, Y.; Islam, N.; Carbonell, R. G.; Rojas, O. J. *Anal. Chem.* **2013**, *85*, 1106
- (207) Berndt, E.; Behnke, S.; Ulbricht, M. *Eur. Polym. J.* **2011**, *47*, 2379
- (208) Tu, Q.; Wang, J.-C.; Liu, R.; He, J.; Zhang, Y.; Shen, S. *Coll. Surf. B: Biointer.* **2013**, *102*, 361
- (209) Ngo, T. C.; Kalinova, R.; Cossement, D.; Hennebert, E.; Mincheva, R.; Snyders, R.; Flammang, P.; Dubois, P.; Lazzaroni, R.; Leclere, P. *Langmuir* **2014**, *30*, 358
- (210) Bao, Z.; Bruening, M. L.; Baker, G. L. *J. Am. Chem. Soc.* **2006**, *128*, 9056

- (211) Tugulu, S.; Barbey, R.; Harms, M.; Fricke, M.; Volkmer, D.; Rossi, A.; Klok, H.-A. *Macromolecules* **2007**, *40*, 168
- (212) Sankhe, A. Y.; Husson, S. M.; Kilbey, S. M., II. *J. Polym. Sci. Part A-Polym. Chem.* **2007**, *45*, 566
- (213) Jain, P.; Dai, J. H.; Baker, G. L.; Bruening, M. L. *Macromolecules* **2008**, *41*, 8413
- (214) Wang, X.; Xiao, X.; Wang, X. H.; Zhou, J. J.; Li, L.; Xu, J. *Macromol. Rapid Commun.* **2007**, *28*, 828
- (215) Xu, D.; Yu, W. H.; Kang, E. T.; Neoh, K. G. *J. Colloid Interface Sci.* **2004**, *279*, 78
- (216) Chen, X. Y.; Armes, S. P.; Greaves, S. J.; Watts, J. F. *Langmuir* **2004**, *20*, 587
- (217) Gao, C.; Vo, C. D.; Jin, Y. Z.; Li, W. W.; Armes, S. P. *Macromolecules* **2005**, *38*, 8634
- (218) Benetti, E. M.; Sui, X. F.; Zapotoczny, S.; Vancso, J. *Adv. Funct. Mater.* **2010**, *20*, 934
- (219) Zhai, G. Q.; Cao, Y.; Gao, J. *J. Appl. Polym. Sci.* **2006**, *102*, 2590
- (220) Pranantyo, D.; Xu, L. Q.; Neoha, K.-G.; Kang, E.-T.; Yang, W.; Lay, S.; Teo, M. *J. Mater. Chem. B* **2014**, *2*, 398
- (221) Xu, F. J.; Zhong, S. P.; Yung, L. Y. L.; Tong, Y. W.; Kang, E. T.; Neoh, K. G. *Tissue Eng.* **2005**, *11*, 1736
- (222) Xu, F. J.; Li, Y. L.; Kang, E. T.; Neoh, K. G. *Biomacromolecules* **2005**, *6*, 1759
- (223) Brantley, E. L.; Jennings, G. K. *Macromolecules* **2004**, *37*, 1476
- (224) Bantz, M. R.; Brantley, E. L.; Weinstein, R. D.; Moriarty, J.; Jennings, G. K. *J. Phys. Chem. B* **2004**, *108*, 9787
- (225) Brantley, E. L.; Holmes, T. C.; Jennings, G. K. *Macromolecules* **2005**, *38*, 9730
- (226) Tugulu, S.; Silacci, P.; Stergiopoulos, N.; Klok, H.-A. *Biomaterials* **2007**, *28*, 2536
- (227) Raynor, J. E.; Petrie, T. A.; Garcia, A. J.; Collard, D. M. *Adv. Mater.* **2007**, *19*, 1724
- (228) Petrie, T. A.; Raynor, J. E.; Reyes, C. D.; Burns, K. L.; Collard, D. M.; Garcia, A. *J. Biomaterials* **2008**, *29*, 2849
- (229) Lavanant, L.; Pullin, B.; Hubbell, J. A.; Klok, H.-A. *Macromol. Biosci.* **2010**, *10*, 101
- (230) Tugulu, S.; Arnold, A.; Sielaff, I.; Johnsson, K.; Klok, H.-A. *Biomacromolecules* **2005**, *6*, 1602

- (231) Xu, F. J.; Li, H. Z.; Li, J.; Eric Teo, Y. H.; Zhu, C. X.; Kang, E. T.; Neoh, K. G. *Biosens. Bioelectron.* **2008**, *24*, 773
- (232) Lee, B. S.; Chi, Y. S.; Lee, K.-B.; Kim, Y.-G.; Choi, I. S. *Biomacromolecules* **2007**, *8*, 3922
- (233) Diamanti, S.; Arifuzzaman, S.; Elsen, A.; Genzer, J.; Vaia, R. A. *Polymer* **2008**, *49*, 3770
- (234) Zhang, F.; Shi, Z. L.; Chua, P. H.; Kang, E. T.; Neoh, K. G. *Ind. Eng. Chem. Res.* **2007**, *46*, 9077
- (235) Sun, L.; Dai, J.; Baker, G. L.; Bruening, M. L. *Chem. Mater.* **2006**, *18*, 4033
- (236) Jain, P.; Sun, L.; Dai, J. H.; Baker, G. L.; Bruening, M. L. *Biomacromolecules* **2007**, *8*, 3102
- (237) Dunn, J. D.; Igrisan, E. A.; Palumbo, A. M.; Reid, G. E.; Bruening, M. L. *Anal. Chem.* **2008**, *80*, 5727
- (238) Sileika, T. S.; Kim, H.-D.; Maniak, P.; Messersmith, P. B. *ACS Appl. Mater. Interfaces* **2011**; *3*, 4602
- (239) Yamamoto, S.; Ejaz, M.; Tsujii, Y.; Fukuda, T. *Macromolecules* **2000**, *33*, 5608
- (240) Primera-Pedrozo, O. M.; Pacheco-Londoño, L. C.; Hernandez-River, S. P. *Goran Nikolic (Ed.), InTech* **2011**, 227
- (241) LeMieux, M. C.; Peleshanko, S.; Anderson, K. D.; Tsukruk, V. V. *Langmuir* **2007**, *23*, 265
- (242) Slim, C.; Tran, Y.; Chehimi, M. M.; Garraud, N.; Roger, J.-P.; Combellas, C.; Kanoufi, F. *Chemistry of Materials* **2008**, *20*, 6677
- (243) Kim, Y. P.; Lee, B. S.; Kim, E.; Choi, I. S.; Moon, D. W.; Lee, T. G.; Kim, H. S. *Analytical Chemistry* **2008**, *80*, 5094
- (244) Navarro, M.; Benetti, E. M.; Zapotoczny, S.; Planell, J. A.; Vancso, G. J. *Langmuir* **2008**, *24*, 10996
- (245) Fan, X. W.; Lin, L. J.; Dalsin, J. L.; Messersmith, P. B. *J. Am. Chem. Soc.* **2005**, *127*, 15843
- (246) Azzaroni, O.; Brown, A. A.; Huck, W. T. S. *Angew. Chem. Int. Ed.* **2006**, *45*, 1770
- (247) Andruzzi, L.; Senaratne, W.; Hexemer, A.; Sheets, E. D.; Ilic, B.; Kramer, E. J.; Baird, B.; Ober, C. K. *Langmuir* **2005**, *21*, 2495
- (248) Gonçalves, S.; Leirós, A.; van Kooten, T.; Dourado, F.; Rodrigues, L. R. *Coll. Surf. B: Biointerfaces* **2013**, *109*, 228
- (249) Yu, K.; Wang, H. F.; Xue, L. J.; Han, Y. C. *Langmuir* **2007**, *23*, 1443

- (250) Yu, K.; Wang, H. F.; Han, Y. C. *Langmuir* **2007**, *23*, 8957
- (251) Dey, T. *Journal of Nanoscience and Nanotechnology* **2006**, *6*, 2479
- (252) Li, D.; He, Q.; Yang, Y.; Möhwald, H.; Li, J. *Macromolecules* **2008**, *41*, 7254
- (253) Chen, X. Y.; Randall, D. P.; Perruchot, C.; Watts, J. F.; Patten, T. E.; von Werne, T.; Armes, S. P. *J. Coll. Interface Sci.* **2003**, *257*, 56
- (254) Bartholome, C.; Beyou, E.; Bourgeat-Lami, E.; Chaumont, P.; Lefebvre, F.; Zydowicz, N. *Macromolecules* **2005**, *38*, 1099
- (255) Tsujii, Y.; Ejaz, M.; Sato, K.; Goto, A.; Fukuda, T. *Macromolecules* **2001**, *34*, 8872
- (256) Nagase, K.; Kobayashi, J.; Kikuchi, A.; Akiyama, Y.; Kanazawa, H.; Okano, T. *Biomacromolecules* **2008**, *9*, 1340
- (257) Babu, K.; Dhamodharan, R. *Nanoscale Research Letters* **2008**, *3*, 109
- (258) Moya, S. E.; Azzaroni, O.; Kelby, T.; Donath, E.; Huck, W. T. S. *J. Phys.Chem. B* **2007**, *111*, 7034
- (259) Kurosawa, S.; Aizawa, H.; Talib, Z. A.; Atthoff, B.; Hilborn, J. *Biosensors & Bioelectronics* **2004**, *20*, 1165
- (260) Li, D. X.; He, Q.; Cui, Y.; Li, J. B. *Chemistry of Materials* **2007**, *19*, 412
- (261) Kaholek, M.; Lee, W. K.; Ahn, S. J.; Ma, H. W.; Caster, K. C.; LaMattina, B.; Zauscher, S. *Chemistry of Materials* **2004**, *16*, 3688
- (262) Choi, E. Y.; Azzaroni, O.; Cheng, N.; Zhou, F.; Kelby, T.; Huck, W. T. S. *Langmuir* **2007**, *23*, 10389
- (263) Yim, H.; Kent, M. S.; Mendez, S.; Balamurugan, S. S.; Balamurugan, S.; Lopez, G. P.; Satija, S. *Macromolecules* **2004**, *37*, 1994
- (264) Zhang, J. M.; Nylander, T.; Campbell, R. A.; Rennie, A. R.; Zauscher, S.; Linse, P. *Soft Matter* **2008**, *4*, 500
- (265) Zhao, C.; Li, L.; Wang, Q.; Yu, Q.; Zheng, J. *Langmuir* **2011**, *27*, 4906
- (266) Zhou, F.; Hu, H. Y.; Yu, B.; Osborne, V. L.; Huck, W. T. S.; Liu, W. M. *Analytical Chemistry* **2007**, *79*, 176
- (267) Spruijt, E.; Choi, E. Y.; Huck, W. T. S. *Langmuir* **2008**, *24*, 11253
- (268) Sakakiyama, T.; Ohkita, H.; Ohoka, M.; Ito, S.; Tsujii, Y.; Fukuda, T. *Chemistry Letters* **2005**, *34*, 1366

## 2. HEMA/OEGMA Polymer Brushes as an Attractive Platform to Prevent Bacteria Adhesion

### 2.1. Introduction

Bacterial adhesion and biofilm formation has a great impact on everyday life, strongly influencing various fields including health systems<sup>1-9</sup>, marine transportation<sup>6,7,10-12</sup>, food processing equipment and packaging<sup>13-17</sup>, industrial and wastewater systems<sup>15,18</sup>, oil industry<sup>19</sup> and domestic environment<sup>20</sup>. By far, the implications in the medical field are most dramatic affecting morbidity and determining important increase of costs in the health care systems worldwide<sup>1,3,8,20-23</sup>. Various medical devices (pacemaker leads, cochlear and dental implants, vascular stents and grafts, catheters, hip and knee prostheses, heart valves, intraocular and contact lenses and many others) are lifesaving but, their use is challenging due to risks involved by biomaterial-associated infections<sup>1,3,5,7-10,21</sup>.

Biointerfacial interactions play a significant role in protein adsorption, bacterial attachment and biofilm formation on surfaces of medical implants hence the key of developing infection-resistant biomaterials is to efficiently control biological and chemical processes on interfaces and surfaces<sup>1,7,8</sup>. The use of specifically designed surfaces for preventing and inhibiting surface fouling by manipulation of physical and chemical surface properties is a promising approach. The resulting surfaces are denominated “passive surfaces” (or antifouling) – they are able to interfere, prevent and even stop protein and/or bacterial adhesion in different stages but, usually, do not kill bacteria<sup>24</sup>. Generally, biopassive approach uses coatings based on hydrophilic or charged polymers<sup>1-12,21,24,25</sup>.

In the last decades, various chemical strategies for obtaining biopassive coatings have been reported. The progress in this field is presented in a series of extensive reviews<sup>1,3,8,24-30</sup>. The use of polymer brushes as *passive antifouling surfaces* has been discussed in a

great number of recent papers<sup>1-5,6-12,20,21,24-30</sup>. Two main approaches are available for the synthesis of polymer brushes with well-defined architecture and a good control over grafting densities and thicknesses: “grafting to” and “grafting from” methods<sup>24,25,30</sup>. In the “grafting to” strategy the polymer chains are first synthesized and then bound to surface by physical bounds (physisorption), or through covalent linkages (chemisorption). In the “grafting from” strategy the polymer brushes are grown directly from the initiator-functionalized surfaces<sup>25</sup>. The main disadvantage of the “grafting to” method relies in the difficulty to produce thick and very dense polymer brushes<sup>25</sup>. Surface-initiated atom transfer radical polymerization (SI-ATRP) is the most frequently used method for the synthesis of “grafted from” protein/bacteria repellent surfaces based on polymer brushes<sup>24-28</sup>. ATRP, a chemically versatile method, compatible with a large assortment of monomers and functional groups, tolerating a relatively high degree of impurities is widely used for the synthesis of polymer brushes<sup>25</sup>. Effective low-fouling coatings have been prepared via SI-ATRP<sup>25,30</sup>.

Due to its demonstrated ability to prevent nonspecific protein adsorption poly(ethylene glycol) (PEG) (poly(ethylene oxide) (PEO)) brush coatings with controlled compositions, architectures and properties have found numerous biomedical and bioengineering applications<sup>1-3,8,20-26,28,30</sup>. Moreover, due to its intrinsic low-fouling properties PEG is nowadays used as “gold standard” material in biomedical applications, mainly for reducing the incidence of nosocomial infections<sup>1,31,32</sup>. Antifouling surfaces obtained by ATRP are based on polyacrylamide (PAM)<sup>33-36</sup>, polymethacrylates as poly(ethylene glycol) methyl ether methacrylate<sup>37</sup>, and zwitterionic polymers such as poly(sulfobetaine methacrylate) and poly(carboxybetaine methacrylate)<sup>38,39</sup>. Oligo(ethylene glycol) methacrylate (OEGMA) and 2-hydroxyethyl methacrylate (HEMA) based polymer brushes have been developed on different surfaces using SI-ATRP. Different OEGMA macromonomers have been grafted on: silicon<sup>40-43</sup>, stainless steel<sup>44</sup>, gold<sup>45-48</sup>, silica<sup>49</sup>, or Ti<sup>50</sup>. The obtained surfaces proved to resist protein adsorption, being repellent to fibrinogen, globulin, peptides, and many others as well as to prevent cell adhesion. Using SI-ATRP anti-fouling polymer brushes based on hydrophilic poly(2-hydroxyethyl methacrylate) (PHEMA) polymer brushes have been “grafted from” on various surfaces. Yoshikawa et al grafted PHEMA brushes from the inner surface of a silica monolith<sup>51</sup> and verified their resistance to protein adsorption. Washburn and co-workers prepared PHEMA-based brushes with well-defined surface chemistry<sup>52</sup> studying the factors affecting protein adsorption. The covalently bound polymer brushes are efficient non-

fouling coatings providing effective physical barriers against protein adhesion due to the exclusion volume around polymer chains and well-developed hydration layer<sup>3</sup>. The polymer chains are densely packed and thus resisting to protein adsorption<sup>24-26</sup>. It is generally accepted that hydrophilic surfaces exhibit repulsive effects preventing bacteria non-specific attachment to surfaces. Contrary to this opinion, Rodriguez-Emmenegger and coworkers<sup>53</sup> proved that poly(*N*-hydroxypropylmethacrylamide) (PHPMA) brushes that are based on a hydrogen bond donor and are moderately hydrophilic can work as antifouling surfaces. Analyzing literature data it is easy to notice that, predominantly, the researchers study the ability of the synthesized surfaces to resist to non-specific peptide/protein adsorption<sup>1,6,10-12,29,30,37,38,42-48,51,54</sup>. It is normal to adopt this perspective as long as it is well-known that the initial step of bacteria attachment is favored by the conditioning plasma protein layer formed on the surface of the material, ensuring the best conditions for the biofilm formation and development. Elucidating the mechanism governing the complex process of the biofilm formation and the laws behind it, biomaterials able to prevent and decrease the number of implant-related infections can be designed. It is worth mentioning that protein or peptide repellent surfaces are not always bacterial repellants as demonstrated by Kingshott and coworkers<sup>55</sup> who reported PEG modified stainless steel surfaces with good protein repellency, but not bacteria repellent. Furthermore, in 2001 Whitesides and coworkers<sup>56</sup> analyzed the factual correlation between these two processes and demonstrated that surfaces with proven good resistance to protein adsorption did not exhibit high ability to reduce bacterial adhesion for *S. aureus* and *S. epidermidis*. The congruence between antifouling surface properties and bacterial antiadhesive activity may depend on the bacterial species and on the particular physiochemical properties of the analyzed surfaces. Although, polymer brush coatings are well-known for their anti-adhesive properties more research is needed to clarify how the protein non-adhesiveness and characteristics of polymer brushes are related to bacteria repellent properties. Roosjen et al. studied the bacteria repellent properties of PEO brushes covalently tethered on glass and silicon surfaces, and they observed a species-related variable bacterial reduction<sup>57-60</sup>. Different reports discuss particular cases considering specific bacterial species attachment to well-defined surfaces. Surface architecture, charge and specific receptor–adhesion to host proteins coating the implant material play an important role in the bacteria binding to substrate<sup>1-12,21,24,25</sup>. The Textor group studied different strategies for the immobilization of PEG using a comb-like polymer with a polycationicpoly(L-lysine) (PLL) backbone and PEG side chains<sup>61-63</sup> and

an alternative biopassive coating based on poly(2-methyl-2-oxazoline) (PMOXA), as well as comb copolymers consisting of a PLL backbone and PMOXA side chains, analogous to PLL-g-PEG systems<sup>64-66</sup>. Further, PMOXA-based coatings have been used to prevent adhesion of *Escherichia coli*<sup>66</sup>. Zwitterionic surfaces obtained from sulfobetaine methacrylate and methacryloyl polymers proved their efficiency in reducing *E. coli*, *S. epidermidis* and *P. aeruginosa* adhesion and biofilm formation both for short and long term studies<sup>67-69</sup>. Recently, hydrophobic surfaces based on a xerogel coating obtained from a mixture of nanostructured fluorinated silica colloids, fluoroalkoxysilane, and a backbone silane<sup>70</sup> as well as through the deposition of a secondary polymer layer locked in place by a micro/nanoporous substrate termed slippery liquid infused porous surfaces (SLIPSS)<sup>1,54,71</sup> were tested and proved to slow bacteria adhesion, but research is still in progress.

Although there are some reports that PHEMA or POEGMA polymer brushes can reduce bacteria adhesion on different surfaces<sup>72-76</sup> to the best of our knowledge there is no in depth study of the effect of polymer brush density and thickness. There are only few reports on surfaces modified with polymer brushes able to reduce *S. epidermidis* attachment, most of them focusing on PEG<sup>56,57,60,69,77-79</sup>. *S. epidermidis* is a coagulase-negative staphylococcus (CNS) usually found on the skin and mucous membranes of the human body<sup>80,81</sup>. It is also one of the most successful pathogens involved in nosocomial infections, mainly associated with implanted medical devices<sup>80-82</sup>. The purpose of this chapter is to investigate *S. epidermidis* adhesion on HEMA or OEGMA polymer brushes on a wide range of grafting densities and film thicknesses. PEG brushes are used as a positive control surface as long as many studies consider it as a “gold standard” in preventing the adhesion of microorganisms to the surfaces. In the present study, silicon substrates were modified with poly(2-hydroxyethyl methacrylate) (PHEMA) and poly(ethylene glycol) monomethacrylate) (POEGMA), using SI-ATRP. Furthermore, POEGMA and PHEMA polymer brushes contain one hydroxyl group per repeat unit along the backbone that can be used to couple a broad range of bioactive compounds, including antimicrobials.



## 2.2. Experimental Section

### 2.2.1. Materials

All chemicals were purchased from Aldrich and used as received unless stated otherwise. Carboxyl-terminated poly(ethylene glycol) (PEG-COOH) was synthesized by refluxing poly(ethylene glycol) monomethyl ether with excess succinyl anhydride in tetrahydrofuran (THF). The resulted PEG-COOH was purified via multiple precipitations from THF solution using diethyl ether. To remove the inhibitor the monomers was passed through a column of activated basic aluminum oxide. Silicon (100) covered with a native silicon oxide layer was used as substrate for surface-initiated polymerization. THF, dichloromethane (DCM) and toluene were purified and dried using a solvent purification system (PureSolv). Deionized water was obtained from a Millipore Direct-Q 5 Ultrapure Water System and ultrahigh quality Milli-Q water was obtained from a Millipore Milli-Q gradient machine fitted with a 0.22  $\mu\text{m}$  filter. The 25-well plates were purchased from BibbySterilin Ltd, Stone, Staffs, UK. Tryptic Soy Broth (TSB) and Mueller-Hinton agar (MHA) were purchased from Difco, BD and Co., France and used according to the manufacturer's instructions. LIVE/DEAD BacLight Bacterial Viability Kit was purchased from Invitrogen, Eugene, Oregon, USA. All non sterile solutions used in the bacteria experiments were autoclaved at 121 °C for 20 minutes. *S. epidermidis* 1457 bacteria strain was kindly provided by Prof. Landmann, University of Basel.

### 2.2.2. Methods

X-ray photoelectron spectroscopy (XPS) was carried out using an Axis Ultra instrument from Kratos Analytical equipped with a conventional hemispheric analyzer. The X-ray source employed was a monochromatic Al K $\alpha$  (1486.6 eV) source operating at 100 W and  $10^{-9}$  mbar. All XPS spectra were calibrated on the aliphatic carbon signal at 285.0 eV. Relative sensitivity factors (RSF) of 0.278 (C<sub>1s</sub>), 0.78 (O<sub>1s</sub>) were used to correct peak area ratios. Attenuated total reflectance Fourier transform infrared spectroscopy (ATR-FTIR) was performed on a nitrogen purged Nicolet 6700 FT-IR spectrometer equipped with a SmartiTR™ (Thermo Fisher Scientific Inc., Waltham, MA, USA) accessory and a diamond crystal. Atomic force microscopy (AFM) was performed in tapping mode on a Veeco Multimode Nanoscope IIIa SPM controller (Digital

Instruments, Santa Barbara, CA) using NSC14/no Al MikroMasch (Tallinn, Estonia) cantilevers. To determine the layer thicknesses, cross-sectional height profiles of micropatterned polymer brushes on silicon substrates were analysed. Micropatterned initiator-coated substrates were prepared using a protocol previously reported in the literature<sup>83</sup>. Brush thicknesses were also determined by means of a SOPRA GES-5 ellipsometer working with a He–Ne laser ( $\lambda = 632.8$  nm) at an angle of incidence of  $70^\circ$ . The calculation method was based on a four-layer silicon/initiator/polymer brush/ambient model, assuming the polymer brush to be isotropic and homogeneous. A fixed refractive index value of 1.5 was used for the polymer layer. Water contact angles were determined using a DataPhysics OCA 35 contact angle measurement instrument.  $^1\text{H-NMR}$  spectra were recorded on a Bruker AVANCE-400 Ultra Shield spectrometer.

### 2.2.3. Procedures

#### 2.2.3.1. Synthesis of SI-ATRP initiator (**1b**)

##### *Synthesis of 5-hexen-1-yl 2-bromo-2-methylpropionate (**1a**)*

5-Hexen-1-ol (6.00 mL, 50 mmol) and triethylamine (7.00 mL, 50 mmol) were dissolved in DCM (30 mL). The solution was stirred under nitrogen and cooled with an ice bath. Next,  $\alpha$ -bromoisobutyryl bromide (6.15 mL, 50 mmol) was added dropwise and the resulting mixture stirred under nitrogen at  $0^\circ\text{C}$  for two hours and additional 4 hours at  $25^\circ\text{C}$ . The precipitate was removed by filtration and the product washed with a saturated ammonium chloride solution. The organic phase was dried over  $\text{MgSO}_4$  and the solvent removed under reduced pressure. 5-hexen-1-yl 2-bromo-2-methylpropionate was obtained as a colorless oil after vacuum distillation ( $80^\circ\text{C}$ , 0.5 mbar). Yield: 78%.

$^1\text{H NMR}$  (400 MHz,  $\text{CDCl}_3$ ,  $\delta$ ): 1.48 (m, 2H, -CH<sub>2</sub>-), 1.67 (m, 2H, -CH<sub>2</sub>-), 1.90 (s, 6H, C-CH<sub>3</sub>), 2.06 (m, 2H, -CH<sub>2</sub>-), 4.12 (t, 2H, O=C-O-CH<sub>2</sub>), 4.95 (m, 2H, C=CH<sub>2</sub>), 5.73 (s, 1H, -CH=CH<sub>2</sub>).  $^{13}\text{C NMR}$  (400 MHz,  $\text{CDCl}_3$ ,  $\delta$ ): 25.72, 28.35 (-CH<sub>2</sub>-), 30.76 (C-CH<sub>3</sub>), 33.77 (-CH<sub>2</sub>-), 55.95 (C-CH<sub>3</sub>), 66.12 (O=C-O-CH<sub>2</sub>), 114.10 (C=CH<sub>2</sub>), 139.12 (C=CH<sub>2</sub>), 171.70 (C=O).

##### *Synthesis of (6-(2-(2-Bromo-2-methyl)propionyloxy)hexyldimethylchlorosilane (**1b**)*

4.46 g (18 mmol) 5-Hexen-1-yl-2-bromo-2-methylpropionate was refluxed for 12 hours under nitrogen at  $50^\circ\text{C}$  with 20 mL (180 mmol) dimethylchlorosilane in presence of 30

mg Pt/C (10% Pt). After the reaction, the solution was filtered over anhydrous sodium sulfate in order to remove the catalyst. The solvent was evaporated under reduced pressure and **1b** was obtained as colorless oil after vacuum distillation (160 °C, 0.5 mbar). Yield: 87%.

<sup>1</sup>H NMR (400 MHz, CDCl<sub>3</sub>, δ): 0.37 (m, 6H, Si-CH<sub>3</sub>), 0.78 (m, 2H, -CH<sub>2</sub>-), 1.36 (m, 6H, -CH<sub>2</sub>-), 1.64 (m, 2H, -CH<sub>2</sub>-), 1.91 (s, 6H, C-CH<sub>3</sub>), 4.12 (t, 2H, O=C-O-CH<sub>2</sub>). <sup>13</sup>C NMR (400 MHz, CDCl<sub>3</sub>, δ): 1.61 (Si-CH<sub>3</sub>), 18.82, 22.81, 25.34, 28.15 (-CH<sub>2</sub>-), 30.74 (C-CH<sub>3</sub>), 32.35 (-CH<sub>2</sub>-), 55.90 (C-CH<sub>3</sub>), 65.95 (O=C-O-CH<sub>2</sub>), 171.62 (C=O).

### 2.2.3.2. Synthesis of SI-ATRP inactive chlorosilane (**2b**)

The ATRP inactive 6-(chloro(dimethyl)silyl)hexyl pivalate **2b** was synthesized via the same protocol than the SI-ATRP initiator **1b** using pivalylol chloride instead of α-bromoisobutyryl bromide.

*Hexen-5-enyl pivalate (2a)* Yield: 72%

<sup>1</sup>H NMR (400 MHz, CDCl<sub>3</sub>, δ): 1.15 (s, 9H, C-CH<sub>3</sub>), 1.42 (m, 2H, -CH<sub>2</sub>-), 1.63 (m, 2H, -CH<sub>2</sub>-), 2.67 (m, 2H, -CH<sub>2</sub>-), 4.03 (t, 2H, O=C-O-CH<sub>2</sub>), 4.96 (m, 2H, C=CH<sub>2</sub>), 5.76 (s, 1H, -CH=CH<sub>2</sub>). <sup>13</sup>C NMR (400 MHz, CDCl<sub>3</sub>, δ): 25.75, 28.32 (-CH<sub>2</sub>-), 30.77 (C-CH<sub>3</sub>), 33.76 (-CH<sub>2</sub>-), 55.95 (C-CH<sub>3</sub>), 66.12 (O=C-O-CH<sub>2</sub>), 114.12 (C=CH<sub>2</sub>), 139.12 (C=CH<sub>2</sub>), 171.70 (C=O).

*6-(chloro(dimethyl)silyl)hexyl pivalate (2b)* Yield: 85%

<sup>1</sup>H NMR (400 MHz, CDCl<sub>3</sub>, δ): 0.36 (m, 6H, Si-CH<sub>3</sub>), 0.81 (m, 2H, -CH<sub>2</sub>-), 1.17 (s, 9H, C-CH<sub>3</sub>), 1.36 (m, 6H, -CH<sub>2</sub>-), 1.62 (m, 2H, -CH<sub>2</sub>-), 4.01 (t, 2H, O=C-O-CH<sub>2</sub>). <sup>13</sup>C NMR (400 MHz, CDCl<sub>3</sub>, δ): 1.61 (Si-CH<sub>3</sub>), 18.84, 22.84, 25.49 (-CH<sub>2</sub>-), 27.16 (C-CH<sub>3</sub>), 28.46, 32.48 (-CH<sub>2</sub>-), 38.64 (C-CH<sub>3</sub>), 64.33 (O=C-O-CH<sub>2</sub>), 178.55 (C=O).

### 2.2.3.3. Immobilization of the ATRP initiator

First, the silicon wafers were sonicated for 5 minutes in acetone and dried. The silicon surfaces were then exposed to oxygen plasma (180 W, 10 min) and subsequently the clean wafers were kept overnight and in the dark in a 10 mM solution of **1b**, or in a 10 mM mixture of **1b** and **2b**, in anhydrous toluene. Afterwards, the slides were extensively rinsed with chloroform, dried under nitrogen and transferred to the appropriate reactors for the polymerizations.

#### 2.2.3.4. HEMA polymer brush synthesis

Surface initiated atom transfer radical polymerizations of HEMA was performed at room temperature in water using a reaction system consisting of HEMA, Cu(I)Cl, Cu(II)Br<sub>2</sub> and 2,2'-bipyridyl in the following molar ratios: 125:3.5:1:10. In a typical experiment 10 mL HEMA (20 mmol), 244 mg bipy (1.56 mmol), water (10 mL) and 36 mg Cu(II)Br<sub>2</sub> (0.16 mmol) were introduced in a Schlenk tube sealed with a septum and mixed until complete homogenization. Then, the mixture was purged with nitrogen for one hour and 55 mg Cu(I)Cl (0.55 mmol) were added. After homogenization the reaction mixture was transferred with a cannula to a nitrogen purged reactor containing the ATRP initiator modified slides and the reaction was allowed to proceed. After the desired time the polymerization mixture was exposed to air, the slides were removed, washed with methanol, 70% ethanol solution, and water and then dried under a flow of nitrogen and then vacuum.

#### 2.2.3.5. OEGMA<sub>6</sub> polymer brush synthesis

Surface initiated atom transfer radical polymerizations of OEGMA<sub>6</sub>, was performed at 60 °C in a water methanol mixture (8:2/v:v) using a reaction system consisting of OEGMA<sub>6</sub>, Cu(I)Cl and 2,2'-bipyridyl in the following molar ratios 80:3.5:10. In a typical experiment 15 mL OEGMA<sub>6</sub> (45 mmol), 860 mg bipy (5.5 mmol) water (12 mL) and methanol (3 mL) were introduced in a Schlenk tube sealed with a septum and mixed until complete homogenization. Then, the mixture was degassed by three freeze-pump-thaw cycles and 193 mg Cu (I)Cl (1.96 mmol) were added. After homogenization the reaction mixture was heated to 60 °C and transferred with a cannula to a nitrogen purged reactor containing the ATRP initiator modified slides. The reactor was placed in a thermostated oil bath at 60 °C and the reaction was allowed to proceed. After the desired time the polymerization mixture was exposed to air, the slides were removed, washed with methanol, 70% ethanol solution, and water and then dried under a flow of nitrogen and then vacuum.

#### 2.2.3.6. Bacterial culture preparation

Stocks of *S. epidermidis* 1457 were prepared using a cryovial bead preservation system (Microbank; Pro-Lab Diagnostics, Richmond Hill, Ontario, Canada) and stored at -75 °C. For the preparation of overnight culture a bead was incubated in 1 mL of TSB for 5 hours at 37 °C, diluted 1:100 in fresh TSB, and incubated overnight at 37 °C. The

overnight culture was diluted to the desired colony-forming units (CFU) based on optical density and then used for the bacterial adhesion tests. All cultures were prepared without shaking and CFU were determined by plating aliquots of 10-fold dilutions of bacterial cultures on Mueller-Hinton agar (MHA), followed by 24 hours of incubation at 37 °C.

### **2.2.3.7. Bacterial adhesion tests**

For all bacterial adhesion tests the surfaces were placed in 25-well plates, 2 mL of TSB with the desired CFU were added and then incubated for a predefined time at 37 °C without shaking.

#### **2.2.3.7.1. Crystal violet staining**

After 24 hours incubation the surfaces were removed, washed four times with 2 mL 0.9% NaCl and then transferred to a fresh 25-well plate. The bacteria were fixed by placing the plate on the heating-surface for 60 minutes at 60 °C and then stained with 0.5% crystal violet (700 µL/well) for 20 minutes at RT. After washing the stained surfaces with tap water they were transferred to a fresh 25-well plate and destained with 33% acetic acid (600 µL/well) under shaking. 100 µL of each solution was transferred to a 96-well flat-bottom plate and the absorbance at 590 nm was read using a plate reader. The samples incubated only in medium without bacteria were treated as described above.

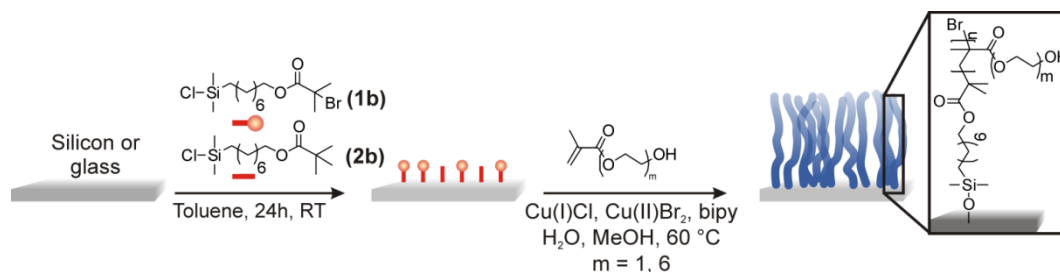
#### **2.2.3.7.2. LIVE/DEAD staining**

LIVE/DEAD BacLight Bacterial Viability Kit was used to visualize the surface-attached bacteria. Dye solution (protected from light) was prepared with 1.5 µL propidium iodide (PI) and 1.5 µL SYTO9 in 1 mL Milli-Q water. After the predefined time of incubation the surfaces were removed, washed two times with 2 mL 0.9% NaCl and then dipped in 0.9% NaCl. The samples were transferred on microscope slide and 14 µL dye solution per each surface was added. A cover slip was placed over the surfaces before microscopic examination (x40; Provis AX70, Olympus AG, Volketswil, Switzerland). At least three randomly selected pictures were acquired from the central part of each surface.

## 2.3. Results and Discussion

### 2.3.1. Polymer-brush synthesis

Two types of polymer brushes were synthesized and tested with respect to their ability to generate bacteria repellent surfaces and thus preventing bacterial adhesion. Polymer brushes have been grown from silicon wafers by SI-ATRP of oligo(ethylene glycol) methyl methacrylate (OEGMA) and 2-hydroxyethyl methacrylate (HEMA). The approach is outlined in Scheme 1. SI-ATRP is robust and chemically versatile method for the synthesis of polymer brushes with good control over thickness and grafting density of the polymer chains. The thickness was controlled by changing the polymerization time and the grafting density by using surfaces previously coated with various ratios of active and inactive initiators. The surfaces were obtained by tethering on the substrate the active ATRP initiator: (6-2-(2-Bromo-2-methyl)propionyloxy)hexyldimethylchlorosilane (**1b**), alone or in mixture with the 6-(chloro(dimethyl)silyl)hexyl pivalate (**2b**) inactive ATRP initiator to decrease the surface density of the ATRP active sites. The synthesis of the used active and inactive initiators was performed in both cases in two steps (Scheme S1, Supporting Information). The first step of reaction involved the esterification of 5-hexen-1-ol with  $\alpha$ -bromoisobutyryl bromide or pivaloyl chloride to obtain active or inactive initiator, respectively. The second step following the esterification was the hydrosilylation with dimethylchlorosilane to synthesize compounds with reactive species able to be tethered to the surfaces. All compounds were characterized by  $^1\text{H-NMR}$  and the spectra are presented in the Supporting Information (Figure S1 – S4). The coupling of the chlorosilane compounds to the silicon wafers could be monitored by an increase in the water-contact angle from  $4^\circ$  to  $80^\circ$ .



**Scheme 1.** Synthetic route for PHEMA (m=1) and POEGMA (m=6) brush synthesis

HEMA and POEGMA polymer brushes were prepared by SI-ATRP using a catalyst system consisting of CuCl/CuBr<sub>2</sub> and bipy in water at room temperature for HEMA and CuCl and bipy in a water-methanol mixture at 60 °C for OEGMA. Figure 1 shows the evolution of thickness with polymerization time for both PHEMA and POEGMA grown from surfaces with 100% active initiator. For the selected reaction conditions, a linear increase in film thickness with polymerization time was observed for HEMA up to 200 minutes and for OEGMA up to 100 minutes and afterwards for both monomers the film thickness is slowly leveling off. The leveling off in the film thickness can be an expression of losing the “living” character of the polymerization. The faster polymerization reaction for OEGMA is due to the absence of Cu<sup>2+</sup> in the catalytic system. Although the use of Cu<sup>2+</sup> leads to a slower, more controlled growth of the polymer brush, for this system, it also leads to the gelation of the polymerization system, due to unexplained reasons.

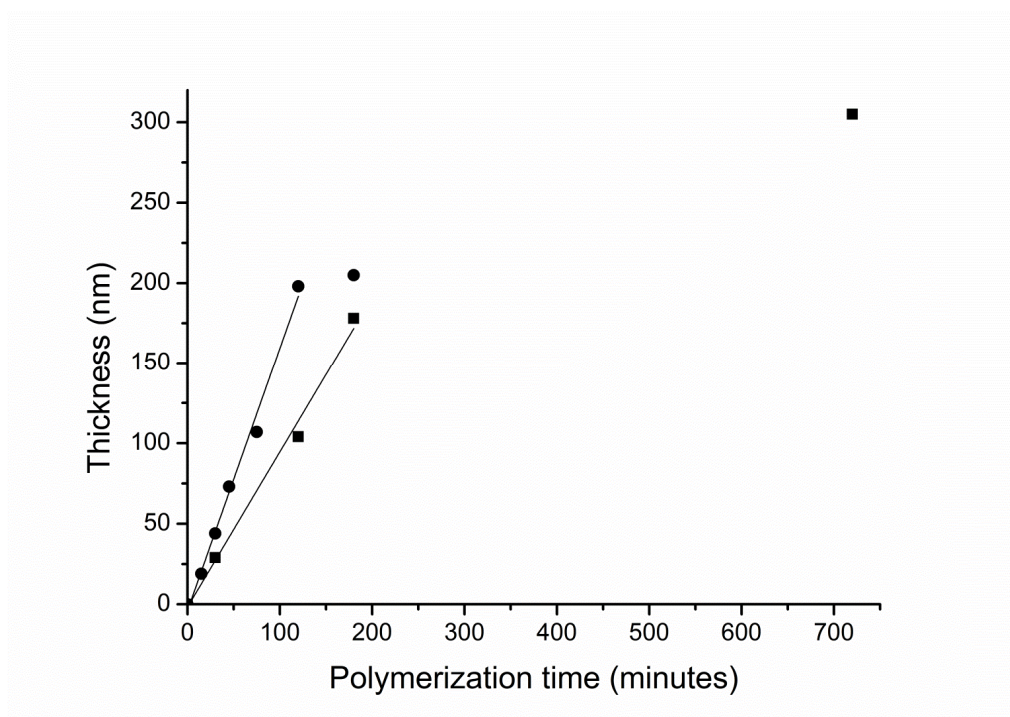


**Figure 1.** Evaluation of film thickness for 100% grafting density PHEMA (■) and POEGMA (●) as measured by AFM

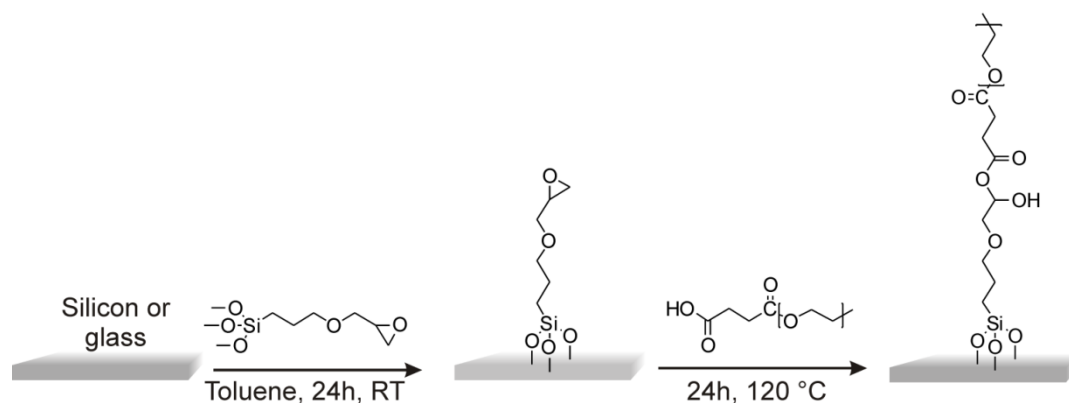
Support for the successful grafting of the polymer brushes is obtained from water contact angle, ATR-FTIR spectroscopy and XPS. The growth of PHEMA and POEGMA

brushes from an ATRP initiator modified substrate resulted in the decrease in the water contact angle from 80 ° to 59 ° and 49 °, respectively.

The FTIR spectra presented in Figure S5 (Supporting Information) for PHEMA and POEGMA brushes coated surfaces shows a broad band at  $\sim 3100 - 3500 \text{ cm}^{-1}$  coming from the hydroxyl groups, the asymmetric and the symmetric  $\text{CH}_2$  vibration between  $2900 \text{ cm}^{-1}$  and  $3000 \text{ cm}^{-1}$  and the carbonyl stretching vibration of the ester group  $\text{C}=\text{O}$  at  $1729 \text{ cm}^{-1}$ . It can be noticed the higher intensity for the peak corresponding the hydroxyl groups and a lower intensity for  $\text{CH}_2$  vibration in the case of PHEMA compared to POEGMA due to the shorter side chains.

The XPS spectra of the PHEMA brush (a) and POEGMA brush (c) presented in Figure S6 (Supporting Information), show the presence of oxygen and carbon in proportions corresponding to the elemental composition. Analysis of the high-resolution  $\text{C}_{1s}$  signal (B - PHEMA, D - POEGMA) could be fitted with three different components corresponding to three types of carbon atoms: 1 - aliphatic backbone atoms, 2 - ethylene glycol units, 3 - ester groups units with ratios within 1:2:3 of 2:2:1 for PHEMA and 2:12:1 for POEGMA.

As a positive control for bacteria adhesion experiments PEG brushes were prepared via the “grafting to” method, outlined in Scheme 2, following a slightly modified procedure<sup>38</sup>. Firstly, the silicon wafer was modified by using toluene solution with epoxysilane volume concentration of 1%. Afterwards, the epoxysilane modified silicon wafer was covered with PEG-COOH powder and then kept for 18 hours in a vacuum oven at 120 °C, then washed with ethanol and dried under a stream of nitrogen. For PEG with a  $M_n$  of  $\sim 5000 \text{ Da}$  the thickness was measured by ellipsometry and had a value of  $4.37 \pm 0.26 \text{ nm}$ , and for PEG with a  $M_n$  of  $\sim 20,000 \text{ Da}$  the value was  $10.84 \pm 0.185$ , respectively. For both PEG brush covered surfaces the water contact angle was 33 °.



**Scheme 2.** Synthetic route for preparation of PEG brushes



Table 1 summarizes all samples prepared for bacterial experiments presenting the thickness in rapport with grafting density and polymerization time. All thicknesses were measured by AFM on pattern samples unless stated otherwise.

**Table 1.** Summary of samples prepared for the bacterial experiments

Sample	Monomer	Active initiator (%)	Polymerization time (min)	Thickness, (nm)	Thickness after being autoclaved (nm)
S1	EG	-	-	4.37±0.26	ND
S2	EG	-	-	10.84±0.185	ND
S3	HEMA	1	30	2.23 ± 2.53*	2.74 ± 2.28*
S4	HEMA	1	120	3.18 ± 1.41*	2.93 ± 2.05*
S5	HEMA	1	720	4.45 ± 2.23*	4.27 ± 2.59*
S6	HEMA	50	30	12	11
S7	HEMA	50	120	38	37
S8	HEMA	50	720	117	115
S9	HEMA	75	30	21	21
S10	HEMA	75	120	73	75
S11	HEMA	75	720	203	201
S12	HEMA	100	30	29	28
S13	HEMA	100	120	104	103
S14	HEMA	100	720	305	302
S15	OEGMA	1	15	ND	ND
S16	OEGMA	1	120	ND	ND
S17	OEGMA	50	15	6.23 ± 0.23*	5.44 ± 0.11*
S18	OEGMA	50	45	27	27
S19	OEGMA	50	75	48	47
S20	OEGMA	50	120	102	100
S21	OEGMA	75	15	11	9
S22	OEGMA	75	45	37	36
S23	OEGMA	75	75	68	69
S24	OEGMA	75	120	138	141
S25	OEGMA	100	15	19	18
S26	OEGMA	100	45	73	75
S27	OEGMA	100	75	107	103
S28	OEGMA	100	120	195	194

\* measured by ellipsometry

ND = not determined

### 2.3.2. Bacteria adhesion tests

The novelty of the research presented in this paper resides in the assessment of biofilms formed by isolates of *S. epidermidis* on surfaces covered with POEGMA and PHEMA brushes with a wide range of grafting densities and thicknesses. Little attention has been paid until now to the analysis of the bacteria repellent properties of PHEMA and POEGMA brushes against this bacterial strain. Thus this study can be considered the first attempt to determine the repellent activity of PHEMA and POEGMA brushes against *S. epidermidis* and to analyze if grafting density and film thickness significantly influence bacterial attachment on brush coated surfaces.

In order to evaluate bacterial adhesion, the surfaces were incubated with *S. epidermidis* 1457. At indicated time points the surfaces were washed to remove the planktonic bacteria, and the bacteria adherent to surfaces were examined using different methods. First, the bacterial adhesion was investigated microscopically using the LIVE/DEAD BacLight Bacterial Viability kit, which employs SYTO 9 and PI, green and red fluorescent nucleic acid dye, respectively. Due to impermeability of intact bacterial membranes for PI, the combination of SYTO 9 and PI allows staining all bacteria in green and bacteria with damaged membranes – in red. The background remains virtually nonfluorescent. Consequently, the ratio of green to red fluorescence intensities may provide an estimation of an index of bacterial viability<sup>84</sup>. The results presented in Figure 2 showed a substantial decrease in the number of bacteria attached to the two studied brush coated surfaces after 3-hours incubation as compared with the silicon wafers used as the negative control. No major differences between the two types of polymer brushes were noted.

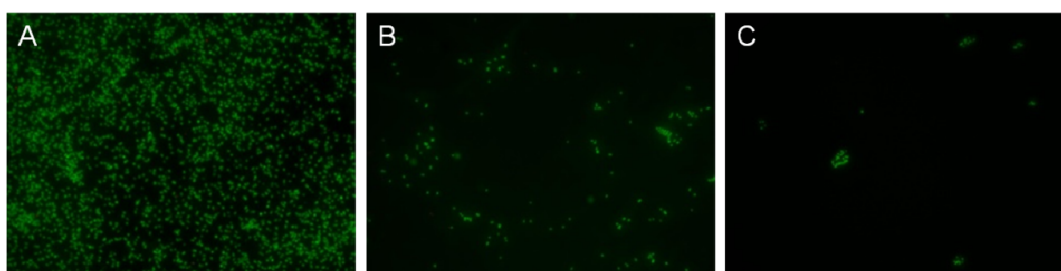


**Figure 2.** Fluorescence micrographs (40x) of Si (A); 100% grafting density 305 nm PHEMA brush (B) and 100% grafting density 195 nm POEGMA brush (C) after incubation with  $5 \times 10^6$  *S. epidermidis* for 3 hours at 37 °C

Although SYTO9/PI staining allows estimating bacterial adhesion it holds the limitations of microscopic methods, including visualization of only a part of investigated surface. Since in this study we were not interested in the viability of the bacteria attached to surfaces we continued the in depth study of bacterial adhesion using the CV staining, which is a cheaper, less time-consuming and more reliable estimation of the entire surface. CV has the property to quantitatively bind to negatively charged molecules, e.g. peptides and proteins of bacteria and extracellular matrix, and upon its detachment by using acetic acid, it gives an absorbance directly proportional to its amount that had been bound to the surface<sup>85-87</sup>. The basic principle of this method is schematically presented in Figure 3.

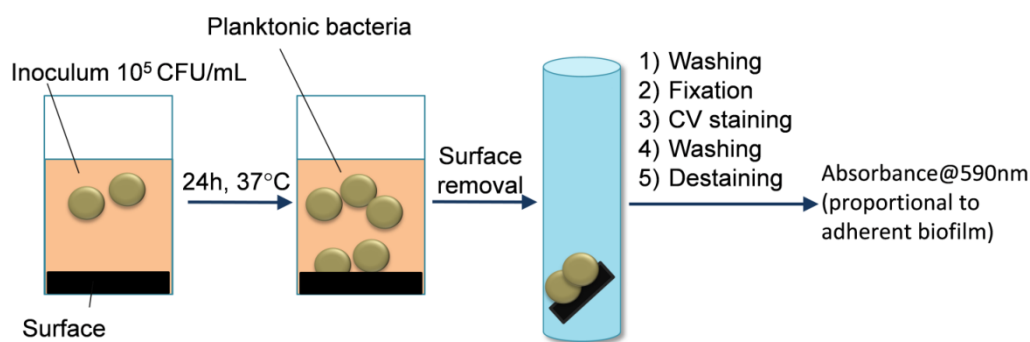


**Figure 3.** Schematic representation of the crystal violet (CV) staining test

Using CV binding assay the surfaces coated with PHEMA and POEGMA polymer brushes were compared with uncoated silicon wafers as negative control samples and silicon wafers on which PEG-brushes have been chemisorbed, as positive control. Studies were performed to evaluate the peptide/protein repellency for POEGMA<sup>40-50</sup> and PHEMA<sup>10,51,52</sup>-brush coatings establishing they are effective in inhibiting non-specific protein adsorption. As for other coatings it was assumed that the ability of coatings to inhibit protein non-specific adsorption is a prerequisite for the ability of the same surface to resist bacteria attachment<sup>56,69</sup>. However earlier work<sup>55,56</sup> suggested that effectiveness in inhibiting non-specific adsorption is a necessary, but not sufficient condition for ensuring good bacteria repellency.

Surfaces coated with POEGMA and PHEMA brushes are known as capable to prevent non-specific protein adsorption; therefore, there was interesting to check to which level they are able to inhibit the attachment of *S. epidermidis*. The brush covered surfaces are hydrophilic and exhibit strong steric exclusion preventing bacteria to approach and reach

surface. Furthermore, ordered hydration layer around the polymer brushes forms a real barrier stopping bacteria to approach and will exert strong repulsive forces.

The results in Figure 4 show significant reduction in CV signal of surfaces coated with PEG, POEGMA or PHEMA brushes as compared with the uncoated silicon wafers. POEGMA and PHEMA brushes at high grafting densities proved to be as good as PEG brushes. In this figure only the minimum and maximum values for grafting densities and thicknesses are shown for all surfaces.

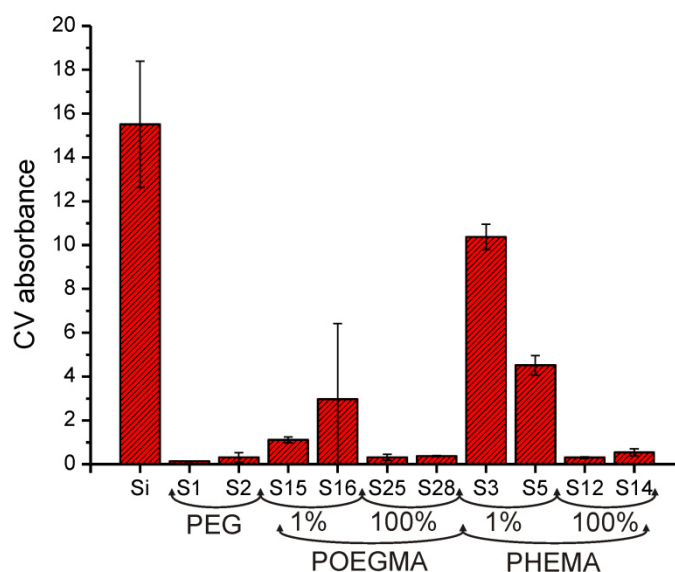


**Figure 4.** CV results for PEG brushes with Mn 5 kDa and 20 kDa; PHEMA and POEGMA brushes at minimum and maximum grafting density and polymerization times (sample description in Table 1), after incubation with  $1 \times 10^5$  *S. epidermidis* for 24 hours at 37 °C. The bars represent the average for three samples.

High value of the absorbance is a clear indication of the colonization of untreated silicon wafers with bacteria, although the signal originating from adherent bacteria or extracellular matrix cannot be discriminated. We concluded that one of the most important characteristics of surfaces coated with polymer brushes in determining their performance as protein and bacteria repellent is the grafting density. Studies mention that higher grafting densities determine higher resistance to non-specific bacterial attachment, but this is not always the case<sup>47,52,88,89</sup>. In some cases high grafting densities can reduce the ability of surface to be protein repellent due to the inability of macromolecular chains to hydrate. Therefore for high grafting densities two concurrent processes have to be

considered regarding their ability to interfere or even inhibit the bacterial adhesion: the repulsion of bacteria due to steric effects, reducing their possibility to penetrate the brush film and to reach the surface, and the increase in the dehydration of the chemisorbed brushes accompanied by an increase in the number of attached bacteria. In an article published in 2012, Santore and coworkers<sup>89</sup>, combining theory and experiment, offer a statistical interpretation of the inconsistency appearing in the literature reports regarding the correlation between the capacity of surfaces to be protein repellent and the ability of the same surfaces to inhibit bacteria attachment. They point out the reasons determining different behavior of brushy surfaces against protein and bacterial adhesion. In specific situations bacteria can adhere easier than proteins and factors as grafting density or film thickness can have different influence on bacterial adhesion.

Thus, as depicted in Figure 4, the lower CV signal observed for the high grafting density coated surfaces is, most likely, a consequence of bacteria inability to penetrate the polymer layer and reach the surface where they can attach. No significant differences could be observed in the bacteria repellent properties as a function of the increased grafting density and reaction time, as a measure of polymer chain length, all samples exhibiting very good capacity to prevent bacteria attachment. The only difference is met for 1% grafting density, for surfaces covered with PHEMA brushes which yield an overall higher CV signal. This is due, probably, to the insufficient surface coverage, allowing bacteria to find free, unprotected zones, to which they can approach and adhere. All the other samples have significantly increased bacteria resistance as compared with the silicon surface. Moreover, the antiadhesive properties of all studied POEGMA brushes and high grafting densities PHEMA are similar to the positive control PEG-brushes. This observation could be important for practical uses establishing the premises for the fabrication of surfaces resistant to bacterial attachment for various conditions of grafting densities and film thicknesses. It is important to notice that, although a few bacteria adhered at the modified surfaces, as indicated by low CV signal, important reduction of bacterial adhesion could be found for all polymer-brush coated compared to the unmodified surfaces. Therefore, such surface modification can result in decreasing the initial bacterial adhesion which could further delay biofilm formation which could further delay biofilm formation and thereby assist the antibiotic therapy and the host immune response in eradicating infection.

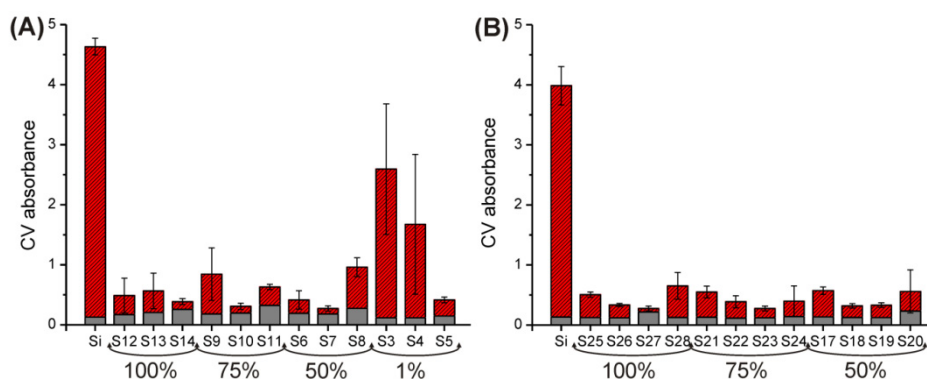


**Figure 5.** CV results for PHEMA (A) and POEGMA (B) with different grafting densities (sample description in Table 1). Grey bars surfaces incubated only in TSB medium and red bars surfaces after incubation with  $1 \times 10^5$  *S. epidermidis* for 24 hours at 37 °C. The bars represent the average for three experiments each performed in triplicates.

Figure 5 presents in more detail the adherence of bacteria to PHEMA (A) and POEGMA (B) brushes modified surface allowing in-depth analysis of effects of different grafting densities and film thickness. Since CV test monitors all adherent entities on a surface all samples were compared with the control without bacteria. In these graphs each group of samples refers to a specific value for grafting density with increase in each group, from left to right, of the polymerization time in other words polymeric chain length or thickness. Even for the lowest grafting density (1%) the CV signal is reduced as compared to the uncoated Si surface. For the 1% PHEMA brushes it is clear that the increase in polymerization time i.e. chain length, reduces the adherence of bacteria, the sample with the highest thickness being comparable in the bacteria repellent effect to all the samples with higher grafting densities. The relatively high bacterial adherence found for low grafting densities PHEMA is, most likely, due to the poor surface coverage, the brushes leaving free and unprotected spaces, which allow bacteria penetrating the protective brush layer. This effect is not observed for 1% grafting density POEGMA brushes (Figure 4) indicating that POEGMA fully covers the surface faster than PHEMA due to the longer side chains. These results underline the possibility to obtain stable, robust and versatile bacteria repellent polymer brushes, largely not influenced by the grafting density and the film thickness.

## 2.4. Conclusions

A library of PHEMA and POEGMA brushes covering a wide range of grafting densities and thicknesses has been prepared using SI-ATRP and tested for bacteria repellent properties. Adhesion of *S. epidermidis* was significantly reduced by the presence of the brush on silicon wafers. The bacteria repellent efficiency of surfaces exhibited little dependence on the nature and properties of the polymer brushes, both POEGMA and PHEMA proving antiadhesive properties similar to PEG, for a wide range of grafting densities and film thicknesses. The exception is the case of surfaces with the very low grafting densities obtained for short polymerization times where insufficient surface coverage reduced the ability of the coating to prevent bacterial adhesion. Both types of polymer brushes are suitable for tailoring surfaces able to delay or prevent bacteria attachment, altering the biological response of the pristine surface. What is more important is that both PHEMA and POEGMA brushes can be a promising alternative for designing bacteria-resistant surfaces with potential application in the production of biomaterials for preventing hospital and mainly implant related infection occurrence. The slow growth of staphylococci, on polymer brush-coatings, may allow more time for treatment with antibiotics before a mature, resistant biofilm can develop.

## 2.5. References

- (1) Harding, J. L.; Reynolds, M. M. *Trends in Biotechnology* **2014**, *32*, 140
- (2) Glinel, K.; Jonas, A. M.; Jouenne, T.; Leprince, J.; Galas, L.; Huck, W. T. S. *BioconjugateChem.* **2009**, *20*, 71
- (3) Hadjesfandiari, N.; Yu, K.; Meiac, Y.; Kizhakkedathu, J. N. *J. Mater. Chem. B* **2014**, *2*, 4968
- (4) Gao, G.; Yu, K.; Kindrachuk, J.; Brooks, D. E.; Hancock, R. E. W.; Kizhakkedathu, J. N. *Biomacromolecules* **2011**, *12*, 3715
- (5) Gao, G.; Lange, D.; Hilpert, K.; Kindrachuk, J.; Zou, Y.; Cheng, J. T. J.; Kazemzadeh-Narbat, M.; Yu, K.; Wang, R.; Straus, S. K.; Brooks, D. E.; Chew, B. H.; Hancock, R. E. W.; Kizhakkedathu, J. N. *Biomaterials* **2011**, *32*, 3899
- (6) Chen, S.; Li, L.; Zhao, C.; Zheng, J. *Polymer* **2010**, *51*, 5283
- (7) Hori, K.; Matsumoto, S. *Biochemical Engineering Journal* **2010**, *48*, 424
- (8) Galanakos, S. P.; Papadakis, S. A.; Kateros, K.; Papakostas, I.; Macheras, G. *Orthopaedics and Trauma* **2009**, *23*, 175
- (9) Wilkins, M.; Hall-Stoodley, L.; Allan, R. N.; Faust, S. N. *Journal of Infection* **2014**, *69*, S47
- (10) Pranantyo, D.; Xu, L. Q.; Neoh, K.-G.; Kang, E.-T.; Yang, W.; Teo, S. L.-M. *J. Mater. Chem. B* **2014**, *2*, 398
- (11) Wan, F.; Pei, X.; Yu, B.; Ye, Q.; Zhou, F.; Xue, Q. *Appl. Mater. Interfaces* **2012**, *4*, 4557
- (12) Yang, W. J.; Neoh, K.-G.; Kang, E.-T.; Teo, S. L.-M.; Rittschof, D. *Progress in Polymer Science* **2014**, *39*, 1017
- (13) Ganesh, C. K.; Anand, S. K. *Int J Food Microbiol* **1998**, *42*, 9
- (14) Yoo, J. A.; Chen, X. D. *Int J Food Microbiol* **2002**, *73*, 11
- (15) Götz, F. *MolMicrobiol* **2002**, *43*, 1367
- (16) Di Ciccio, P.; Vergara, A.; Festino, A. R.; Paludi, D.; Zanardi, E.; Ghidini, S.; Ianieri, A. *Food Control* **2015**, *50*, 930
- (17) Zhang, M.; Yang, F.; Pasupuleti, S.; Oh, J. K.; Kohli, N.; Lee, I-S.; Perez, K.; Verkhoturov, S. V.; Schweikert, E. A.; Jayaraman, A.; Cisneros-Zevallos, L.; Akbulut, M. *Int. J. Food Microbiol.* **2014**, *185*, 73
- (18) Huq, A.; Whitehouse, C. A.; Grim, C. J.; Alam, M.; Colwell, R. R. *Current Opinion in Biotechnology* **2008**, *19*, 244
- (19) Nemati, M.; Jenneman, G. E.; Voordouw, G.. *BiotechnolBioeng* **2001**, *74*, 424



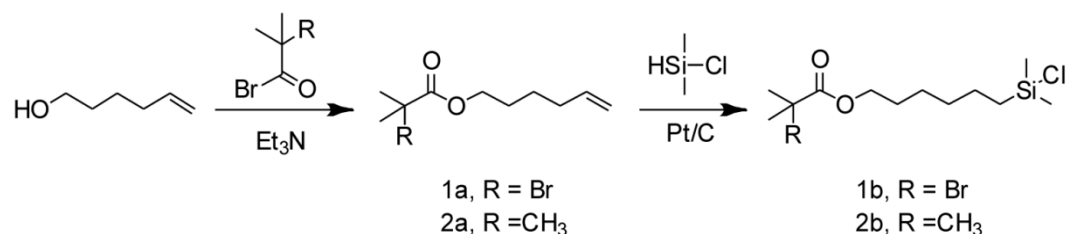
- (20) Garrett, T. R.; Bhakoo, M.; Zhang, Z. *Progress in Natural Science* **2008**, *18*, 1049
- (21) Yue, C.; Yang, B. *J. Bionic Eng.* **2014**, *11*, 589
- (22) Sharma, G.; Rao, S.; Bansal, A.; Dang, S.; Gupta, S.; Gabrani, R. *Biologicals* **2014**, *42*, 1
- (23) Lynch, A. S.; Robertson, G. T. *Annu. Rev. Med.* **2008**, *59*, 415
- (24) Charnley, M.; Textor, M.; Acikgoz, C. *React. Funct. Polym.* **2011**, *71*, 329
- (25) Barbey, R.; Lavanant, L.; Paripovic, D.; Schuwer, N.; Sugnaux, C.; Tugulu, S.; Klok, H.-A. *Chem. Rev.* **2009**, *109*, 5437
- (26) Salwiczek, M.; Qu, Y.; Gardiner, J.; Strugnell, R. A.; Lithgow, T.; McLean, K. M.; Thissen, H. *Trends in Biotechnology* **2014**, *32*, 82
- (27) Raynor, J. E.; Capadona, J. R.; Collard, D. M.; Petrie, T. A.; Garcia, A. J. *Biointerphases* **2009**, *4*, FA3
- (28) Siedenbiedel, F.; Tiller, J. C. *Polymers* **2012**, *4*, 46
- (29) Magin, C. M.; Cooper, S. P.; Brennan, A. B. *Mater. Today* **2010**, *13*, 36
- (30) Xua, F. J.; Neoh, K. G.; Kang, E. T. *Prog. Polym. Sci.* **2009**, *34*, 719
- (31) Li, J.; Kao, W. J. *Biomacromolecules* **2003**, *4*, 1055
- (32) Zdyrko, B.; Klep, V.; Li, X.; Kang, Q.; Minko, S.; Wen, X.; Luzinov, I. *Mat. Sci. Eng. C* **2009**, *29*, 680
- (33) Li, W.; Zhou, J.; Gu, J.-S.; Yu, H.-Y. *J. Appl. Polym. Sci.* **2010**, *115*, 2302
- (34) Xiao, D.; Zhang, H.; Wirth, M. *Langmuir* **2002**, *18*, 9971
- (35) Jewrajka, S. K.; Mandal, B. M. *Macromolecules* **2003**, *36*, 311
- (36) Cringus-Fundeanu, I.; Luijten, J.; van der Mei, H. C.; Busscher, H. J.; Schouten, A. J. *Langmuir* **2007**, *23*, 5120
- (37) Li, X.; Wang, M.; Wang, L.; Shi, X.; Xu, Y.; Song, B.; Chen, H., *Langmuir* **2013**, *29*, 1122
- (38) Feng, W.; Gao, X.; McClung, G.; Zhu, S.; Ishihara, K.; Brash, J. L. *Acta Biomater.* **2011**, *7*, 3692
- (39) Smith, R. S.; Zhang, Z.; Bouchard, M.; Li, J.; Lapp, H. S.; Brotske, G. R.; Lucchino, D. L.; Weaver, D.; Roth, L. A.; Coury, A.; Biggerstaff, J.; Sukavaneshvar, S.; Langer, R.; Loose, C. *Sci. Transl. Med.* **2012**, *4*, 153ra132
- (40) Xu, F. J.; Zhong, S. P.; Yung, L. Y. L.; Kang, E. T.; Neoh, K. G. *Biomacromolecules* **2004**, *5*, 2392

- (41) Gao, X.; Feng, W.; Zhu, S.; Sheardown, H.; Brash, J. L. *Langmuir* **2008**, *24*, 8303
- (42) Xu, F. J.; Li, Y. L.; Kang, E. T.; Neoh, K, G. *Biomacromolecules* **2005**, *6*, 1759
- (43) Stadler, V.; Kirmse, R.; Beyer, M.; Breitling, F.; Ludwig, T.; Bischoff, F. R. *Langmuir* **2008**, *24*, 8151
- (44) Ignatova, M.; Voccia, S.; Gilbert, B.; Markova, N.; Cossement, D.; Gouttebaron, R.; Jerome, R.; Jerome, C. *Langmuir* **2006**, *22*, 255
- (45) Ma, H.; Hyun, J.; Stiller, P.; Chilkoti, A. *Adv Mater* **2004**, *16*, 338
- (46) Ma, H.; Wells, M.; Beebe, T. P.; Chilkoti, A. *Adv Funct Mater* **2006**, *16*, 640
- (47) Singh, N.; Cui, X.; Boland, T.; Husson, S. M. *Biomaterials* **2007**, *28*, 763
- (48) Ma, H.; Li, D.; Sheng, X.; Zhao, P.; Chilkoti, A. *Langmuir* **2006**, *22*, 3751
- (49) Tugulu, S.; Klok, H. A. *Biomacromolecules* **2008**, *9*, 906
- (50) Fan, X.; Lin, L.; Messersmith, P. B. *Biomacromolecules* **2006**, *7*, 2443
- (51) Yoshikawa, C.p; Goto, A.; Tsujii, Y.; Ishizuka, N.; Nakanishi, K.; Fukuda, T. *J PolymSci A: PolymChem* **2007**, *45*, 4795
- (52) Mei, Y.; Wu, T.; Xu, C.; Langenbach, K. J.; Elliott, J. T.; Vogt, B. D.; Beers, K. L.; Amis, E. J.; Washburn, N. R. *Langmuir* **2005**, *21*, 12309
- (53) Rodriguez-Emmenegger, C.; Brynda, E.; Riedel, T.; Houska, M.; Subr, V.; Alles, A. B.; Hasan, E.; Gautrot, J. E.; Huck, W. T. S. *Macromol. Rapid Commun.* **2011**, *32*, 952
- (54) Epstein, A. K.; Wong, T.-S.; Belisle, R. A.; Boggs, E. M.; Aizenberg, J. *Proc. Natl. Acad. Sci. U.S.A.* **2012**, *109*, 13182
- (55) Wei, J.; Ravn, D. B.; Gram, L.; Kingshott, P. *Colloids Surf B* **2003**, *32*, 275
- (56) Ostuni, E.; Chapman, R. G.; Liang, M. N.; Meluleni, G.; Pier, G.; Ingber, D. E.; Whitesides, G. M. *Langmuir* **2001**, *17*, 6336
- (57) Roosjen, A.; Kaper, H. J.; Van der Mei, H. C.; Norde, W.; Busscher, H. J. *Microbiology* **2003**, *149*, 3239
- (58) Roosjen, A.; Busscher, H. J.; Norde, W.; Van der Mei, H. C. *Microbiology* **2006**, *152*, 2673
- (59) Roosjen, A.; De Vries, J.; Van Der Mei, H. C.; Norde, W.; Busscher, H. J. *J. Biomed. Mat. Res. - Part B Applied Biomaterials* **2005**, *73*, 347
- (60) Roosjen, A.; Van der Mei, H. C.; Busscher, H. J.; Norde, W. *Langmuir* **2004**, *20*, 10949

- (61) Harris, L. G.; Tosatti, S.; Wieland, M.; Textor, M.; Richards, R. G. *Biomaterials* **2004**, *25*, 4135
- (62) Maddikeri, R. R.; Tosatti, S.; Schuler, M.; Chessari, S.; Textor, M.; Richards, R. G.; Harris, L. G. *J. Biomed. Mater. Res. Part A* **2008**, *2*, 425
- (63) Harris, L. G.; Richards, R. G. *J. Mater. Sci. Mater. M* **2004**, *15*, 311.
- (64) Konradi, R.; Pidhatika, B.; Mühlebach, A.; Textor, M. *Langmuir* **2008**, *24*, 613
- (65) Pidhatika, B.; Möller, J.; Benetti, E. M.; Konradi, R.; Rakhmatullina, E.; Mühlebach, A.; Zimmermann, R.; Werner, C.; Vogel, V.; Textor, M. *Biomaterials* **2010**, *31*, 9462
- (66) Pidhatika, B.; Moller, J.; Vogel, V.; Konradi, R. *Chimia* **2008**, *62*, 264
- (67) Chang, Y.; Liao, S. C.; Higuchi, A.; Ruaan, R. C.; Chu, C. W.; Chen, W. Y. *Langmuir* **2008**, *24*, 5453
- (68) Chen, S. F.; Zheng, J.; Li, L. Y.; Jiang, S. Y. *J. Am. Chem. Soc.* **2005**, *127*, 14473
- (69) Cheng, G.; Zhang, Z.; Chen, S.; Bryers, J. D.; Jiang, S. *Biomaterials* **2007**, *28*, 4192
- (70) Privett, B. J.; Youn, J.; Hong, S. A.; Lee, J.; Han, J.; Shin, J. H.; Schoenfishc, M. H. *Langmuir* **2011**, *27*, 9597
- (71) Li, J. S.; Kleintschek, T.; Rieder, A.; Cheng, Y.; Baumbach, T.; Obst, U.; Schwartz, T.; Levkin, P. A. *ACS Appl. Mater. Interfaces* **2013**, *5*, 6704
- (72) Rodriguez-Emmenegger, C.; Decker, A.; Surman, F.; Preuss, C. M.; Sedláková, Z.; Zydziak, N.; Barner-Kowollik, C.; Schwartz, T.; Barner, L.; *RSC Adv.* **2014**, *4*, 64781
- (73) Chiag, Y.-C.; Chang, Y.; Chen, W.-Y.; Ruaan, R.-C. *Langmuir* **2012**, *28*, 1399
- (74) Goncalves, S.; Leirós, A.; van Kooten, T.; Dourado, F.; Rodrigues, L. R. *Colloids Surf B Biointerfaces* **2013**, *109*, 228
- (75) Zhang, F.; Shi, Z. L.; Chua, P. H.; Kang, E. T.; Neoh, K. G. *Ind. Eng. Chem. Res.* **2007**, *46*, 9077
- (76) Zhao, C.; Li, L.; Wang, Q.; Yu, Q.; Zheng, J. *Langmuir* **2011**, *27*, 4906
- (77) Nejadnik, M. R.; van der Mei, H. C.; Norde, W.; Busscher, H. J. *Biomaterials* **2008**, *29*, 4117
- (78) Swartjes, J. J. T. M.; Veeregowda, D. H.; van der Mei, H. C.; Busscher, H. J.; Sharma, P. K. *Adv. Funct. Mater.* **2014**, *24*, 4435
- (79) Sileika, T. S.; Kim, H.-D.; Maniak, P.; Messersmith, P. B. *ACS Appl. Mater. Interfaces* **2011**, *3*, 4602

- (80) Otto, M. *Nature Reviews Microbiology* **2009**, *7*, 555
- (81) Sousa, C.; Teixeira, P.; Oliveira, R. *Int. J. Biomat.* **2009**, Article ID 718017, 9 pages
- (82) Mack, D.; Davies, A. P.; Harris, L. G.; Jeeves, R.; Pascoe, B.; Knobloch, J. K.-M.; Rohde, H.; Wilkinson, T. S. *Biomaterials Associated Infection: Immunological Aspects and Antimicrobial Strategies*, Springer Science + Business Media New York **2013**
- (83) Tugulu, S.; Harms, M.; Fricke, M.; Volkmer, D.; Klok, H.-A. *Angew. Chem., Int. Ed.* **2006**, *45*, 7458–7461
- (84) <http://www.thelabrat.com/protocols/bacterialviability.shtml>
- (85) Stepanovic, S.; Cirkovic, I.; Ranin, L.; Svabic-Vlahovic, M. *Letters in Applied Microbiology* **2004**, *38*, 428
- (86) Adetunji, V. O.; Isola, T. O. *Global Veterinaria* **2011**, *6*, 06
- (87) Okajima, Y.; Kobayakawa, S.; Tsuji, A.; Tochikubo, T. *IOVS* **2006**, *47*, 2971
- (88) Andruzzi, L.; Senaratne, W.; Hexemer, A.; Sheets, E. D.; Ilic, B.; Kramer, E. J.; Baird, B.; Ober, C. K. *Langmuir* **2005**, *21*, 2495
- (89) Gon, S.; Kumar, K.-N.; Nüsslein, K.; Santore, M. M. *Macromolecules* **2012**, *45*, 8373

## 2.6. Supporting Information



**Scheme S1.** Synthesis of the SI-ATRP initiator (**1b**) and the ATRP inactive equivalent (**2b**)

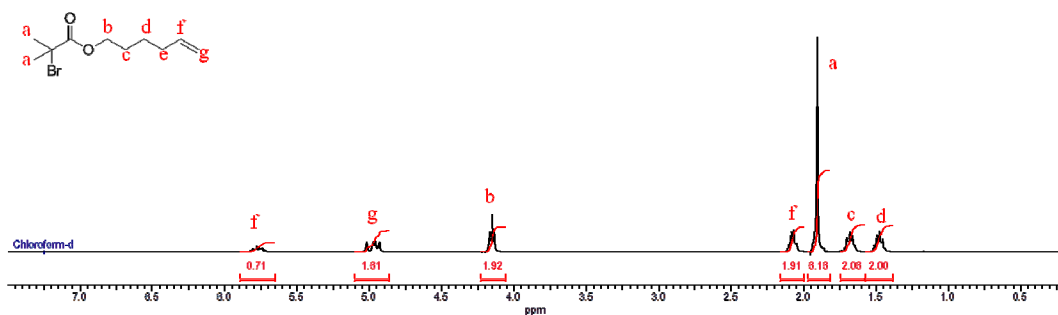


**Figure S1.**  $^1\text{H-NMR}$  of 5-hexen-1-yl 2-bromo-2-methylpropanoate (**1a**)

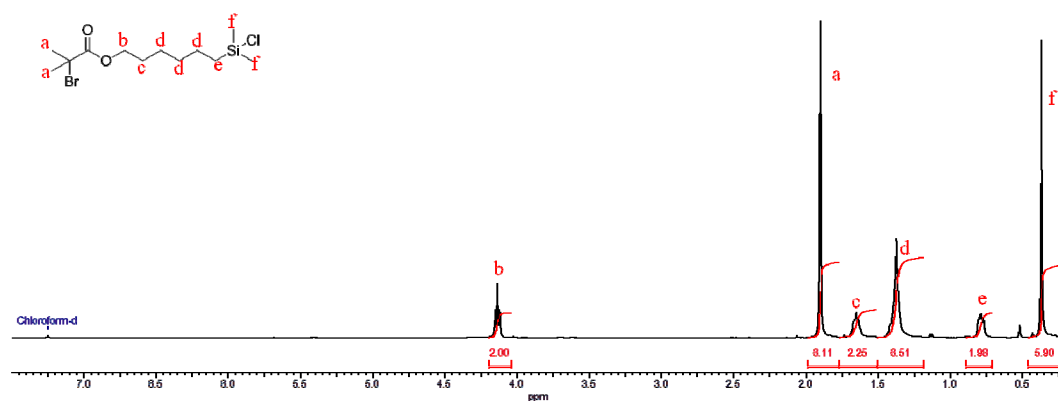


**Figure S2.**  $^1\text{H-NMR}$  of (6-(2-(2-Bromo-2-methylpropanoyloxy)hexyldimethylchlorosilane) (**1b**)

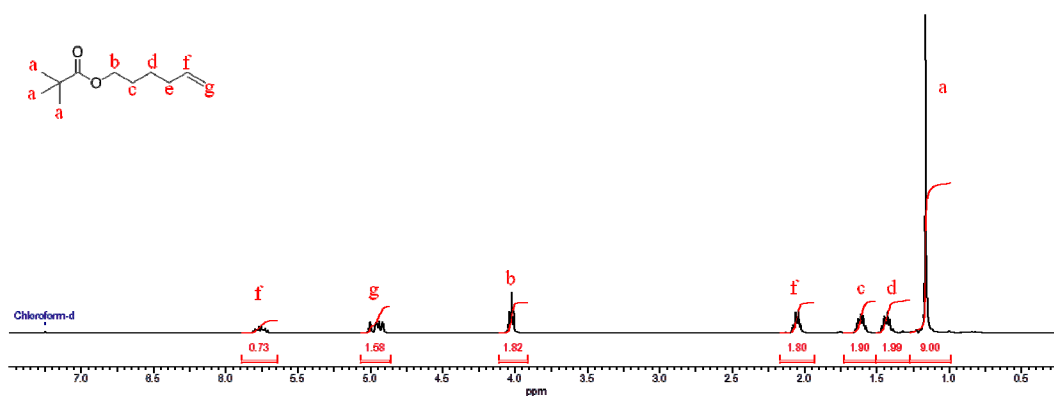


Figure S3. <sup>1</sup>H-NMR of Hexen-5-enyl pivalate (2a)

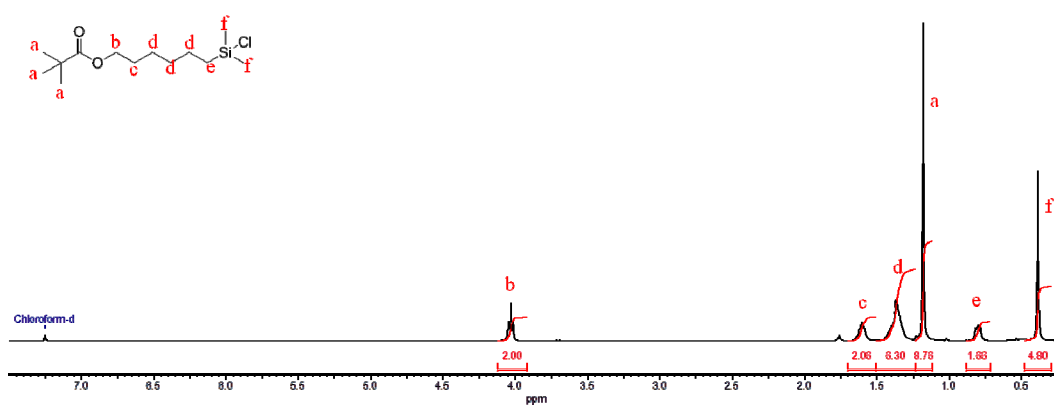
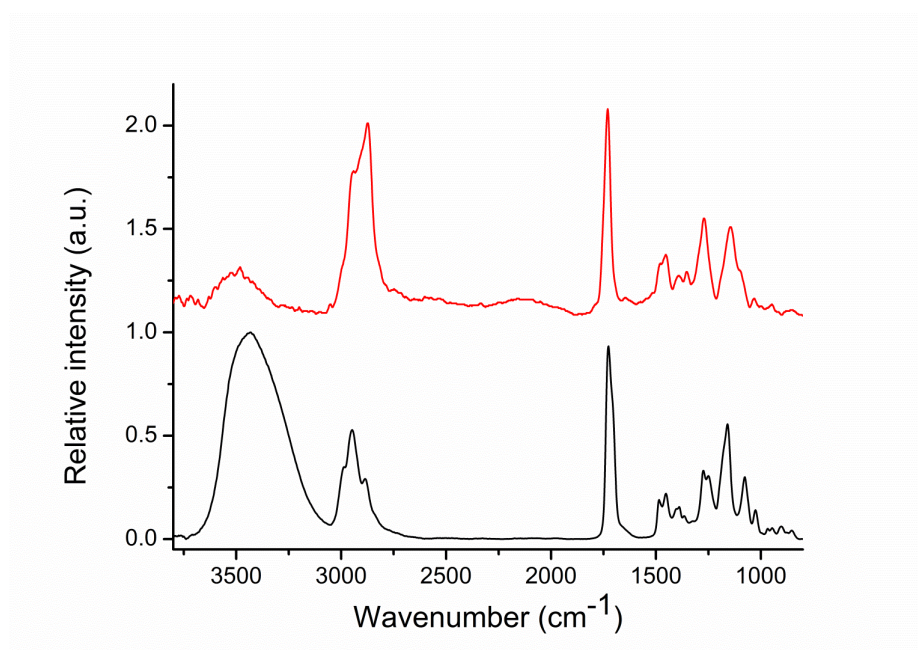
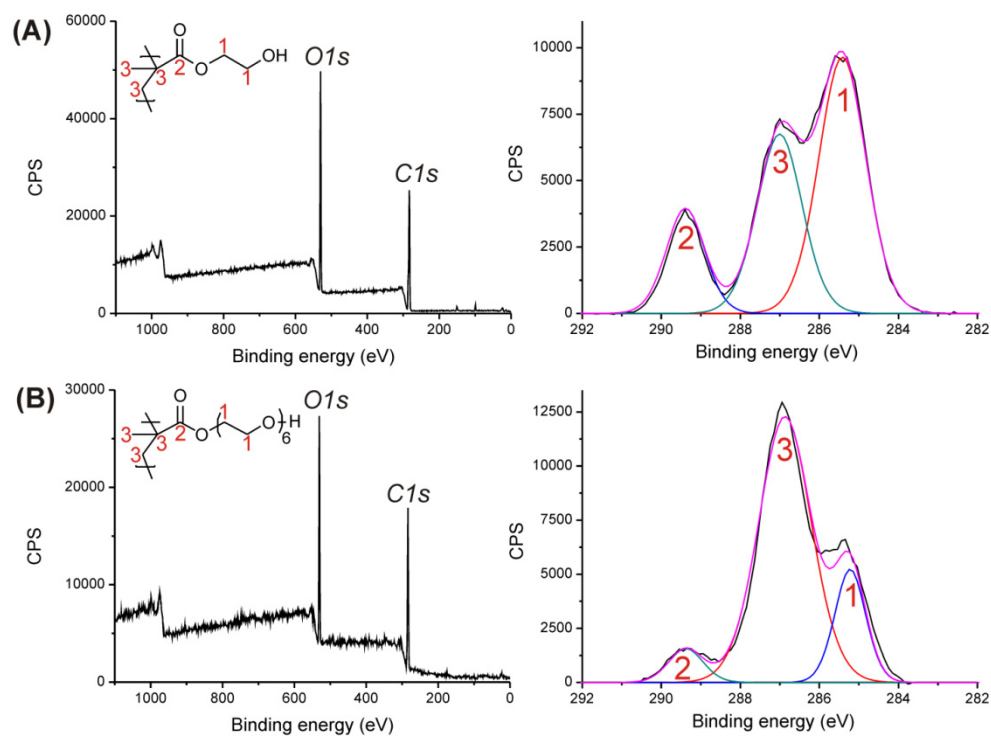


Figure S4. <sup>1</sup>H-NMR of 6-(chloro(dimethyl)silyl)hexyl pivalate (2b)



**Figure S5.** FTIR spectra of PHEMA (black line) and POEGMA (red line) brushes



**Figure S6.** XPS spectra: A – PHEMA survey (left) Hi-res  $C_{1s}$  (right); B – POEGMA survey (left) Hi-res  $C_{1s}$  (right)





### 3. Dual Biopassive-Bioactive Antibacterial Coatings Based on Vancomycin Functionalized Polymer Brushes

#### 3.1. Introduction

Implant-related infections may cause serious complications after surgery, imposing prolonged antibiotic treatments and often causing development of antibiotic resistant bacteria strains. In many cases, after a while, the only solution is to surgically remove the implant. The demand for specific materials to prevent and treat implant-related infection has dramatically increased in the last years and, as a result, many researchers focused their interest on developing antibacterial surfaces able to prevent bacteria adhesion on surfaces and to kill approaching bacteria<sup>1-4</sup>.

There are multiple strategies to prevent bacteria adhesion and to avoid biofilm formation on surfaces: (i) biopassive approaches intended to prevent bacteria attachment on surfaces and thus to inhibit the first stages of biofilm development and (ii) bioactive approaches based on non-leaching or leaching antimicrobial surfaces. The first approach is mainly based on hydrophilic polymers physisorbed or chemisorbed on implant surfaces. The second strategy is based on incorporating antimicrobial agents that are able to kill bacteria on contact when coupled to a surface (“contact killing surfaces”) or to release it thus killing the approaching bacteria (leaching or release surfaces)<sup>3-5</sup>. Both strategies have advantages and disadvantages. The main disadvantage of the biopassive (non-fouling) surfaces resides in their inability to ensure prolonged *in vivo* use. This behavior is due mainly to their sensitivity to deterioration in physiological media as well as to the difficulty to obtain uniform, defect-free coatings<sup>5</sup>. Also the oxidation process of these coatings can reduce their long-term *in vivo* efficiency as implant protective surfaces, process observed mainly for PEG brushes<sup>6</sup>. Moreover, during the first stages of biofilm formation a conditioning film forms, usually reducing the efficiency of biopassive coatings<sup>7</sup>. Bioactive coatings, although highly efficient for different bacterial strains, may release too fast the active component and therefore losing their bactericidal properties. Furthermore, dead bacteria debris can accumulate on the surface and hinder the active

centers<sup>1,5</sup>. In the case of leaching antibacterial surfaces, the quantity of the released bactericidal agent can become insufficient after a period<sup>7</sup>.

To obtain contact killing coatings, different methods have been used for attaching polymers to surfaces: layer-by-layer deposition<sup>8,9</sup> plasma polymerization<sup>10</sup> and chemical grafting techniques<sup>11,12</sup>. Two strategies, namely “grafting to” and “grafting from” methods were used to obtain antibacterial polymer brush-based surfaces and the scope and limitations of their use have been extensively analyzed<sup>1,4,5,12-19</sup>; “grafting from” method being usually preferred due to the ability to produce polymer brushes with accurate control over brush thickness, composition, and architecture<sup>13</sup>. Surface-initiated controlled radical polymerization reactions (SI-CRP) have been used to synthesize effective non-fouling or/and antibacterial surfaces, due to the extensive possibility of controlling and tailoring the molecular weight, molecular weight distribution and architecture of the synthesized compounds. A lot of well-documented reviews discuss the up-to-date achievements in this field, adopted strategies and mechanisms of action underlining the challenges and unanswered questions<sup>1,3-5,12,13-18</sup>. Non-leaching antibacterial surfaces can be obtained by covalently attaching a bactericidal agent on the substrate; common used bactericidal agents are based on quaternary ammonium compounds, antimicrobial peptides, bacteriophages, lysozyme, chitosan or antibiotics<sup>1,5</sup>. Bactericidal agents can be covalently or physically immobilized on surfaces and kill bacteria by disrupting and penetrating bacterial cell membrane or can action on specific biomolecules on the bacterial wall, hence causing the death of bacteria upon contact<sup>1</sup>.

Antimicrobial coatings based on quaternary ammonium compounds (QAC) have found applications in preventing nosocomial infections<sup>1,5,18,20-25</sup>. Although exhibiting remarkable properties as contact-killing bacteria surfaces, the coatings based on quaternary ammonium compounds have the disadvantage of reduced cyto- and bio-compatibility<sup>26,27</sup>. Another well-known non-leaching antibacterial approach is based on surface immobilized antimicrobial peptides (AMPs)<sup>1,3-5,11-13,17,18</sup>. AMPs are usually derived from natural sources, so they are biocompatible and non-toxic and characterized by a large spectrum of antibacterial activity<sup>17,18</sup>. Contact killing bacteria surfaces based on immobilized AMPs have been developed on different surfaces: stainless steel<sup>28</sup>, silicon wafers<sup>29</sup>, silicon substrates<sup>30-34</sup>, silica and paramagnetic silica microparticles<sup>35</sup>, silicon wafer coated with titanium and titanium implants<sup>36-38</sup>. Although antibacterial non-leaching coatings based on immobilized AMPs proved effective against a series of bacteria strains, they still represent a new and expensive category of products. AMPs applications in therapy are

still unclear, as clinical trials are ongoing. Side-effects as allergies, potential local toxicity, sensitivity to proteases and pH are not sufficiently clarified<sup>39-41</sup>. Moreover, they were not yet tested against the most relevant bacteria for biomaterial-associated infections, namely *S. epidermidis* and *S. aureus*. Non-leaching antibacterial coatings have been also obtained by covalent attachment of antibiotics to surfaces. This method is strongly dependent on the nature of the antibiotic, the type of the considered bacteria and the way the bactericidal agent is tethered on the surface. Generally, the number of antibiotics that can be used is limited to those not requiring internalization in order to be active, such as  $\beta$ -lactam antibiotics and vancomycin.  $\beta$ -L antibiotics are antimicrobial agents containing a  $\beta$ -lactam ring in their structure and work by inhibiting the biosynthesis of the bacterial cell wall. Vancomycin is a glycopeptide antibiotic effective against a broad spectrum of Gram-positive bacteria and its bacterial action relies on the interference in the cross-linking of the peptidoglycan layer of the bacterial cell wall<sup>42</sup>. For penicillin V and cephadrine conjugated with PEG-Lysine<sup>43</sup> and for penicillin<sup>44</sup> and ampicillin<sup>45</sup> attached to microwave plasma modified poly(tetrafluoroethylene) (subsequently hydrolyzed and esterified with PEG) generally, the modified surfaces were found to be less active than the corresponding non-bound antibiotic, in some cases non-leaching surfaces did not kill bacteria, but the corresponding releasing systems kept the antibacterial character<sup>43</sup>. Vancomycin has been linked in multiple ways to different surfaces and the antibacterial activity was always maintained<sup>46-50</sup> even though slightly reduced in some cases<sup>51,52</sup>. Even though such coatings proved antibacterial properties, the antibiotic efficiency can be reduced due to the steric effects, impeding their contact with bacterial cell membrane. Also, debris of the dead bacteria accumulated on surface can reduce antibiotic activity<sup>5</sup>.

Recently, a new strategy was proposed to overcome some of disadvantages presented above for different non-leaching antibacterial coatings. This approach refers to the immobilization of bactericidal agents on non-fouling surfaces, thus realizing dual “biopassive-bioactive” coatings. First attempts were reported by Huck’s group; they immobilized Magainin I on surfaces covered with a copolymer of 2-(2-methoxyethoxy)ethyl methacrylate and hydroxyl-terminated oligo(ethylene glycol) methacrylate, that was bacteria repellent by itself<sup>29</sup>. Unfortunately, no information are given if the AMP modified polymer brush retains its bacteria repellent properties. The attachment of vancomycin to anachelin chromophore through a PEG linker realized by Gademann and his coworkers<sup>46</sup> was reported to be effective against *Bacillus subtilis*, and

to suppress the attachment of dead cells and dead cell debris. These studies, however, have used only a small number of bacterial strains not representative for the most relevant microorganisms involved in biomaterial-related infections.

The work presented in this Chapter is focused on developing dual functional biopassive/bioactive coatings based on vancomycin immobilized on PHEMA and POEGMA brushes. PHEMA and POEGMA brushes with different grafting densities have been synthesized on silicon wafers using SI-ATRP and then vancomycin were coupled to the functionalized surfaces. Vancomycin has two reactive groups available for coupling to polymer brushes: a primary amine and carboxylic acid and both approaches have been tried in this study. ELISA tests and XPS were employed to evidence the coupling of vancomycin on surfaces. Vancomycin modified surfaces have been tested for antibacterial activity against *S. epidermidis*.

## 3.2. Experimental Section

### 3.2.1. Materials

All chemicals were purchased from Aldrich and used as received unless stated otherwise. Vancomycin antibody (ab19968), IgG-HRP antibody (ab6721) were purchased from Abcam and used as received. Tetrahydrofuran (THF), dichloromethane (DCM), Dimethylformamide (DMF) and toluene were purified and dried using a solvent purification system (PureSolv). Deionized water was obtained from a Millipore Direct-Q 5 Ultrapure Water System and ultrahigh quality Milli-Q water was obtained from a Millipore Milli-Q gradient machine fitted with a 0.22  $\mu\text{m}$  filter. The 25-well plates were purchased from Bibby Sterilin Ltd, Stone, Staffs, UK. Tryptic Soy Broth (TSB) and Mueller-Hinton agar (MHA) were purchased from Difco, BD and Co., France and used according to the manufacturer's instructions. All non sterile solutions used in the bacteria experiments were autoclaved at 121  $^{\circ}\text{C}$  for 20 minutes. Vancomycin, Syto9, propidium iodide (PI) and the bacteria strains (*Staphylococcus epidermidis* 1457 and *Bacillus subtilis* 6633) were kindly provided by Prof. Landmann, University of Basel. Silicon (100) covered with a native silicon oxide layer and quartz slides were used as substrates for surface-initiated polymerization. PHEMA and POEGMA<sub>6</sub> brushes with different grafting densities and thicknesses were prepared as described in Chapter 2.

### **3.2.2. Methods**

X-ray photoelectron spectroscopy (XPS) was carried out using an Axis Ultra instrument from Kratos Analytical equipped with a conventional hemispheric analyzer. The X-ray source employed was a monochromatic Al K $\alpha$  (1486.6 eV) source operating at 100 W and 10<sup>-9</sup> mbar. All XPS spectra were calibrated on the aliphatic carbon signal at 285.0 eV. Relative sensitivity factors (RSF) of 0.278 (C<sub>1s</sub>), 0.78 (O<sub>1s</sub>), 0.477 (N<sub>1s</sub>) were used to correct peak area ratios. Attenuated total reflectance Fourier transform infrared spectroscopy (ATR-FTIR) was performed on a nitrogen purged Nicolet 6700 FT-IR spectrometer equipped with a SmartiTR™ (Thermo Fisher Scientific Inc., Waltham, MA, USA) accessory and a diamond crystal. Atomic force microscopy (AFM) was performed in tapping mode on a Veeco Multimode Nanoscope IIIa SPM controller (Digital Instruments, Santa Barbara, CA) using NSC14/no Al MikroMasch (Tallinn, Estonia) cantilevers. To determine the layer thicknesses, cross-sectional height profiles of micropatterned polymer brushes on silicon substrates were analysed. UV-Visible absorbance spectra were recorded using a Varian Cary 100 Bio UV-Visible spectrophotometer at room temperature on polymer brush coated quartz substrates.

### **3.2.3. Procedures**

#### **3.2.3.1. p-Nitrophenyl chloroformate (NPC) activation of PHEMA and POEGMA<sub>6</sub> brushes**

The polymer brushes were activated by applying 20 mL of a freshly prepared solution of NPC (121 mg, 0.6 mmol) and triethylamine (167  $\mu$ L, 1.2 mmol) in anhydrous THF for 1 hour at room temperature under vigorous shaking. Excess NPC was removed from the surfaces in the following way: rinsing with anhydrous THF, washing twice with anhydrous THF for 5 minutes under vigorous shaking, rinsing with DMF, rinsing with anhydrous THF, and washing with anhydrous THF for 5 minutes. The slides were subsequently dried under a flow of nitrogen and stored in a nitrogen atmosphere until used for further functionalization.

#### **3.2.3.2. Vancomycin coupling via the amine group**

NPC-activated brushes were functionalized with vancomycin via the amine group by treatment with a solution containing 1 mM vancomycin, 2.5 mM 4-(dimethylamino)pyridine (DMAP) and 2.5 mM triethylamine (Et<sub>3</sub>N) in anhydrous DMF

for 16 hours at room temperature under gentle shaking in the dark. After that, the samples were washed with DMF, rinsed and washed three times for one hour with 70% ethanol solution and two times with water to remove residual physisorbed vancomycin and finally dried in a stream of nitrogen.

#### **3.2.3.3. Vancomycin coupling via the carboxylic acid group**

Over the NPC activated polymer brushes a 0.1 M 2,2'-(Ethylenedioxy)bis(ethylamine) solution with 0.2 M DMAP was added. After 12 hours the surfaces were washed with DMF and then incubated overnight in a 1 mM solution of vancomycin with 0.1 M 1-(3-Dimethylaminopropyl)-3-ethylcarbodiimide hydrochloride and 0.1 M *N*-hydroxysuccinimide (prepared 12 hours before). After 16 hours the samples were washed with DMF, rinsed and washed three times for one hour with 70% ethanol solution and two times with water to remove residual physisorbed vancomycin and finally dried in a stream of nitrogen.

#### **3.2.3.4. ELISA testing**

The surfaces were placed in a 24 well plate and incubated at 4 °C for 24 hours with 10 mg/mL BSA in PBS solution for blocking. Then the samples were washed and incubated (0.5 mL, 30 minutes at room temperature) with rabbit anti-vancomycin (2.5 µg/mL) in blocking solution (10 mg/mL, BSA/PBS) followed by washing five times with 0.05% Tween20 in PBS and five times with PBS to remove traces of Tween20. Then the samples were incubated (0.5 mL, 30 minutes, RT) with goat anti-rabbit (1 µg/mL) in blocking solution. After 30 minutes the samples were washed five times with 0.05% Tween20 and five times with PBS to remove Tween20. Then the samples were rinsed once more with PBS and moved to new wells where 300 µL of 3,3',5,5'-tetramethylbenzidine (TMB) was added. After 30 minutes 300 µL of 1M sulphuric acid was added to stop the reaction. 200 µL from each well were transferred in a 96 well plate and the absorbance at 450 nm was read using a plate reader.

#### **3.2.3.5. Bacteria culture preparation**

Stocks of *S. epidermidis* 1457 were prepared using a cryovial bead preservation system (Microbank; Pro-Lab Diagnostics, Richmond Hill, Ontario, Canada) and stored at -75 °C. For the preparation of overnight culture a bead was incubated in 1 mL of TSB for 5 hours at 37 °C, diluted 1:100 in fresh TSB, and incubated overnight at 37 °C. The overnight culture was diluted to the desired colony-forming units (CFU) based on optical

density and then used for the bacterial adhesion tests. All cultures were prepared without shaking and CFU were determined by plating aliquots of 10-fold dilutions of bacterial cultures on Mueller-Hinton agar (MHA), followed by 24 hours of incubation at 37 °C.

#### **3.2.3.6. LIVE/DEAD staining**

LIVE/DEAD BacLight Bacterial Viability Kit was used to visualize the surface-attached bacteria. Dye solution (protected from light) was prepared with 1.5 µL propidium iodide (PI) and 1.5 µL SYTO9 in 1 mL Milli-Q water. All surfaces were placed in 25-well plates, 2 mL of TSB with the desired CFU were added and then incubated for a predefined time at 37 °C. After the predefined time of incubation the surfaces were removed, washed two times with 2 mL 0.9% NaCl and then dipped in 0.9% NaCl. The samples were transferred on microscope slide and 14 µL dye solution per each surface was added. A cover slip was placed over the surfaces before microscopic examination (x40; Provis AX70, Olympus AG, Volketswil, Switzerland). At least three randomly selected pictures were acquired from the central part of each surface.

### **3.3. Results and Discussion**

#### **3.3.1. Synthesis of vancomycin modified polymer brushes**

To prepare dual functional biopassive/bioactive coatings, PHEMA and POEGMA brushes were used as platform since their ability to prevent bacteria adhesion was demonstrated in Chapter 2. Vancomycin was selected as bioactive agent as it is effective against most gram-positive staphylococci responsible for a great number of implant-associated infections. There are also studies which demonstrate that vancomycin is active when coupled to a surface<sup>46-52</sup>. Vancomycin is a glycopeptide antibiotic and its bactericidal action relies on the interference in the biosynthesis of the peptidoglycan layer of the bacterial cell wall. The antibiotic binds to L-Lys-D-Ala-D-Ala termini of the nascent peptidoglycan disturbing the cross-linking between glycan chains and affecting osmotic stability of the bacterial membrane<sup>42,47</sup>. PHEMA and POEGMA brushes with different grafting densities have been synthesized as described in the previous Chapter. Vancomycin has two functional groups available for coupling reactions (Figure 1). For the glycosidic primary amine, Lawson et al.<sup>51,52</sup> reported a decreased but still present

activity when vancomycin is modified in this position. Gademann<sup>46</sup> and Antoci<sup>47-50</sup> coupled vancomycin as a monolayer via the carboxylic acid group and showed that the antibiotic is still active.

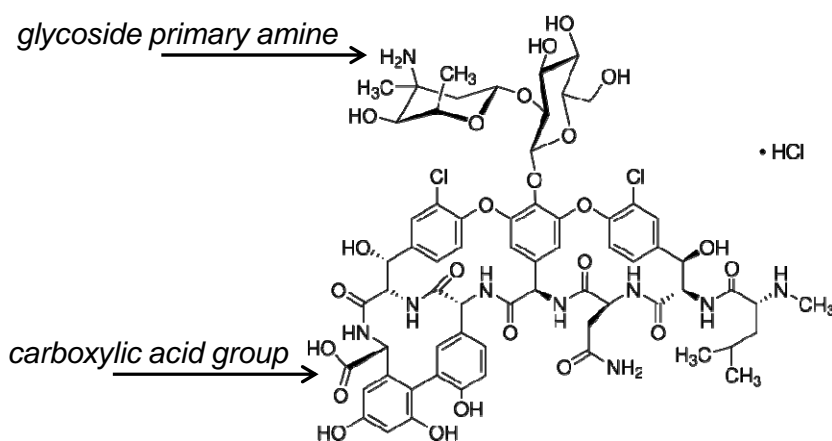
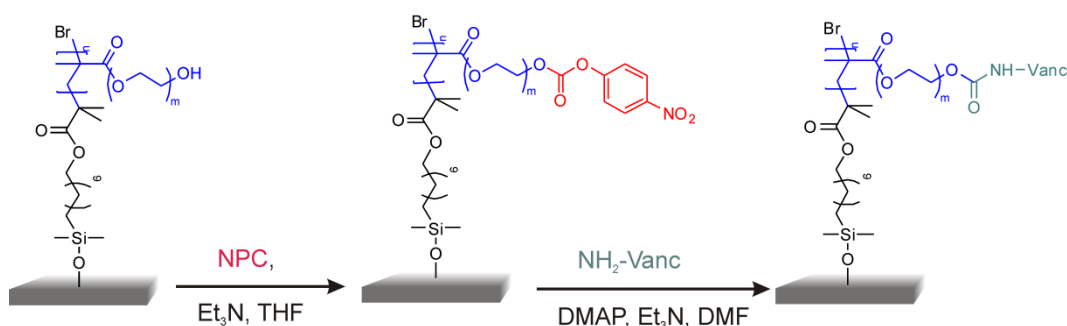


**Figure 1.** Structure of vancomycin

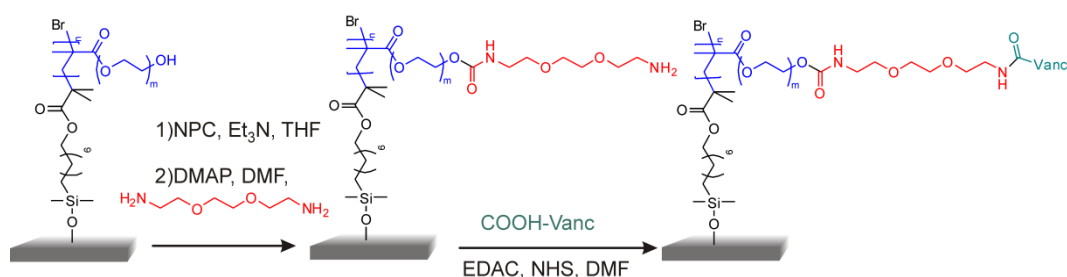
The method used to couple vancomycin via its primary amine group to PHEMA or POEGMA brushes is briefly presented in Scheme 1. The first step involves polymer brush modification with *p*-nitrophenyl chloroformate (NPC) leading to the modification of the hydroxyl groups on the side chain to an active ester, which favors reactions with primary amines. Although vancomycin contains a carboxylic acid group, several hydroxyl groups and a secondary amine group all of which can potentially react with NPC activated brushes, coupling will predominantly occur via the primary amine due to its higher nucleophilicity and the influence of any side reaction is expected not to be significant<sup>51,53,54</sup>.



**Scheme 1.** Synthetic route for coupling vancomycin via its primary amine group to PHEMA or POEGMA brushes



In Scheme 2 the strategy for coupling the vancomycin via its carboxylic acid group to polymer brushes is schematically represented. Initially, the brushes were activated with NPC and then reacted with a large excess of 2,2'-(ethylenedioxy)bis(ethylamine) (DADO) to obtain polymer brushes with amine terminated side chains. Vancomycin was coupled to the amine terminated polymer brushes using EDAC/NHS chemistry<sup>55,56</sup>. The strategy of modifying the hydroxyl side-chains of PHEMA and POEGMA into amine and then coupling vancomycin using EDAC/NHS chemistry was employed since direct coupling of vancomycin via its carboxylic acid group to hydroxyl side-chains of polymer brushes yielded worst results.



**Scheme 2.** Synthetic route for coupling vancomycin via its carboxylic acid group to PHEMA or POEGMA brushes

For some experiments, as a control surface, vancomycin was directly coupled to silicon wafers using the strategy presented in Scheme S1 (Supporting Information). For this, the silicon wafers were modified with (3-aminopropyl)triethoxysilane (APTES) and, subsequently vancomycin was coupled using EDAC/NHS chemistry.

### 3.3.2. Characterization of vancomycin modified polymer brushes

The vancomycin modified surfaces were characterized using UV-Vis and ATR-FTIR spectroscopy, XPS analysis as well as ELISA tests. Due the fact that vancomycin has specific absorbance at 270 nm, polymer brushes modified with vancomycin were synthesized on quartz wafers and characterized using UV-Vis spectroscopy. Figure 2 shows UV-Vis spectra of an unmodified PHEMA brush as well as two vancomycin modified brushes with different film thicknesses. It is easy to notice the appearance of the vancomycin characteristic peak, and its intensity increased with increasing brush thickness. However, for the other samples, most likely due to the lower amounts of vancomycin per unit of area, the characteristic absorbance for vancomycin is under the detection limits, so this method could not be used for all samples.

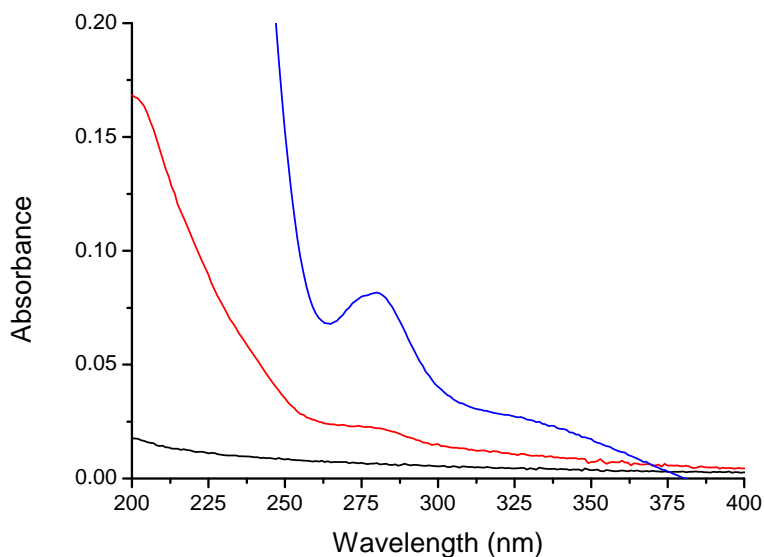


**Figure 2.** UV-Vis absorbance of a PHEMA brush with a thickness of 100 nm (black line) and two vancomycin modified PHEMA brushes with thickness of 100 nm (red line) and 300 nm (blue line).

The coupling of vancomycin to polymer brushes was also evidenced by FTIR spectroscopy. Figure 3A shows the characteristic FTIR spectrum for PHEMA brushes. By NPC activation (Figure 3B) a large decrease in the hydroxyl band ( $3100 - 3600 \text{ cm}^{-1}$ ), appearance of the aromatic  $\text{CH}_2$  band (approx.  $3100 \text{ cm}^{-1}$ ) and the new carbonyl at  $1800 \text{ cm}^{-1}$  can be observed. Also, the appearance of an amide peak most likely due to the DMF still present in the sample can be observed at  $1650 \text{ cm}^{-1}$ . It is worth mentioning that NPC modified brushes could not be properly washed before analysis due to high reactivity of the NPC ester group. The presence of DMF in the NPC modified brushes was considered to have no influence on the next reactions steps. Analysis of Figure 3C evidences that, as expected, by coupling vancomycin to polymer brushes the hydroxyl peak increases, the NPC carbonyl signal completely disappears and a new amide band appears at  $1650 \text{ cm}^{-1}$ . Regardless of the brush used (PHEMA or POEGMA) and the way in which vancomycin was coupled no significant difference was noticed in the FTIR spectra, the only change being the intensity of the amide peak.

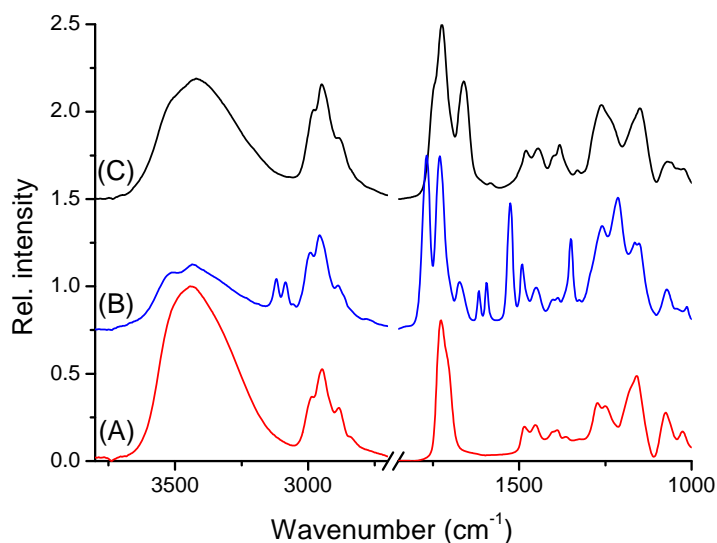


**Figure 3.** FTIR spectra of (A) PHEMA, (B) NPC modified PHEMA and (C) vancomycin modified PHEMA

XPS characterization was performed to confirm, once again, the presence of vancomycin coupled to polymer brushes. As expected, in all samples the nitrogen signal could be noticed suggesting the vancomycin coupling was successful. Table 1 reports the chemical composition as resulted from XPS for PHEMA and POEGMA brushes with 100% grafting density and 200 nm thickness modified with vancomycin via its primary amine and carboxylic acid group. From the nitrogen to carbon ratios the conversion of the hydroxyl to vancomycin in the top ten nm was estimated at 30.21% for PHEMA and 22.63% for POEGMA, when vancomycin was coupled via its primary amine group. For the samples with vancomycin coupled via its carboxylic acid group, assuming 100% conversion of hydroxyl to amine groups in the side chain, the conversions were estimated to be 22.31 % and 13.51 % for PHEMA and POEGMA, respectively. Due to the high number of different C atoms, the  $C_{1s}$  peak could not be deconvoluted.

**Table 1.** Sample composition as resulted from XPS for PHEMA and POEGMA brushes modified with vancomycin

Polymer brush	Vancomycin group used for coupling	Sample composition			Conversion (%)
		C%	O%	N%	
PHEMA	Primary amine	64.89	32.30	2.82	30.21
PHEMA	Carboxylic acid	65.39	32.25	2.37	22.31
POEGMA	Primary amine	64.27	33.89	1.84	22.63
POEGMA	Carboxylic acid	64.14	34.61	1.25	13.51

The coupling of vancomycin on PHEMA and POEGMA brushes was also confirmed by antibody labeling. ELISA (*enzyme-linked immunosorbent assay*) is a biochemical technique employing specific antibodies and color change to detect the presence of a substance<sup>57,58</sup>. The ELISA test is schematically represented in Figure S2 (Supporting Information) and is based on the interaction of vancomycin with a commercially available vancomycin antibody. The antibody binds to the vancomycin present on the surfaces, then a secondary HRP containing antibody is added. After washing the surfaces to remove traces of unbound antibodies TMB is added. TMB is a chromogen that yields a blue color when oxidized by HRP i.e. leads to an absorbance proportional with the vancomycin content on the surface. All samples used in the antibacterial experiments were tested with ELISA and the results are presented in Figure 4. The sample code description and the characteristics of the polymer brushes can be found in Table 2. From the graph higher absorbance can be easily noticed for all samples containing vancomycin (S3, S6, S8, S13-S16) as compared to their counterparts without the antibiotic. No significant difference among vancomycin modified samples can be observed, but generally slightly higher values appear when vancomycin was coupled via its primary amine group (S8, S13, S14). For different grafting densities no significant surface concentrations in vancomycin were evidenced. This effect may be due to the fact that ELISA measures only vancomycin on the upper layer of the surface, not inside the brush.

**Table 2.** Samples used for ELISA and antibacterial tests

Sample name	Surface Modification	Post polymerization modification	Active Initiator (%)	Thickness (nm)	Vancomycin coupling
S1	-	-	-	ND	-
S2	APTES	-	-	ND	-
S3	APTES	-	-	ND	-COOH
S4	PHEMA	-	50	117	-
S5	PHEMA	DADO	50	ND	-
S6	PHEMA	-	50	ND	-COOH
S7	PHEMA	-	100	305	-
S8	PHEMA	-	100	ND	-NH <sub>2</sub>
S9	POEGMA	-	50	102	-
S10	POEGMA	-	100	195	-
S11	POEGMA	DADO	50	ND	-
S12	POEGMA	DADO	100	ND	-
S13	POEGMA	-	50	ND	-NH <sub>2</sub>
S14	POEGMA	-	100	ND	-NH <sub>2</sub>
S15	POEGMA	-	50	ND	-COOH
S16	POEGMA	-	100	ND	-COOH

ND=not determined

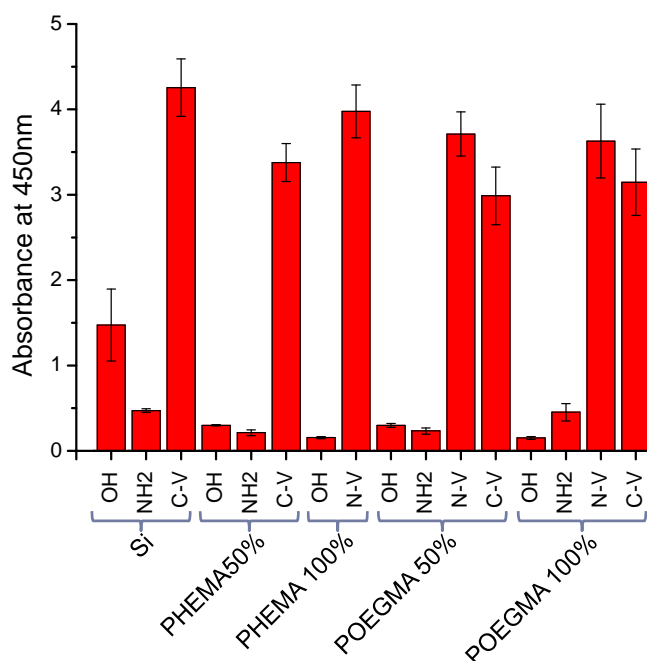


**Figure 4.** ELISA tests results for all samples used in the antibacterial experiments; where N-V represents vancomycin coupled via amine; C-V vancomycin coupled via carboxylic acid; OH hydroxyl terminated surface or side-chain in the case of polymer brushes and NH<sub>2</sub> the intermediary amine modified surface or polymer brushes

### 3.3.3. Antibacterial testing of vancomycin modified polymer brushes

In the last two decades, various strategies to create coatings that reduce the risk of biomaterial-associated infections have been developed. The problem of implant-related infections is complicated due to the large number of bacterial strains involved and the large variety of biomaterials employed in the fabrication of medical devices. Different biopassive, as well as bioactive coatings have been reported as effective against specific bacterial strains, but also have limitations. A new approach relies on combining non-fouling surface properties with the effective killing of bacteria, therefore, creating dual-functional antimicrobial platforms. As mentioned above, the aim and novelty of this study was to develop combined biopassive/bioactive surfaces, where an antimicrobial compound (bioactive) – vancomycin was attached on biopassive PHEMA and POEGMA brushes. All brush surfaces were exposed to *B. subtilis* and *S. epidermidis* to assess their biological activity. The live/dead kit<sup>59</sup> was used to assess and differentiate live and dead bacteria on surface by fluorescence. The two stains included in the kit, SYTO9 and propidium iodide (PI) are evidencing both the bacterial cells with intact membrane (live) and those with damaged cytoplasmic membranes (dead). Living bacteria are stained fluorescent green by SYTO9, while the dead ones are stained fluorescent red by PI. Initially, as reported in Gademann's study<sup>4</sup>, all surfaces were tested against *Bacillus subtilis*, which is known to be sensitive to vancomycin. The surfaces were incubated for 24 hours in a 540 CFU/mL *Bacillus subtilis* 6633 inoculum at 37 °C, rinsed with 0.9% NaCl solution, and stained with SYTO9/PI. The fluorescence micrographs are presented in Figure S2 (Supporting Information). Surprisingly, no specific activity could be evidenced; almost no bacteria adhered on any of the surfaces, not on bare silicon wafers, suggesting that perhaps *B. subtilis* 6633 is not the most appropriate bacterial strain to study bacteria adhesion on the considered surfaces. Considering the high incidence of *Staphylococcus epidermidis* in the implant related infections we tested the biological activity of all surfaces against this bacterial strain and assessed both the bacteria repellent and the bactericidal effect of the synthesized platforms. As vancomycin was coupled to polymer brushes both via its glycoside primary amine group and via its carboxylic acid group, hence it was also possible to evaluate and compare the biological activity of vancomycin in both cases.

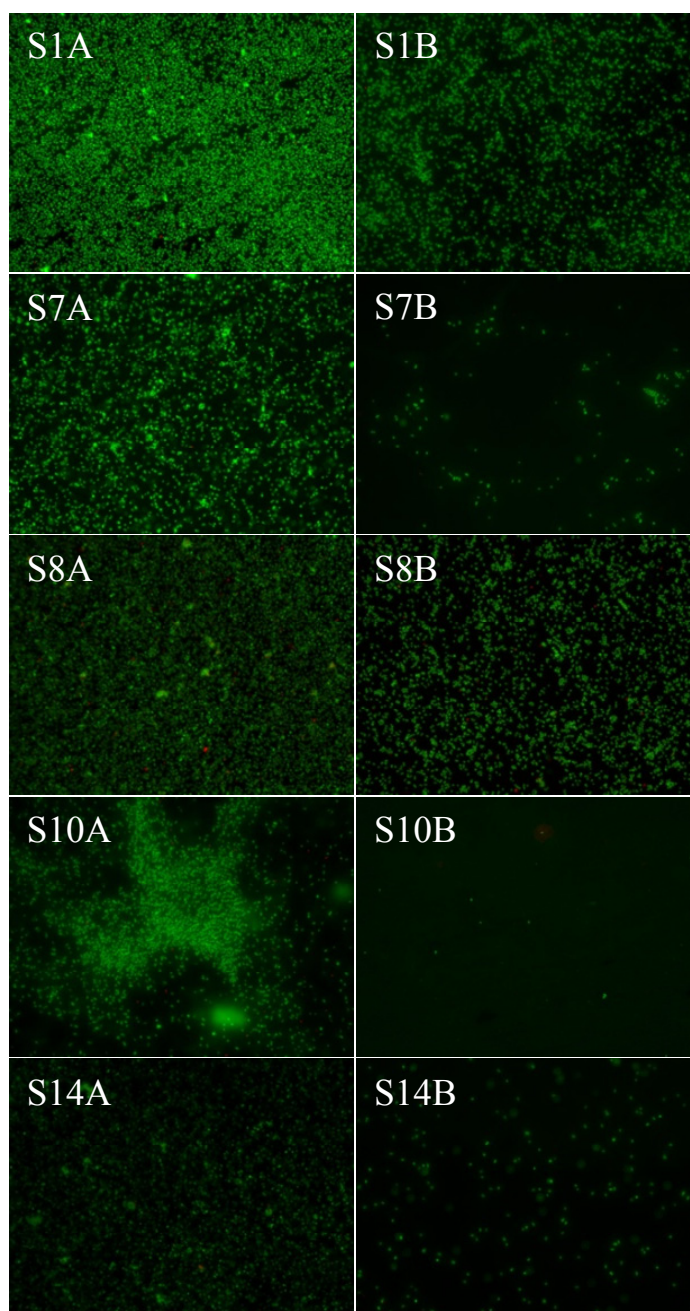


**Figure 5.** Fluorescence micrographs (40x) of Si and polymer brushes, with and without vancomycin coupled via its primary amine group; A – without washing; B – with washing; after 3 hours of incubation in  $5.32 \times 10^6$  SE at 37 °C; samples code description in Table 2

Initially, the systems with vancomycin coupled via its glycoside primary amine group were studied. All samples were incubated in a  $5.32 \times 10^6$  CFU/ml bacterial solution for 3

hours at 37 °C. After removing the bacterial supernatant, the samples were washed with a 0.9% NaCl solution to remove non-adherent bacteria. The fluorescence micrographs were recorded for all samples before and after washing (Figure 5). The purpose was to investigate if dead bacteria can be removed by rinsing or if they remain on the surface. As noticed from the images in Figure 5, contrary to *B. subtilis*, *S. epidermidis* colonized, preferentially, the uncoated negative control silicon sample (Figure 5: S1A, S1B). As demonstrated in the previous chapter, both PHEMA and POEGMA brush coated surfaces exhibit bacteria repellent activity, no significant difference being observed between the two types of brushes. The micrographs from the right side column emphasize that the brushes suppressed the attachment of bacteria on surfaces; after rinsing the initial adherent bacteria were removed. When the vancomycin functionalized surfaces are analyzed it is interesting to notice that PHEMA brushes (Figure 5: S8B) lose the bacteria repellent properties, while POEGMA brushes (Figure 5: S14B) still keep the antifouling character. This is due, probably, to the increased length of the PEG chain, which attenuates the effect of the large vancomycin molecule on the conformation of the polymer brushes. Unfortunately, no dead bacteria could be observed (even for the unwashed samples) for all vancomycin modified surfaces. This means that vancomycin loses its activity when coupled to polymer brushes via its primary amine group. It can also be a problem arising from steric effects among brushes and vancomycin molecule. Overall, this experiment demonstrated that fewer bacteria adhered on all polymer brush coated surfaces as compared to the uncoated silicon wafers. The vancomycin modified surfaces lost a part of their bacteria repellent properties, phenomenon more obvious for PHEMA brush based coatings. The absence of dead bacteria on both washed and unwashed samples suggests the loss of antibacterial activity of the vancomycin functionalized brushes.

The antimicrobial activity of surfaces with vancomycin coupled to polymer brushes via its carboxylic acid group was also analyzed. There are studies proving that vancomycin covalently bonded to titanium (presumably a monolayer) via the C-terminal carboxylic acid remains bactericidal<sup>46-50</sup>. Consequently, we coupled vancomycin to the brushes using this functional group. Moreover, for these experiments, as a control surface, vancomycin was directly coupled to silicon wafers using the strategy presented in Scheme S1 (Supporting Information).



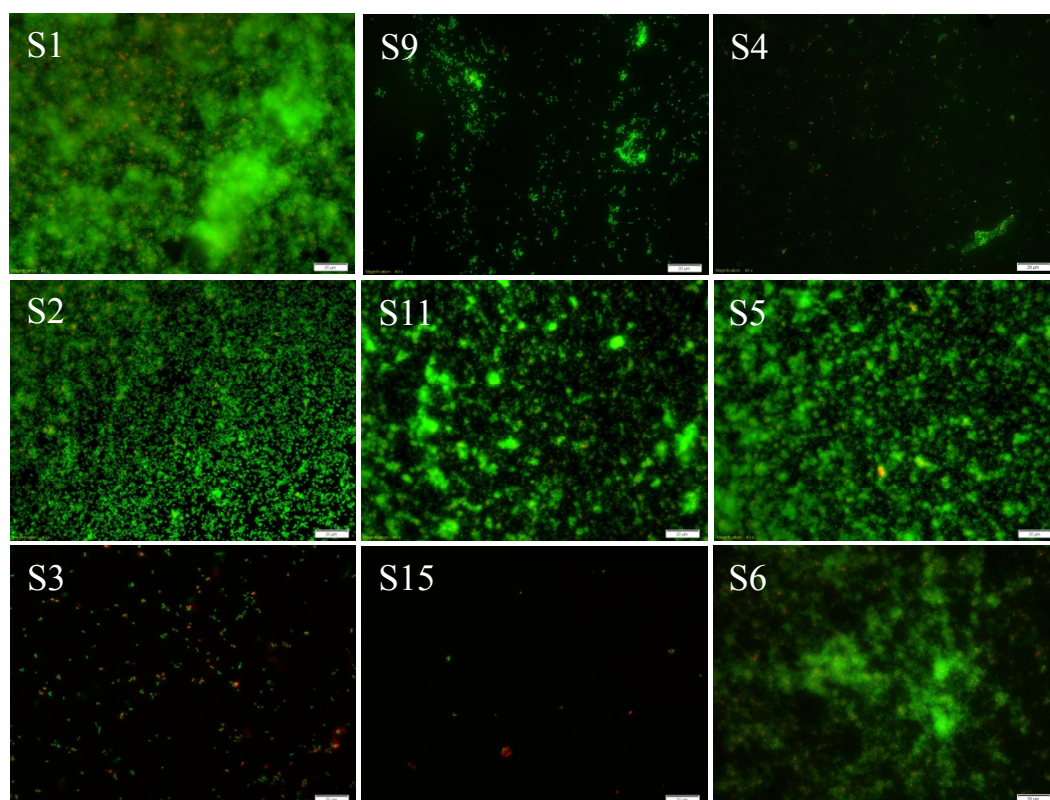


**Figure 6.** Fluorescence micrographs (40x) of control samples and polymer brushes with and without vancomycin coupled via its carboxylic acid group, after 24 hours of incubation in 970 CFU/ml SE at 37 °C (washed samples); samples code description in Table 2

Silicon wafers and, brush covered surfaces with and without vancomycin were incubated for 24 hours in a *S. epidermidis* inoculum of 970 CFU/ml at physiological temperature and rinsed with 0.9 % NaCl solution. After staining with SYTO9/PI, the samples were analyzed using fluorescence microscopy and the results are presented in Figure 6. It is obvious from the predominantly green staining in Figure 6 for sample S1 that a lot of bacteria adhered to uncoated Si surface. Both POEGMA (Figure 6: S9) and PHEMA (Figure 6: S4) brush coatings are bacteria repellent as compared with bare silicon wafers (Figure 6: S1), the results in this experiment being consistent with all previous observations. It was also interesting to investigate if the amine functionalized surfaces (the intermediary step in coupling vancomycin via the carboxyl group) could interfere with antibacterial properties of the analyzed surfaces and the results are presented in the second row of Figure 6. It is obvious that all three  $-NH_2$  modified surfaces were covered by a substantial layer of adherent bacteria, evenly distributed on

the surface. The bacteria strongly adhered and could not be removed by rinsing. It is interesting that both for POEGMA and PHEMA brushes the surfaces lost almost entirely the non-fouling properties. As easily can be noticed in Figure 6 for POEGMA (S11) and PHEMA (S5) a thick layer of adherent bacteria was formed on surfaces and the microorganisms stayed attached also after washing. Finally, the antibacterial activity of vancomycin modified surfaces was assessed and presented in the last row in Figure 6. Analyzing the image for sample S3 it is easy to notice that covalently bound vancomycin keeps its activity also when directly linked on silicon wafers. The surface is covered with live and dead bacteria but the layer is considerably diminished as compared with control Si samples (Figure 6: S1 and S2). Similar with POEGMA brushes with vancomycin coupled via its primary amine group, POEGMA brushes with vancomycin coupled via carboxylic acid group keeps its bacteria repellent properties. Moreover, looking at the second column in Figure 6 it is easy to notice that the surface switches from non-fouling POEGMA (S9) to fouling when amine functionalized (S11) and back to non-fouling after coupling vancomycin (S15), suggesting the activity of the covalently bound antibiotic. Furthermore, comparing vancomycin coupling via its primary amine group with vancomycin coupled via its carboxylic acid group on POEGMA-brushes several dead bacteria could be noticed suggesting that the coupling via the carboxylic acid group is more effective and the surface may be bactericidal. The situation is completely different for vancomycin modified PHEMA brushes (Figure 6: S6). PHEMA brushes lost their bacteria repellent properties, the intense green staining of the surface standing for a significant number of adherent bacteria colonizing the surface. Almost no red dots are visible, meaning there are few dead bacteria on the surface, and the activity of the coupled antibiotic is significantly reduced. Again, this can be attributed to the shorter PEG side-chain of PHEMA compared to POEGMA that may restrict the accessibility of the antibiotic.

Although POEGMA brushes modified with vancomycin coupled via its carboxylic acid group seemed to exhibit simultaneous bioactive – biopassive properties it was not possible to evaluate the bactericidal efficiency due to the low number of bacteria cells observed on the surfaces. To clarify this aspect we tested again POEGMA brushes with and without vancomycin coupled both via its primary amine group and carboxylic acid group, removing the rinsing step after the incubation with bacteria. Furthermore, we tested samples with two grafting densities (50 % and 100 %) to assess if there is any influence on the bactericidal activity of vancomycin modified POEGMA brushes. The

results are presented in Figure 7 and it can be easily observed that only sample S15 presents more dead bacteria as compared with the other analyzed surfaces. This observation is consistent with the previous experiments that showed that vancomycin was active only when coupled to POEGMA brushes via its carboxylic acid group. However the results are not as significant as expected, considering the low number of bacteria killed by vancomycin. This may be due to the polymer brush which is preventing the interaction of the antibiotic with bacteria cell wall.

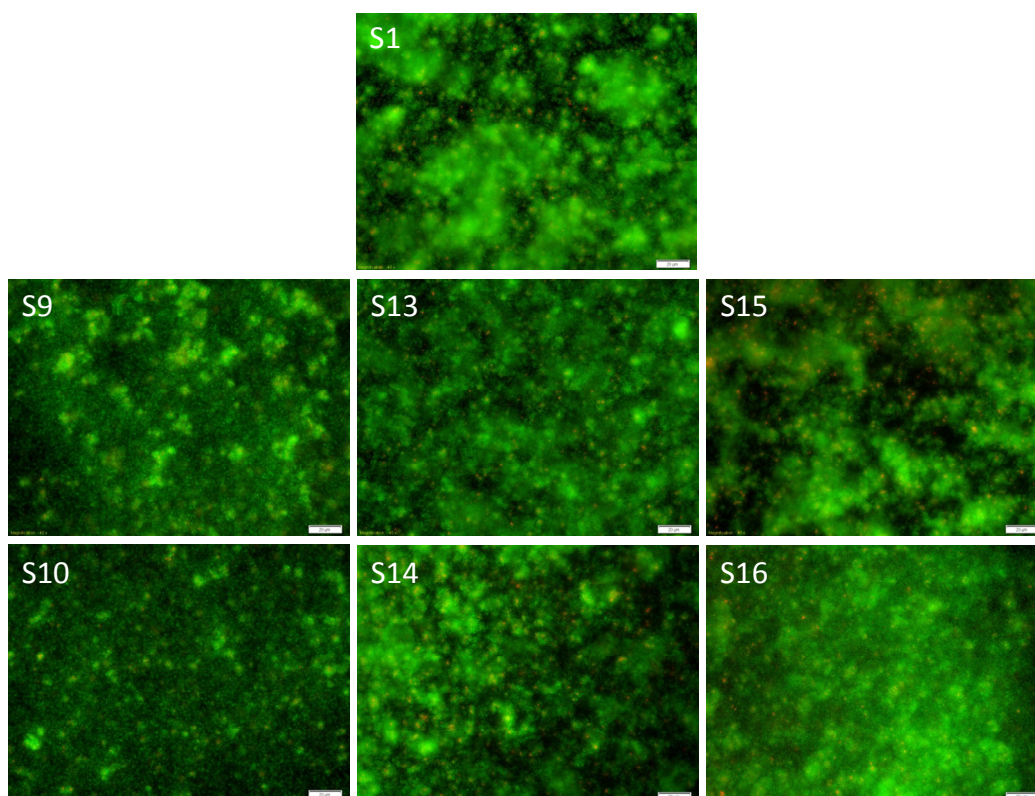


**Figure 7.** Fluorescence micrographs (40x) of control samples and POEGMA brushes, with two grafting densities, with and without vancomycin coupled via its primary amine or its carboxylic acid group, after 24 hours of incubation in 945 CFU/ml SE at 37 °C (unwashed samples); samples code description in Table 2

For higher grafting densities (Figure 7: S14 and S16), the antibacterial activity is reduced probably due to steric hindrance among brushes and vancomycin molecules. Moreover, steric effects may reduce brushes mobility and thus the possibility of the antibiotic molecules to reach bacterial membrane and to impede the cross-linking process between the glycan chains.

### 3.4. Conclusions

Bacteria repellent POEGMA and PHEMA brushes with different grafting densities have been synthesized using SI-ATRP. Vancomycin was successfully coupled on the polymer brushes both via glycoside primary amine group and C-terminal carboxylic acid using NPC and EDAC/NHS chemistry, respectively. The coupling was confirmed using UV-Vis, FTIR and XPS. The presence of vancomycin on the functionalized surfaces was also evidenced by antibody labeling using ELISA test. To the best of our knowledge this is the first attempt to create dual-functional biopassive-bioactive surfaces by coupling vancomycin on silicon using POEGMA or PHEMA brush platforms. Bactericidal activity of the obtained surfaces was evaluated using live/dead cells assays based on SYTO9/PI staining.

While HEMA polymer brushes lost their non-fouling proprieties after coupling of vancomycin both via its primary amine and carboxylic acid groups, vancomycin modified POEGMA brushes retained the bacteria repellent property. When vancomycin was coupled via the primary amine group no signs of bactericidal activity could be noticed regardless of the employed substrate. Coupling vancomycin to POEGMA brush surface via the C-terminal carboxylic acid of the antibiotic produced dual-functional bacteria repellent – bactericidal surfaces although the bactericidal effect was smaller than expected. Vancomycin modified POEGMA brushes with lower grafting densities had higher efficiency against *S. epidermidis* bacterial strain.

The different behavior of the two types of brushes when modified with vancomycin can be attributed to the enhanced ethylene glycol spacer length and enhanced water solubility of the POEGMA brushes, leading to increased ligand mobility and increased ability of the antibiotic molecules to reach and interfere with bacterial membrane. These vancomycin-modified brushes combine the bacteria repellent character of POEGMA with the possibility to selectively immobilize antibiotics, which makes them attractive candidates for the development of dual-functional biopassive/bioactive platforms, with interesting biomedical applications for combating implant-related infections.

### 3.5. References

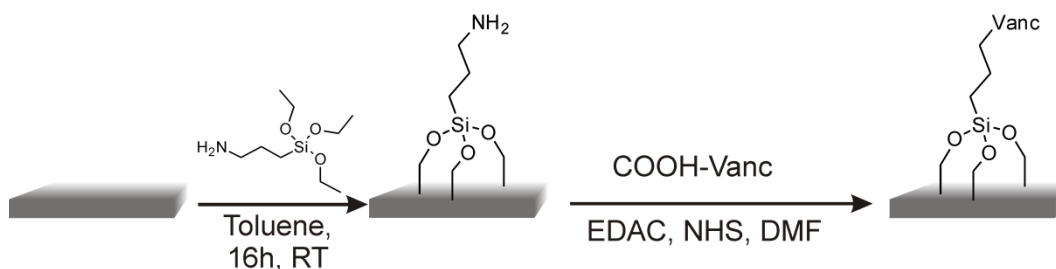
- (1) Hadjesfandiari, N.; Yu, K.; Meiac, Y.; Kizhakkedathu, J. N. *J. Mater. Chem. B* **2014**, *2*, 4968
- (2) Mack, D.; Davies, A. P.; Harris, L. G.; Jeeves, R.; Pascoe, B.; Knobloch, J. K.-M.; Rohde, H.; Wilkinson, T. S. *Biomaterials Associated Infection: Immunological Aspects and Antimicrobial Strategies*, Springer Science + Business Media New York **2013**
- (3) Salwiczek, M.; Qu, Y.; Gardiner, J.; Strugnell, R. A.; Lithgow, T.; McLean, K. M.; Thissen, H. *Trends in Biotechnology* **2014**, *32*, 82
- (4) Siedenbiedel, F.; Tiller, J. C. *Polymers* **2012**, *4*, 46
- (5) Charnley, M.; Textor, M.; Acikgoz, C. *React. Func. Polym.* **2011**, *71*, 329
- (6) Cheng, G.; Zhang, Z.; Chen, S.; Bryers, J. D.; Jiang, S. *Biomaterials* **2007**, *28*, 4192
- (7) Hetrick, E. M.; Schoenfisch, M. H. *Chem. Soc. Rev.* **2006**, *35*, 780
- (8) Hammond, P. T. *AIChE J.* **2011**, *57*, 2928
- (9) Lyklema, J.; Deschenes, L. *Adv. Colloid Interface Sci.* **2011**, *168*, 135
- (10) Friedrich, J. *Plasma Processes Polym.* **2011**, *8*, 783
- (11) Advincula, R. *Adv. Polym. Sci.* **2006**, *197*, 107
- (12) Edmondson, S.; Osborne, V. L.; Huck, W. T. S. *Chem. Soc. Rev.* **2004**, *33*, 14
- (13) Barbey, R.; Lavanant, L.; Paripovic, D.; Schuwer, N.; Sugnaux, C.; Tugulu, S.; and Klok, H.-A. *Chem. Rev.* **2009**, *109*, 5437
- (14) Xua, F. J.; Neoh, K. G.; Kang, E. T. *Prog. Polym. Sci.* **2009**, *34*, 719
- (15) Moroni, L.; Gunnewiek, M. K.; Benetti, E. M. *Acta Biomaterialia* **2014**, *10*, 2367
- (16) Meyers, S. R.; Grinstaff, M. W. *Chem. Rev.* **2012**, *112*, 1615
- (17) Harding, J. L.; Reynolds, M. M. *Trends in Biotechnology* **2014**, *32*, 140
- (18) Timofeeva, L.; Kleshcheva, N. *Appl. Microbiol. Biotechnol.* **2011**, *89*, 475
- (19) Zdyrko, B.; Klep, V.; Li, X.; Kang, Q.; Minko, S.; Wen, X.; Luzinov, I. *Mat. Sci. Eng. C* **2009**, *29*, 680
- (20) Murata, H.; Koepsel, R. R.; Matyjaszewski, K.; Russell, A. J., *Biomaterials* **2007**, *28*, 4870
- (21) Waschinski, C. J.; Zimmermann, J.; Salz, U.; Hutzler, R.; Sadowski, G.; Tiller, J. *C. Adv. Mater.* **2008**, *20*, 104
- (22) Lee, S. B.; Koepsel, R. R.; Morley, S. W.; Matyjaszewski, K.; Sun, Y. J.; Russell, A. J. *Biomacromolecules* **2004**, *5*, 877
- (23) Lin, J.; Qiu, S. Y.; Lewis, K.; Klivanov, A. M., *Biotechnol. Prog.* **2002**, *18*, 1082

- (24) Haldar, J.; An, D. Q.; de Cienfuegos, L. A.; Chen, J. Z.; Klibanov, A. M. *Proc. Natl. Acad. Sci. USA* **2006**, *103*, 17667
- (25) Milovic, N. M.; Wang, J.; Lewis, K.; Klibanov, A. M., *Biotechnol. Bioeng.* **2005**, *90*, 715
- (26) Knetsch, M. L. W.; Koole, L. H. *Polymers* **2011**, *3*, 340
- (27) Hegstad, K.; Langsrud, S.; Lunestad, B. T.; Scheie, A. A.; Sunce, M.; Yazdankhah, S. P. *Microb. Drug Resist.* **2010**, *16*, 91
- (28) Waterhouse, A.; Wise, S. G.; Yin, Y.; Wu, B.; James, B.; Zreiqat, H.; McKenzie, D. R.; Bao, S.; Weiss, A. S.; Ng, M. K. C.; Bilek, M. M. M. *Biomaterials* **2012**, *33*, 7984
- (29) Glinel, K.; Jonas, A. M.; Jouenne, T.; Leprince, J.; Galas, L.; Huck, W. T. S. *Bioconjugate Chem.* **2009**, *20*, 71
- (30) Mohorčič, M.; Jerman, I.; Zorko, M.; Butinar, L.; Orel, B.; Jerala, R.; Friedrich, J. *J Mater Sci: Mater Med* **2010**, *21*, 2775
- (31) Li, Y.; Santos, C. M.; Kumar, A.; Zhao, M.; Lopez, A. I.; Qin, G.; McDermott, A. M.; Cai, C. *Chem. - Eur. J.* **2011**, *17*, 2656
- (32) Basu, A.; Mishra, B.; Leong, S. S. J. *J. Mater. Chem. B* **2013**, *1*, 4746
- (33) Li, X.; Li, P.; Saravanan, R.; Basu, A.; Mishra, B.; Lim, S. H.; Su, X.; Tambyah, P. A.; Leong, S. S. J. *Acta Biomater.* **2014**, *10*, 258
- (34) Mishra, B.; Basu, A.; Chua, R. R. Y.; Saravanan, R.; Tambyah, P. A.; Ho, B.; Chang, M. W.; Leong, S. S. J. *J. Mater. Chem. B* **2014**, *2*, 1706
- (35) Blin, T.; Purohit, V.; Leprince, J.; Jouenne, T.; Glinel, K. *Biomacromolecules* **2011**, *12*, 1259
- (36) Gao, G.; Yu, K.; Kindrachuk, J.; Brooks, D. E.; Hancock, R. E. W.; Kizhakkedathu, J. N. *Biomacromolecules* **2011**, *12*, 3715
- (37) Gao, G.; Lange, D.; Hilpert, K.; Kindrachuk, J.; Zou, Y.; Cheng, J. T. J.; Kazemzadeh-Narbat, M.; Yu, K.; Wang, R.; Straus, S. K.; Brooks, D. E.; Chew, B. H.; Hancock and, R. E. W.; Kizhakkedathu, J. N. *Biomaterials* **2011**, *32*, 3899
- (38) Gao, G.; Cheng, J. T. J.; Kindrachuk, J.; Hancock, R. E. W.; Straus, S. K.; Kizhakkedathu, J. N. *Chem. Biol.* **2012**, *19*, 199
- (39) Seo, M. D.; Won, H. S.; Kim, J. H.; Mishig-Ochir, T.; Lee, B. J. *Molecules* **2012**, *17*, 12276
- (40) Glinel, K.; Thebault, P.; Humblot, V.; Pradier, C. M.; Jouenne, T. *Acta Biomater* **2012**, *8*, 1670



- (41) Campoccia, D.; Montanaro, L.; Arciola, C. R. *Biomaterials* **2013**, *34*, 8533
- (42) Nicolaou, K. C.; Chen, J. S.; Dalby, S. M. *Bioorg.Med. Chem.* **2009**, *17*, 2290
- (43) Nathan, A.; Zalipsky, S.; Ertel, S. I.; Agathos, S. N.; Yarmush, M. L.; Kohn, J. *Bioconjug. Chem.* **1993**, *4*, 54
- (44) Aumsuwan, N.; Heinhorst, S.; Urban, M. W. *Biomacromolecules* **2007**, *8*, 713
- (45) Aumsuwan, N.; Danyus, R. C.; Heinhorst, S.; Urban, M. W. *Biomacromolecules* **2008**, *9*, 1712
- (46) Wach, J. Y.; Bonazzi, S.; Gademann, K. *Angew. Chem. Int. Ed.* **2008**, *47*, 7123
- (47) Jose, B.; Antoci, V. Jr.; Zeiger, A. R.; Wickstrom, E.; Hickok, N. J. *Chemistry & Biology* **2005**, *12*, 1041
- (48) Antoci Jr., V. Jr.; King, S. B.; Jose, B.; Parvizi, J.; Zeiger, A. R.; Wickstrom, E.; Freeman, T. A.; Composto, R. J.; Ducheyne, P.; Shapiro, I. M.; Hickok, N. J.; Adams, C. S. *J. Orthop. Res.* **2007**, *25*, 858
- (49) Edupuganti, O. P.; Antoci, V. Jr.; King, S. B.; Jose, B.; Adams, C. S.; Parvizi, J.; Shapiro, I. S.; Zeiger, A. R.; Hickok, N. J.; Wickstrom, E. *Bioorg.Med. Chem. Lett.* **2007**, *17*, 2692
- (50) Antoci, V. Jr.; Adams, C. S.; Parvizi, J.; Davidson, H. M.; Composto, R. J.; Freeman, T. A.; Wickstrom, E.; Ducheyne, P.; Jungkind, D.; Shapiro, I. M.; Hickok, N. J. *Biomaterials* **2008**, *29*, 4684
- (51) Lawson, M. C.; Shoemaker, R.; Hoth, K. B.; Bowman, C. N.; Anseth, K. S. *Biomacromolecules* **2009**, *10*, 2221
- (52) McKinley, C. L.; Hoth, K. C.; DeForest, C. A.; Bowman, C. N.; Anseth, K. S. *Clin. Orthop. Relat. Res.* **2010**, *468*, 2081
- (53) Stefano Tugulu, Anke Arnold, India Sielaff, Kai Johnsson, Harm-Anton Klok, *Biomacromolecules*, *6*, 1602-1607, **2005**
- (54) Tugulu, S.; Silacci, P.; Stergiopoulos, N.; Klok, H.-A. *Biomaterials* **2007**, *28*, 2536
- (55) Sjöwall, C.; Wetterö, J.; Bengtsson, T.; Askendal, A.; Skogh, T.; Tengvall, P. *Biochem. Biophys. Res. Comm. - BBRC* **2007**, *1*, 251
- (56) Fischer, M. J. E. *Methods in Molecular Biology* 627, Springer Science + Business Media, LLC **2010**
- (57) <http://www.elisa-antibody.com/ELISA-Introduction>
- (58) <http://www.abdserotec.com/an-introduction-to-elisa.html>
- (59) Berney, M.; Hammes, F.; Bosshard, F.; Weilenmann, H.-U.; Egli, T. *Appl. Environm. Microbiol.* **2007**, *73*, 3283

### 3.6. Supporting Information



**Scheme S1.** Synthetic route for the direct coupling of vancomycin to silicon wafers

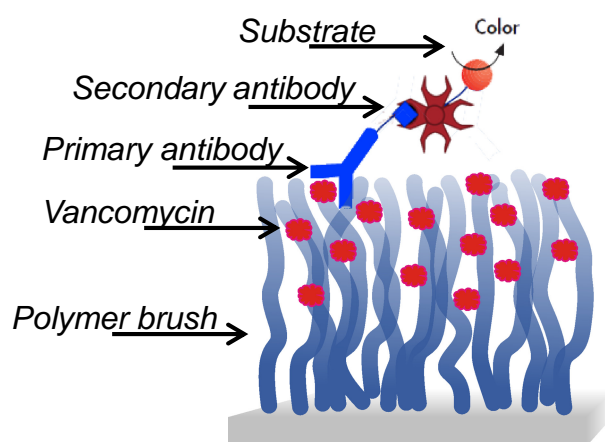


**Figure S1.** Schematic representation of ELISA test for vancomycin modified polymer brushes

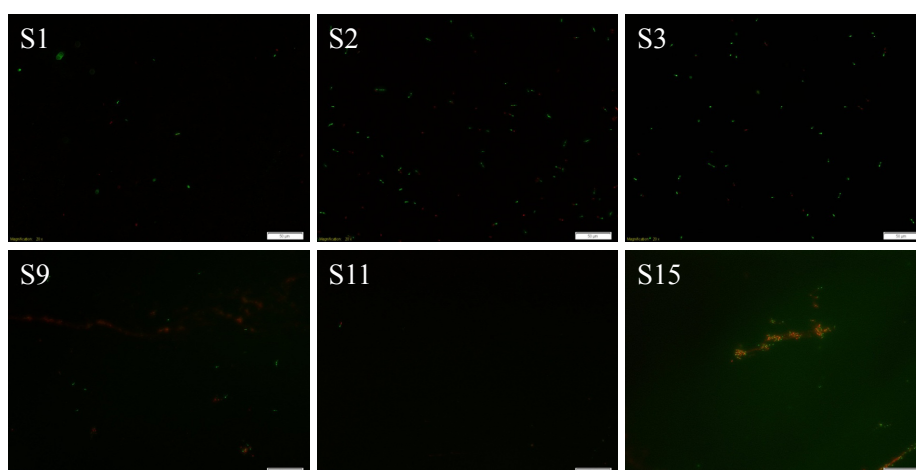


**Figure S2.** Fluorescence micrographs (40x) of control samples and POEGMA brushes with and without vancomycin coupled via its carboxylic acid group after 24 hours in 540 CFU/ml BS at 37 °C (washed samples); samples code description in Table 2



## 4. Polymer brushes as a platform for bacteria triggered release

### 4.1. Introduction

Long-term infective resistance of biomaterials becomes a high priority in the fight against hospital acquired infections<sup>1-7</sup>. The first step in preventing implant-related infections is to prevent and inhibit protein and then bacteria adhesion on surfaces. Different classes of bacteria repelling and antiadhesive surfaces have been developed in the last decades considering the complex mechanisms involved in the bacterial attachment on surfaces<sup>1-7</sup>. In the design of biomaterials for medical devices it has to be considered that several mechanisms are generally valid for all bacterial strains, while others are specific for different species or even more, for only one type of bacteria<sup>1,2,7</sup>. Moreover, repelling bacteria is a necessary, but not sufficient condition for avoiding or decreasing the number of nosocomial infections<sup>5</sup>. Therefore, another approach aimed to the development of bioactive surfaces able not only to repel bacteria but to kill the approaching microorganisms<sup>5,8,9</sup>. It was demonstrated that polymers including or coupled with antimicrobial agents can effectively kill bacteria on contact<sup>2,4,7,8</sup>.

In the last years active strategies based on coatings able to release bactericidal agents have been developed. The concept of active protection involves the entrapment of pharmacologically active substances in matrices or on surfaces and their subsequent leaching or triggered release<sup>4,8</sup>. Until now the studied release systems include the release of silver in ionized and elementary forms or as silver zeolites and as nanoparticles<sup>4,9,10</sup> as well as chlorhexidine from polymers<sup>11</sup>. Antibiotics have also been released from different types of coatings, to increase and prolong their efficacy. Different antibiotics including vancomycin, tobramycin, cefamandol, cephalothin, carbenicillin, amoxicillin, and gentamicin<sup>4,12,13</sup> have been released from polyurethane<sup>14-16</sup>, hydroxyapatite<sup>12</sup>, biodegradable polymer coatings<sup>13</sup> or from collagen matrices for wound dressings<sup>17</sup>. Such controlled release systems have as a main advantage the possibility to deliver the active principle directly to the site of implantation, ensuring the therapeutic level of the drug.

The disadvantages of such release system rely in the impossibility to control the kinetics of the active principle release, involving high dosages for short time after implantation and decreased levels for longer periods. Moreover, it is hard to deliver the drug only in the close vicinity of the infected site, and only in the presence of bacteria. For these reasons a more attractive approach is to deliver the active component in the presence of bacteria. Tanihara et al. studied in 1998-99<sup>18,19</sup> a gentamicin release system triggered by the increased thrombin activity in the presence of *S. aureus*. Although this approach seems promising, the main limitation lies in the fact that thrombin-like activity is a host generated signal and is not generated only during infections but also due to the foreign body response in the presence of implant alone. Therefore, a more attractive way will be to use a bacteria generated signal, that is present only during infection. Several bacterial signals can be exploited: cell wall hydrolases or autolysins<sup>20-23</sup>,  $\beta$ -lactamase<sup>24,25</sup>, DD-peptidases<sup>26-28</sup> or human immunoglobulin A1 (IgA1) proteases<sup>29,30</sup>. Cell wall hydrolases or autolysins are specific bacterial enzymes involved in cell wall breakdown, preserving its integrity during cell division<sup>20</sup>. Recent studies<sup>21,22</sup> have identified several short-peptide sequences that can be cleaved by autolysins which could be potentially used as linkers between the antimicrobial agent and polymer brushes.  $\beta$ -lactamase secreted by bacteria that have acquired resistance to penicillin is an antibiotic degrading enzyme having a specific four-atom ring in its structure ( $\beta$ -lactam). The mechanism involved in the deactivation of antibiotics by  $\beta$ -lactamase involves breaking of the  $\beta$ -lactam ring through hydrolysis. Several groups have explored the possibility of using the activity of  $\beta$ -lactamases to release an active agent in solution<sup>25,31-36</sup>. Typically the active agent is coupled to cephalosporin through an ester, carbamate, tertiary amine or ether bond and the presence of lactamase causes degradation of  $\beta$ -lactam ring and could lead to the release of an antimicrobial agent. Another bacteria signal that could be considered is D-amino acid proteases<sup>27,28</sup>. A DD-peptide linker could be used between the active component and substrate and afterwards hydrolysed by DD-peptidases secreted by bacteria. Although this strategy seems straightforward it is not very well studied and it is not yet clear which bacteria secrete these proteases, if they are extracellularly secreted and what amino acid sequence is required for cleavage by the D-amino acid proteases. Human immunoglobulin A1 (IgA1) proteases are another class of enzymes that are of potential interest to develop biological trigger release systems. These are proteolytic enzymes secreted by several species of bacteria which cleave host IgA1 antibodies in the hinge region and thereby reduce the removal of the bacteria by the host's immune system<sup>30</sup>. At

the moment, however, there are not enough data regarding what bacteria cleaves what region of IgA1 and searching for the right sequence to use might prove to be time consuming laborious work.

Although there are studies referring to the bacterial signals, there is a lack of literature concerning bacteria triggered release systems. In this Chapter we used two different linkers sensitive to two specific bacterial signals i.e. autolysins and  $\beta$ -lactamase for the attachment of a dye to PHEMA brushes. PHEMA brushes were used because they are easy to synthesize through SI-ATRP with control over grafting densities and thicknesses. They also have a hydroxyl group on each repeating unit that has been reported to undergo post-polymerization modification reactions<sup>37-39</sup>. Then we used these systems as a proof-of-concept for the possibility to release an active compound, in this case the dye, from the polymer brushes in the presence of the selected bacterial enzymes.

## 4.2. Experimental Section

### 4.2.1. Materials

All chemicals were purchased from Aldrich and used as received unless stated otherwise. The Mca functionalized peptide (Mca-Ala-D-isoGln-Lys-D-Ala-Arg-OH) was purchased from GL Biochem (Shanghai) Ltd with a purity of 95%. The  $\beta$ -lactamase enzymes were bought from Fluorochem and use as received. Tetrahydrofuran (THF), dichloromethane (DCM), Dimethylformamide (DMF) and toluene were purified and dried using a solvent purification system (PureSolv). Deionized water was obtained from a Millipore Direct-Q 5 Ultrapure Water System and ultrahigh quality. Tryptic Soy Broth (TSB) and Mueller-Hinton agar (MHA) were purchased from Difco, BD and Co., France and used according to the manufacturer's instructions. All non sterile solutions used in the bacteria experiments were autoclaved at 121 °C for 20 minutes. *Staphylococcus epidermidis* 1457 bacteria strains was kindly provided by Prof. Landmann, University of Basel. Silicon (100) covered with a native silicon oxide layer and quartz slides were used as substrates for surface-initiated polymerization. PHEMA brushes with different grafting densities and thicknesses were prepared as described in Chapter 2.

## 4.2.2. Methods

Attenuated total reflectance Fourier transform infrared spectroscopy (ATR-FTIR) was performed on a nitrogen purged Nicolet 6700 FT-IR spectrometer equipped with a SmartiTR™ (Thermo Fisher Scientific Inc., Waltham, MA, USA) accessory and a diamond crystal. UV-Visible absorbance spectra were recorded using a Varian Cary 100 Bio UV-Visible spectrophotometer at room temperature on polymer brush coated quartz substrates. Atomic force microscopy (AFM) was performed in tapping mode on a Veeco Multimode Nanoscope IIIa SPM controller (Digital Instruments, Santa Barbara, CA) using NSC14/no Al MikroMasch (Tallinn, Estonia) cantilevers. To determine the layer thicknesses, cross-sectional height profiles of micropatterned polymer brushes on silicon substrates were analyzed.

## 4.2.3. Procedures

### 4.2.3.1. Peptide functionalization of PHEMA brushes

PHEMA brushes were activated using p-nitrophenyl chloroformate (NPC) as reported in Chapter 3. NPC-activated brushes were peptide functionalized by treatment with a solution containing 1 mM peptide and 2.5 mM 4-(dimethylamino)pyridine (DMAP) in anhydrous DMF for 16 hours at room temperature under gentle shaking in the dark. Afterwards, the samples were sonicated in DMF for 5 minutes, rinsed and washed three times for 1 hour with 70% ethanol solution and two times with water to remove residual physisorbed peptide and finally dried in a stream of nitrogen.

### 4.2.3.2. Autolysin triggered release experiment

The culture of *S. epidermidis* 1457 with the desired CFU was prepared as described in Chapter 2. The PHEMA brushes functionalized with the Mca peptide, prepared on quartz slides, were placed into sterile 14 mL polypropylene round-bottom tubes containing 3 mL of bacteria inoculum of approx.  $10^5$  CFU/mL and incubated for 24 h at 37 °C without shaking. After the incubation the adherent bacteria were removed from the surfaces in the following way: rinsing with 70% ethanol, washing twice with 70% ethanol for 5 minutes under shaking, sonication for 5 minutes with 1.5% EDTA and 0.45% NaCl, rinsing with 70% ethanol, and washing with 70% ethanol for 5 minutes. The slides were subsequently dried under a flow of nitrogen and the “after incubation” UV-Vis spectrum was recorded.

#### 4.2.3.3. $\beta$ -Amino-3-(hydroxymethyl)cephalosporinic acid (7-HACA) synthesis

7 $\beta$ -aminocephalosporanic acid (7-ACA) (1 g, 3.6 mmol) was added to MeOH (5 mL) and H<sub>2</sub>O (5 mL); the mixture was cooled to  $-30$  °C giving a suspension and to this 3.0 M aq NaOH (2 mL) was added slowly. The mixture was stirred for 2 hours at  $-30$  °C to give a clear solution, and then at a temperature under 0 °C, 5% aq HCl was added dropwise to the resulting solution until it was pH 3.5. The mixture was stirred for 1 hour at this temperature; a precipitate formed. The precipitate was collected by suction filtration, washed with MeOH and dried under vacuum.

#### 4.2.3.4. Coupling of dansylcadaverine to PHEMA

NPC activated PHEMA was reacted with a dry DMF solution containing 3 mM of dansylcadaverine and 6mM of DMAP for 18hours. After the reaction the polymer brushes where washed two times with DMF for 2 hours, two times with 70% ethanol solution for 2 and 12 hours respectively, and then dried in a stream of nitrogen.

#### 4.2.3.5. Coupling of dansylcadaverine via 7-HACA linker

NPC activated PHEMA was first reacted with a dry DMF solution containing 10mM of 7 $\beta$ -amino-3-(hydroxymethyl)cephalosporinic acid (7-HACA), 15 mM of DMAP and 15 mM of Et<sub>3</sub>N. The 7-HACA modified PHEMA was washed with DMF and 70% ethanol then activated a second time with NPC following the same protocol. After washing the NPC activated 7-HACA was reacted with a dry DMF solution containing 3 mM of dansylcadaverine and 6 mM of DMAP for 18 hours. After the reaction the polymer brushes where washed two times with DMF for 2 hours, two times with 70% ethanol solution for 2 and 12 hours respectively, and then dried in a stream of nitrogen.

#### 4.2.3.6. Release experiment $\beta$ -lactamase

The dansylcadaverine modified polymer brushes, prepared on quartz slides, were incubated for 16 hours in 10mM PBS buffer containing 10 units of Beta I and one unit of Beta II per mL. Afterwards the samples were washed two times with 10 mM PBS buffer for 2 hours, rinsed with water and dried in a stream of nitrogen. The UV-Vis spectra of the slide before and after incubation with the enzyme were recorded.

### 4.3. Results and Discussion

The research presented herein is focused on the synthesis and characterization of polymer brushes that should release an active component only in the presence of bacterial enzymes. There are many bacterial signals that could be used but, considering previous reports, we selected two that seemed more promising: *autolysins* and  $\beta$ -*lactamase*. Therefore, we coupled a dye on HEMA polymer brushes via a peptide linker susceptible to be cleaved by autolysins or via a penicillin-like linker that could be hydrolyzed by  $\beta$ -lactamase. The concept is schematically represented in Figure 1. The PHEMA brushes used as platform, with different grafting densities and thicknesses, were synthesized by SI-ATRP, as described in Chapter 2.

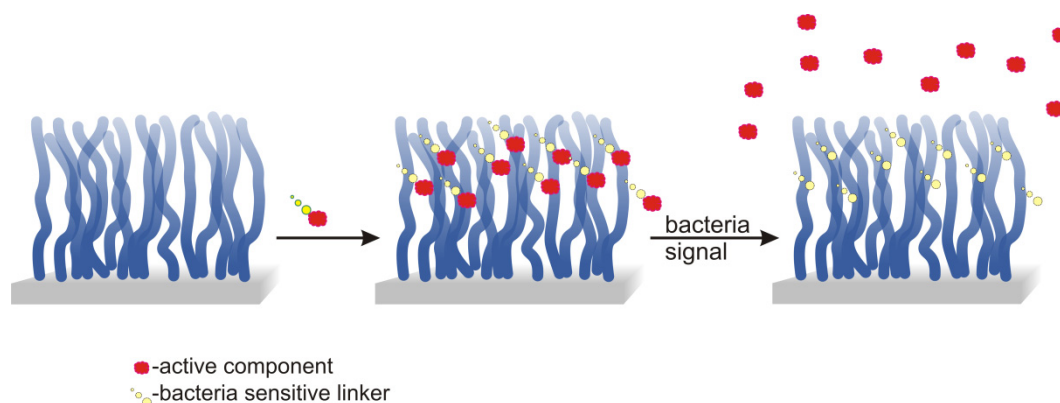


**Figure 1.** The concept of bacteria-triggered enzymatic release from chemically modified polymer brushes

#### 4.3.1. Autolysin triggered release

In staphylococci, there are five well-defined autolysins classified according to their specific cleavage sites, i.e. *N*-acetylmuramidases, *N*-acetylglucosaminidases, *N*-acetylmuramyl-L-alanine amidases, endopeptidases, and transglycosylases<sup>20</sup> and they play an important role in bacteria attachment on implant surfaces. The autolysins specific for both *S. aureus* and *S. epidermidis* are known to be bifunctional, containing an amidase and a glucosaminidase domain<sup>23</sup>. The research performed in Kalbacher's group<sup>21,22</sup> analyzed the structure and mode of action of the main autolysin in *S. epidermidis* and proved the catalytic (amidase) domain named AmiE in *S. epidermidis* can break the

amide bond of *N*-acetylmuramyl-L-alanine in the peptidoglycan structure<sup>22,23</sup>. Also, they found a new substrate for autolysin, substrate based on the sequence L-Lys-D-isoGln-L-Ala-MurNAc. They found certain modifications to this substrate can be tolerated without affecting binding and recognition by the enzyme. The key positions they focus for modifying were the sugar moiety at the N terminus, the amine lysine side chain as well as the C terminus. They have proved that adding D-Ala-Arg-OH on the C terminus of the peptide can increase the solubility, and they also coupled a fluorescent (7-Methoxycoumarin-4-yl)-acetyl (Mca) reporter group at the N terminus replacing MurNAc and modified the L-Lys amino side chain with a fluorescent quencher. All these changes did not seem to modify the recognition by the enzyme and the incubation with AmiE led to an increase in fluorescence suggesting that the cleavage site is somewhere between Mca and Lys. Therefore the peptide selected was Mca-Ala-D-isoGln-Lys-D-Ala-Arg-OH (Figure 2) and the amine from Lys was used for coupling to the polymer brush.

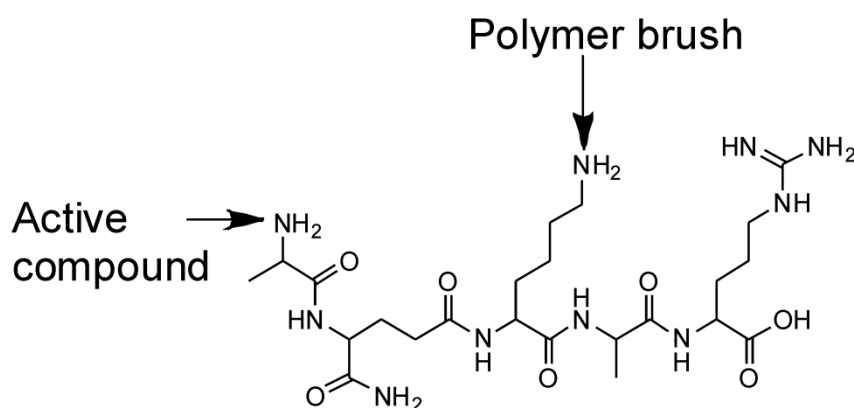
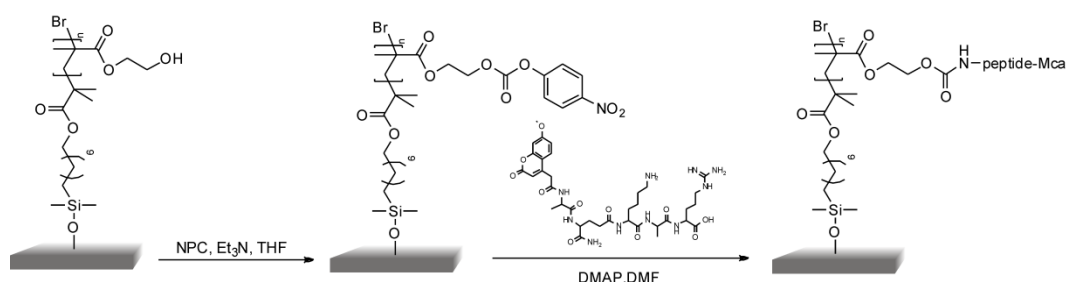


**Figure 2.** Structure of the peptide substrate used for coupling of the active compound to the polymer brush

The binding of the Mca-modified linker to PHEMA brushes is represented in Scheme 1. Functionalization of HEMA polymer brushes starts with a first step involving activation of the hydroxyl groups on the side chain with *p*-nitrophenyl chloroformate (NPC) in anhydrous THF in the presence of triethylamine, which is frequently used to couple primary amines. In the next step of the reaction, the peptide was bound to the NPC-activated surfaces in anhydrous DMF with 4-(dimethylamino)-pyridine (DMAP) as acylation catalyst<sup>37</sup>. The influence of any side reaction such as coupling *via* guanidine is expected to be insignificant since it should not affect the release of Mca, as the cleavage point of the substrate is somewhere between Mca and Lys. All reaction steps were

monitored by FTIR and UV-Vis spectroscopy. The FTIR spectra presented in Figure 3 confirmed the introduction of the *p*-nitrophenyl groups on PHEMA brushes by the appearance of an additional carbonyl stretching vibration around  $1800\text{ cm}^{-1}$ , due to the formation of the new carbonate linkage. The coupling of Mca peptide was evidenced by the appearance of specific amide 1 and amide 2 bands, at  $1657\text{ cm}^{-1}$  and  $1614\text{ cm}^{-1}$ , respectively. Furthermore, UV-Vis spectroscopy (Figure 4) revealed the NPC activation of PHEMA resulted in a strong UV-Vis absorption centered at 270 nm. The coupling of the peptide to the polymer brushes was evidenced by the appearance of the Mca specific absorbance at 325 nm. Moreover, no residual NPC groups could be observed.



**Scheme 1.** Synthetic route for coupling of the Mca modified peptide to PHEMA brushes

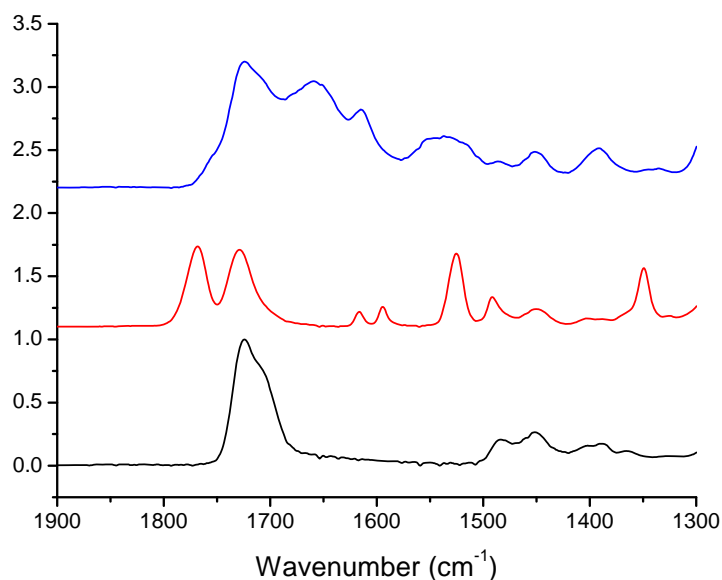


**Figure 3.** FTIR spectra of PHEMA (black line) NPC activated PHEMA (red line) and Mca modified peptide coupled to PHEMA (blue line) with a brush thickness of 102 nm and a grafting density of 100%



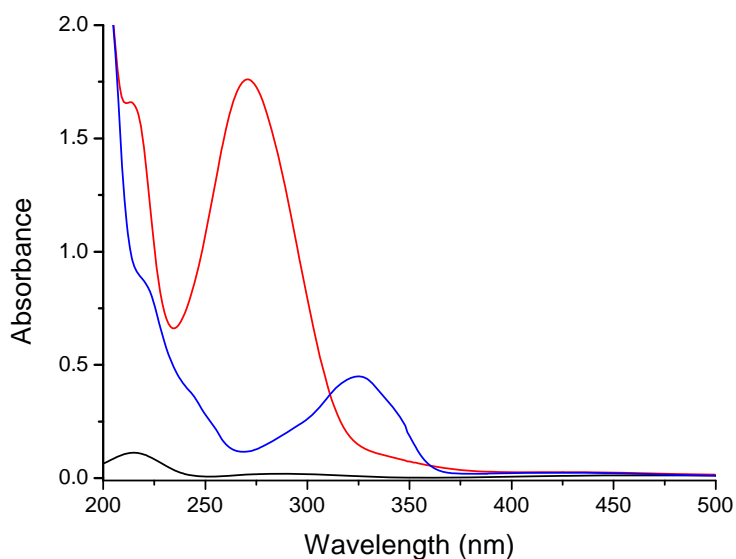


**Figure 4.** UV-Vis spectra of PHEMA (black line) NPC activated PHEMA (red line) and Mca modified peptide coupled to PHEMA (blue line) with a brush thickness of 102 nm and a grafting density of 100%

In order to see if the peptide can be cleaved after coupling to PHEMA brushes, surfaces were incubated in a culture of *S. Epidermidis* 1457 for 24 hours at 37°C. We tested samples with three grafting densities (10%, 50 % and 100 %) to assess if there is any influence on the release of the dye coupled to PHEMA brushes via the peptide (Figure 5). The UV-Vis spectra before and after incubation were recorded. In Figure 5 the characteristic peak for Mca at 325 nm clearly appears for 50% and 100% grafting density PHEMA brushes both before and after incubation suggesting the autolysine specific for *S. epidermidis* could not cleave the amide bond as we expected. For less dense polymer brushes, it seems the autolysine binds and cleaves the bond and the dye is released. The characteristic peak of Mca disappears for PHEMA brushes with 10 % grafting density. The lack of the enzyme lytic activity could be due to different conformations adopted by polymer brushes with high grafting densities, hindering the labile bond and making it not accessible to the enzyme.

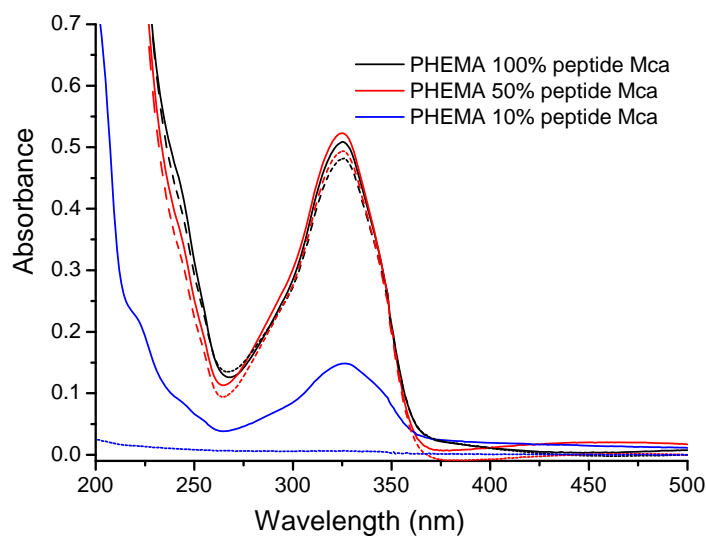


**Figure 5.** UV-Vis spectra of the modified polymer brushes before (straight line) and after (dotted line) incubation for 24 hours in *SEI457*

Based on the observations in this experiment we decided to analyze the behavior of polymer brushes with the lowest grafting density (for which the cleavage of the linker and the dye release was noticed), in more detail. The PHEMA brushes with the dye linked via the peptide were incubated in a bacteria growth medium with and without bacteria to test their stability. As easily can be observed from Figure 6 the characteristic peak for Mca disappears after incubating thick PHEMA brushes (black lines) both in presence and in absence of bacteria. Considering the thin HEMA polymer brushes (red lines) a different behavior is noticed, the characteristic Mca peak disappearing only when the surfaces are incubated in bacteria culture medium. The different behaviors of thick and thin brushes could be attributed to the effect of two simultaneous processes: polymer brushes degradation in the bacteria growth medium and linker cleavage in the presence of autolysin secreted by bacteria. Only for thin polymer brushes the selectivity of these processes could be assessed and the autolysin triggered release of the dye was evidenced. This observation is in concordance with previous experiments which proved thin brushes as being more stable than thick ones<sup>39</sup>.

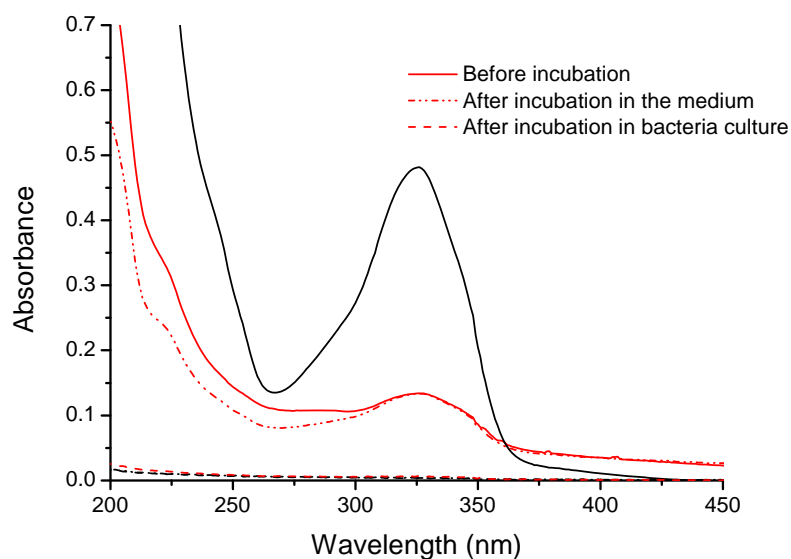
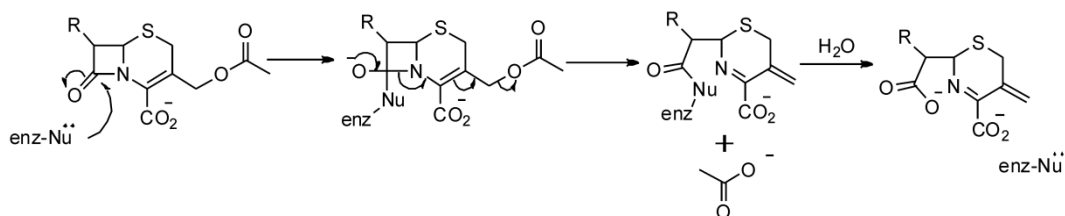


**Figure 6.** UV-Vis spectra of 10% PHEMA thin (red lines) and thick (black lines) polymer brushes modified with the fluorescent substrate for AmiE before and after incubation for 24h

#### 4.3.2. $\beta$ lactamase triggered release from PHEMA brushes



**Scheme 2.** Mechanism of  $\beta$ -lactamase attack on cephalosporins

The mechanism of the  $\beta$ -lactamase activity leading to cleavage of the  $\beta$ -lactam centers on the covalent acylation of the  $\beta$ -lactam by serine in the active site, and then hydrolysis which leads to the reactivation of the  $\beta$ -lactamase and release of the inactivated  $\beta$ -lactam<sup>40</sup>. Therefore for a linker to be sensitive to  $\beta$ -lactamase activity the serine ester hydrolysis mechanism has to be favored and the active site has not to be hindered by substituents attached to the  $\beta$ -lactam ring. The mechanism of the  $\beta$ -lactamase action on a cephalosporin is based on the reaction sequences presented in Scheme 2. Active species

can be attached via a leaving group, leading to the cleavage of the active compounds from the  $\beta$ -lactam ring<sup>25</sup>. Several research groups have explored the possibility of using the activity of  $\beta$ -lactamases to release an antimicrobial agent in solution<sup>25,31-36</sup>. Usually, an ester, carbamate, tertiary amine or ether bond can be used to couple the active agent to cephalosporin, a structure that is well established as a mono-release nucleus that leads to the rapid elimination of the substituent in the leaving group position following  $\beta$ -lactamase catalyzed breaking of the  $\beta$ -lactam ring. Therefore a cephalosporin-like linker could be used to couple the antibacterial agent to the surface as presented in Figure 7. Since the most of the gram positive bacteria have acquired resistance to  $\beta$ -lactam antibiotics they secrete  $\beta$ -lactamase that could hydrolyzed by  $\beta$ -lactamase the proposed linker.

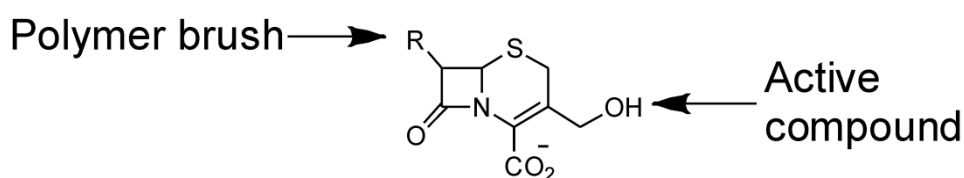
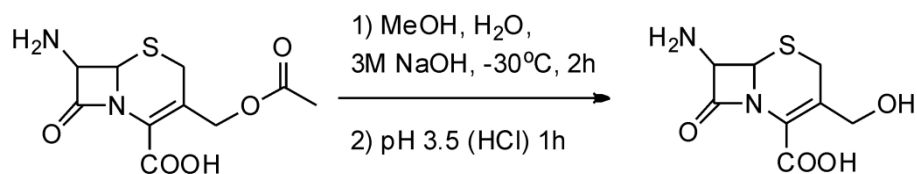


**Figure 7.** Structure of the cephalosporin-like linker used for coupling of the active compound to the polymer brush

In this study a dye was coupled to the polymer brushes using a proper linker susceptible to cleavage by  $\beta$ -lactamase. To synthesize the linker we started from 7 $\beta$ -aminocephalosporanic acid (7-ACA) which is a key intermediate for the synthesis of cephalosporin antibiotics and is known to be vulnerable to enzyme-catalyzed scission. To obtain the desired linker the methylacetoxymethyl group of the 7 $\beta$ -aminocephalosporanic acid was deacetylated to obtain a hydroxyl group thus resulting the 7 $\beta$ -amino-3-(hydroxymethyl)cephalosporinic acid (7-HACA) as presented in Scheme 3. The reaction took place at -30 °C, in a mixture MeOH/H<sub>2</sub>O. The structure of the 7-HACA linker was confirmed by <sup>1</sup>H-NMR (Figure 8). Afterwards, the hydroxyl group was used to couple an antibiotic (or a dye) and try to see if the presence of  $\beta$ -lactamase causes the release of the active substance.



**Scheme 3.** Synthesis of 7-HACA starting for 7-ACA

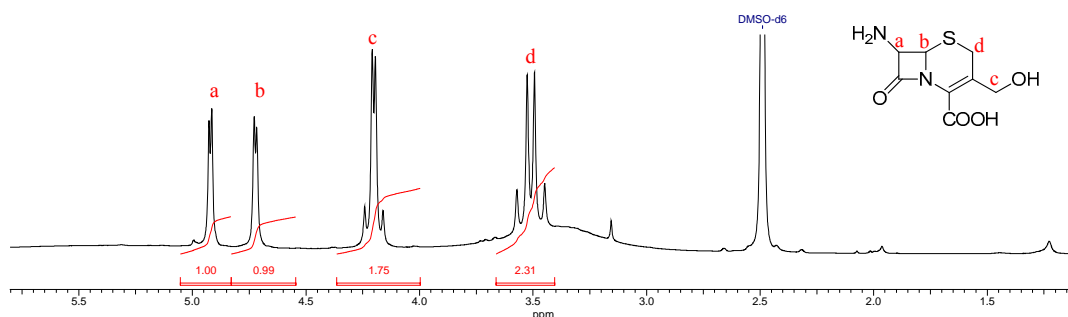
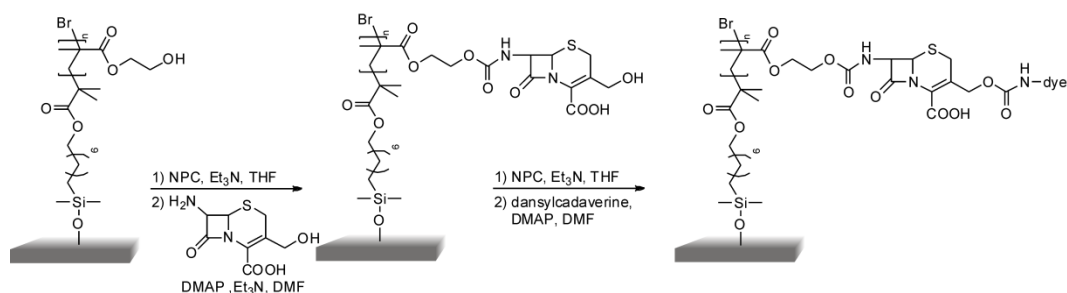


**Figure 8.** <sup>1</sup>H-NMR of 7-HACA

For the study of the  $\beta$ -lactamase triggered release systems, dansylcadaverine (Figure S1 – Supporting Information), a dye was used as marker to monitor the possibility of enzyme induced cleavage of the linker. Dansylcadaverine was bound to PHEMA brushes via 7-HACA linker following the procedure presented in Scheme 4. For this purpose NPC activated PHEMA brushes were first reacted with a dry DMF solution containing 7 $\beta$ -amino-3-(hydroxymethyl)cephalosporinic acid (7-HACA), DMAP and Et<sub>3</sub>N. The 7-HACA modified PHEMA brushes were washed with DMF and 70% ethanol then activated a second time with NPC following the same protocol. After washing, the NPC activated 7-HACA-PHEMA brushes were reacted with a dry DMF solution containing dansylcadaverine and DMAP for 18 hours. Finally, the polymer brushes were washed two times with DMF and two times with 70% ethanol solution. As a control sample the dansylcadaverine was coupled directly to NPC activated HEMA polymer brushes without the 7-HACA linker as presented in Scheme S1 – Supporting Information.



**Scheme 4.** Synthetic route for coupling of dansylcadaverine via a 7-HACA linker to PHEMA brushes

All reaction steps have been monitored using UV-Vis and FTIR spectroscopy. UV-Vis spectroscopy for dansylcadaverine bound to PHEMA brushes via 7-HACA linker is presented in Figure 9 and for direct coupling of the dye to PHEMA brushes in Figure S2 – Supporting Information. In both cases the NPC activation is confirmed by the appearance of the NPC specific peak at 270 nm. The coupling of 7-HACA to PHEMA brushes could also be confirmed by UV-Vis spectroscopy by the disappearance of the NPC specific absorbance and the appearance of a new peak around 260 nm. The NPC activation of the hydroxyl groups on 7-HACA was again evidenced by the appearance of the specific absorbance at 270 nm. The absorbance for the second NPC activation has a reduced intensity most likely indicating a lower yield for the second NPC activation step. The coupling of dansylcadaverine for systems with and without 7-HACA linker was evidenced by the disappearance of the NPC absorbance and the appearance of the specific dye absorbance at 350 nm and 265 nm. FTIR spectra (Figure 10 for dye coupling via 7-HACA and Figure S3-Supporting Information for direct coupling of the dye to PHEMA brushes) also confirmed the NPC activation of PHEMA by the appearance of the second carbonyl peak. The next reaction steps could not be clearly evidenced by FTIR, the main observable difference being the broadening of the carbonyl peak at  $1750\text{ cm}^{-1}$ . This is probably due to the low number of amide groups introduced in the polymer brush appearing to wavelength too close to the initial carbonyl peak. Nevertheless, UV-Vis spectroscopy confirmed the successful coupling of the dye on PHEMA brushes both directly and via 7-HACA linker, so no further characterization was considered necessary.

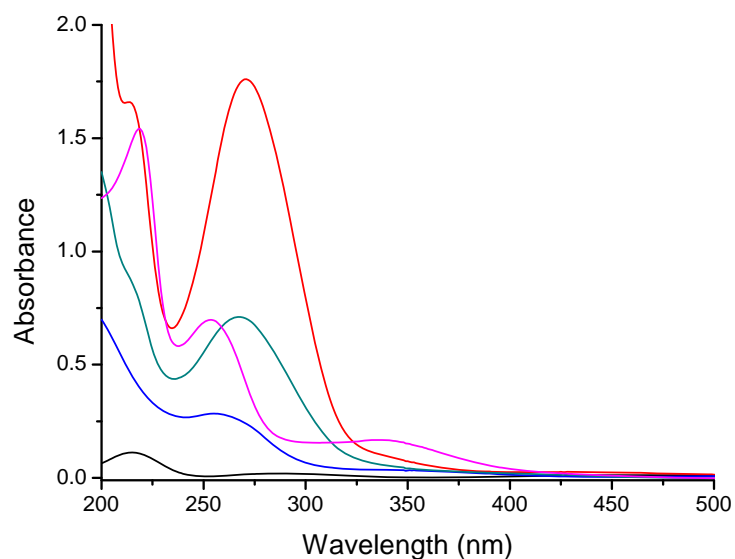


**Figure 9.** UV-Vis spectra of PHEMA (—), NPC activated PHEMA (—), 7-HACA modified PHEMA (—), NPC activated 7-HACA-PHEMA (—) and dansylcadaverine coupled via 7-HACA to PHEMA (—) brushes with a thickness of the initial PHEMA brush of 97 nm and a grafting density of 100%

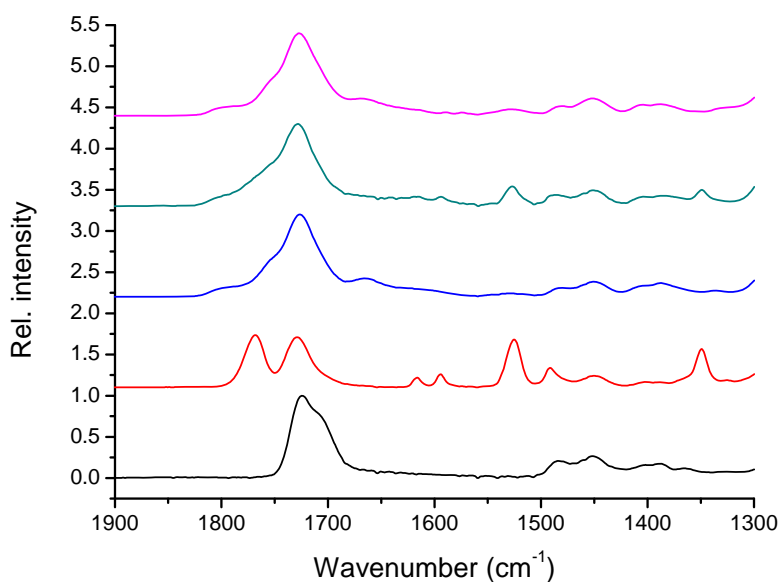


**Figure 10.** FTIR spectra of PHEMA (—), NPC activated PHEMA (—), 7-HACA modified PHEMA (—), NPC activated 7-HACA-PHEMA (—) and dansylcadaverine coupled via 7-HACA to PHEMA (—) brushes with a thickness of the initial PHEMA brush of 97 nm and a grafting density of 100%

To evaluate if the conformation of polymer brushes can influence  $\beta$ -lactamase triggered release of the dye from the synthesized substrates, PHEMA brushes with different grafting densities (10%, 50% and 100%) were prepared, with a polymerization time of 16 hours and subsequently modified with dansylcadaverine via 7-HACA linker following the previously described protocol. All the reaction steps were monitored by UV-Vis spectroscopy and the results for each step are presented in Figure 11A-11D. From UV-Vis spectra it is easy to notice the appearance of specific absorbance for each step and the influence of the grafting density. It is obvious that the dye binding to PHEMA brushes depends on the grafting density, the UV-Vis absorption being stronger for higher grafting densities, as expected.

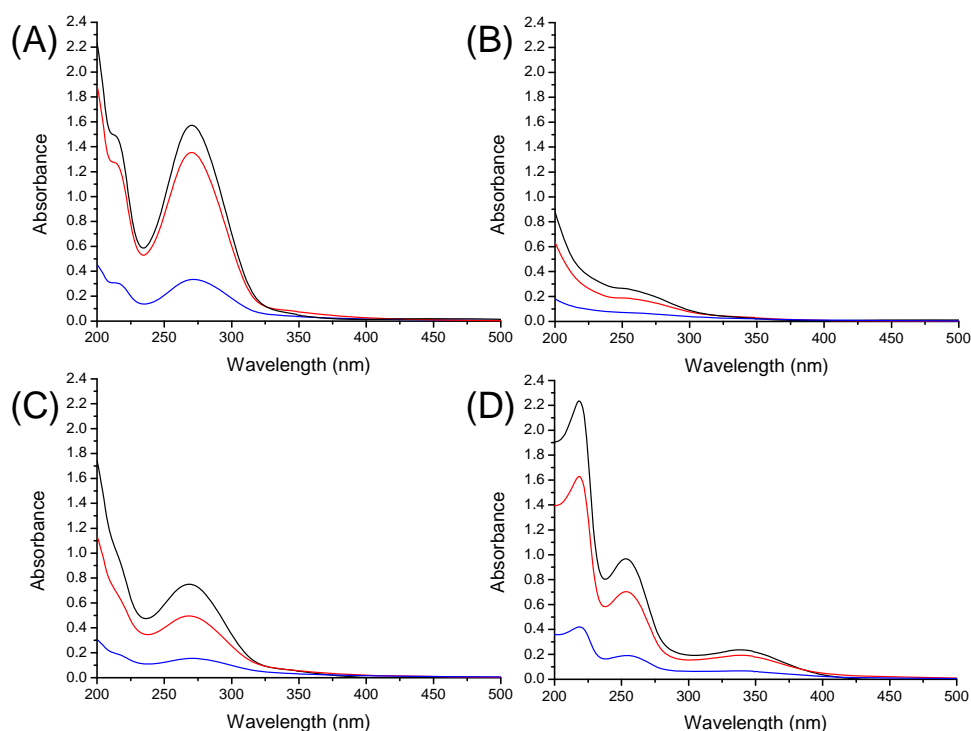


**Figure 11.** UV-Vis spectra of first NPC step (A), 7-HACA modified PHEMA brushes (B), second NPC step (C) and dansylcadaverine coupled via 7-HACA linker to PHEMA brushes (D) with different grafting densities (10% - black line; 50% - red line and 100% - blue line)

All dansylcadaverine modified brushes were tested to monitor if they release the dye in the presence of  $\beta$ -lactamases. Since, contrary to autolysins,  $\beta$ -lactamases are commercially available, we preferred to perform the triggered release experiments



directly using the enzymes. The  $\beta$ -lactamase used is vialied to contain more than 500 Beta I units per vial and more than 50 Beta II units per vial. One unit of activity is defined as the amount of enzyme that will catalyze the hydrolysis of 1 micromole of penicillin (Beta I) or cephalosporin (Beta II) per minute under the assay method conditions. For this experiment all the dye modified polymer brushes were incubated for 16 hours in PBS buffer containing 10 units of Beta I and 1 unit of Beta II per ml. The UV-Vis spectra were recorded before and after incubation and are presented in Figure 12. Unfortunately, no dye was released from the polymer brushes, regardless of grafting density. Some assumptions can be made to explain this behavior. The hydrophobicity of the resulting surfaces (both 7-HACA and dansylcadaverine are not water soluble) may play a role, hindering the interaction between the polymer brush and the enzyme. Moreover, it is not yet fully understood what modifications are allowed to the 7-HACA linker without affecting its recognition by the enzyme. Coupling the linker to the polymer brush or the modification with the dye may prevent the recognition of its cephalosporin core by the  $\beta$ -lactamase. Although several side reactions may compete with the binding of the dye to PHEMA brushes via 7-HACA linker resulting in different ways of dye binding to the polymer brush this could still not explain total absence of release from the studied surfaces.

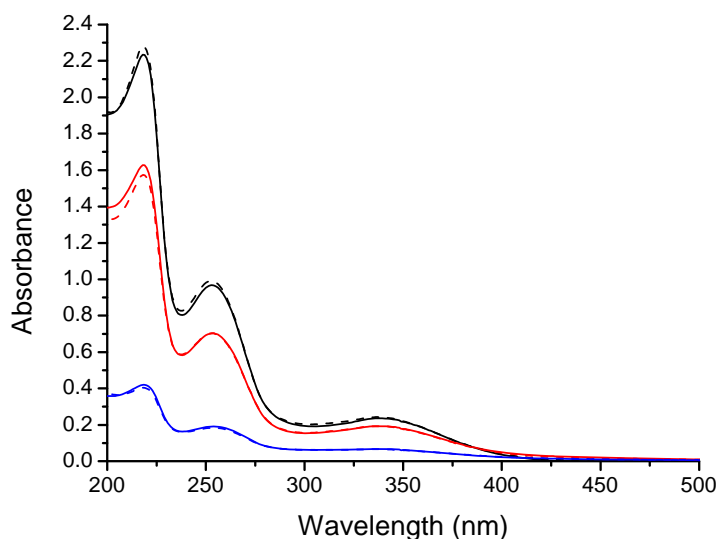


**Figure 12.** UV- Vis spectra of PHEMA brushes with three different grafting densities (10% - black line; 50% - red line and 100% - blue line) modified with dansylcadaverine via a 7-HACA linker before (full line) and after (dotted line) incubation in a  $\beta$ -lactamase solution for 16 hours

## 4.4. Conclusions

The aim of this Chapter was to explore the possibility of using different linkers that could be employed to attach an active compound (or a dye) to the surface, which would then be cleaved by a bacterial generated signal. Two different bacterial signals were considered, based on specific enzymes secreted by bacteria: autolysins and  $\beta$ -lactamase. To the best of our knowledge this is the first attempt to release an active compound from polymer brushes in the presence of selected bacterial signals. HEMA polymer brushes were used as a substrate as they can be easily synthesized through SI-ATRP and they present a hydroxyl group on each repeating unit that can undergo post-polymerization modification reactions. Different dyes were used as a substitute of an actual antibacterial agent to better monitor the potential bacterial triggered release. A fluorescent (7-Methoxycoumarin-4-yl)-acetyl (Mca) dye linked to polymer brushes *via* a peptide was used to evaluate the triggered release induced by autolysins, while dansylcadaverine was coupled via 7-HACA linker to PHEMA brushes to assess the ability of  $\beta$ -lactamase to cleave the linker and release it. FTIR and UV-Vis spectroscopy confirmed that the dye modified peptide was successfully linked to polymer brushes and dansylcadaverine was coupled via 7-HACA linker to PHEMA brushes. No dye release was noticed as response to  $\beta$ -lactamase action for all polymer systems under study maybe due to of the polymer brushes which did not allow the enzyme to interact or recognize the 7-HACA linker. Autolysins succeeded to induce the dye release only for low grafting density thin polymer brushes which seem to be more stable in the selected experimental conditions than thick polymer brushes. The research performed in this Chapter crated the premises to develop surfaces able to release the active component only in the presence of bacteria or infection, but more studies are needed to design the most appropriate system for specific bacterial signals and to understand the interactions involved.

## 4.5. References

- (1) Campoccia, D.; Montanaro, L.; Arciola, C. R. *Biomaterials* **2013**, *34*, 8533
- (2) Hadjesfandiari, N.; Yu, K.; Meiac, Y.; Kizhakkedathu, J. N. *J. Mater. Chem. B* **2014**, *2*, 4968
- (3) Meyers, S. R.; Grinstaff, M. W. *Chem. Rev.* **2012**, *112*, 1615
- (4) Hetrick, E. M.; Schoenfisch, M. H. *Chem. Soc. Rev.* **2006**, *35*, 780
- (5) Glinel, K.; Thebault, P.; Humblot, V.; Pradier, C. M.; Jouenne, T. *Acta Biomaterialia* **2012**, *8*, 1670
- (6) Harding, J. L.; Reynolds, M. M. *Trends in Biotechnology* **2014**, *32*, 140
- (7) Timofeeva, L.; Kleshcheva, N. *Appl. Microbiol. Biotechnol.* **2011**, *89*, 475
- (8) Charnley, M.; Textor, M.; Acikgoz, C. *Reactive and Functional Polymers* **2011**, *71*, 329
- (9) Knetsch, M. L. W.; Koole, L. H. *Polymers* **2011**, *3*, 340
- (10) Monteiro, D. R.; Gorup, L. F.; Takamiya, A. S.; Ruvollo-Filho, A. C.; de Camargo, E. R.; Barbosa, D. B. *International Journal of Antimicrobial Agents* **2009**, *34*, 103
- (11) Harris, L. G.; Mead, L.; Müller-Oberländer, E.; Richards, R. G., *J. Biomed. Mater. Res. Part A* **2006**, *78A*, 50
- (12) Stigter, M.; Bezemer, J.; de Groot, K.; Layrolle, P. *J. Controlled Release* **2004**, *99*, 127
- (13) Price, J. S.; Tencer, A. F.; Arm, D. M.; Bohach, G. A. *J. Biomed. Mater. Res.* **1996**, *30*, 281
- (14) Schierholz, J. M.; Steinhäuser, H.; Rump, A. F. E.; Berkels, R.; Pulverer, G. *Biomaterials* **1997**, *18*, 839
- (15) Rossi, S.; Azghani, A. O.; Omri, A. *J. Antimicrob. Chemother.* **2004**, *54*, 1013
- (16) Kwok, C. S.; Horbett, T. A.; Ratner, B. D. *J. Controlled Release* **1999**, *62*, 301
- (17) Zilberman, M.; Elsner, J. J. *J Control Release.* **2008**, *130*, 202
- (18) Suzuki, Y.; Tanihara, M.; Nishimura, Y.; Suzuki, K.; Kakimaru, Y.; Shimizu, Y. *J Biomed Mater Res* **1998**, *42*, 112
- (19) Tanihara, M.; Suzuki, Y.; Nishimura, Y.; Suzuki, K.; Kakimaru, Y.; Fukunishi, Y. *J. Pharm. Sci* **1999**, *88*, 510

- (20) Renzoni, A.; Barras, C.; François, P.; Charbonnier, Y.; Huggler, E.; Garzoni, C.; Kelley, W. L.; Majcherczyk, P.; Schrenzel, J.; Lew, D. P.; Vaudaux, P. *Antimicrobial Agents and Chemotherapy* **2006**, *50*, 3048
- (21) Lützner, N.; Pätzold, B.; Zoll, S.; Stehle, T.; Kalbacher, H. *Biochemical and Biophysical Research Communications* **2009**, *380*, 554
- (22) Zoll, S.; Pätzold, B.; Schlag, M.; Götz, F.; Kalbacher, H.; Stehle, T. *PLoS Pathog* **2010**, *6*, e1000807
- (23) Biswas, R.; Voggu, L.; Simon, U. K.; Hentschel, P.; Thumm, G.; Gotz, F. *FEMS Microbiol Lett* **2006**, *259*, 260
- (24) McCann, J. R.; McDonough, J. A.; Pavelka Jr., M. S.; Braunstein, M. *Microbiology* **2007**, *153*, 3350
- (25) Grant, J. W.; Smyth, T. P. *J. Org. Chem.* **2004**, *69*, 7965
- (26) Pratt, R. F. *Cell. Mol. Life Sci.* **2008**, *65*, 2138
- (27) Cabaret, D.; Adediran, S. A.; Pratt, R. F.; Wakselman, M. *Biochemistry* **2003**, *42*, 6719
- (28) Adediran, S. A.; Cabaret, D.; Lohier, J.-F.; Wakselman, M.; Pratt, R. F. *Bioorganic & Medicinal Chemistry* **2010**, *18*, 282
- (29) Vitovski, S.; Sayer, J. R. *Infection and Immunity* **2007**, *75*, 2875
- (30) Mistry, D.; Stockley, R. A. *The International Journal of Biochemistry & Cell Biology* **2006**, *38*, 1244
- (31) Shamis, M.; Lode, H. L.; Shabat, D. *J. Am. Chem. Soc.* **2004**, *126*, 1726
- (32) Smyth, T. P.; O'Donnell, M. E.; O'Connor, M. J.; St Ledger, J. O. *J. Org. Chem.* **1998**, *63*, 7600
- (33) Smyth, T. P.; O'Connor, M. J.; O'Donnell, M. E. *J. Org. Chem.* **1999**, *64*, 3132
- (34) Smyth, T. P.; O'Donnell, M. E.; O'Connor, M. J.; St Ledger, J. O. *Tetrahedron* **2000**, *56*, 5699
- (35) Ruddle, C. C.; Smyth, T. P. *Chem. Commun.* **2004**, 2332
- (36) Ruddle, C. C.; Smyth, T. P. *Org. Biomol. Chem.* **2007**, *5*, 160
- (37) Tugulu, S.; Arnold, A.; Sielaff, I.; Johnsson, K.; Klok, H. A. *Biomacromolecules* **2005**, *6*, 1602
- (38) Tugulu, S.; Silacci, P.; Stergiopoulos, N.; Klok, H. A. *Biomaterials* **2007**, *28*, 2536
- (39) Tugulu, S.; Klok, H. A. *Biomacromolecules* **2008**, *9*, 906
- (40) Livermore, D. M. *Journal of Antimicrobial Chemotherapy* **1998**, *41*, Suppl. D, 25

## 4.6. Supporting Information

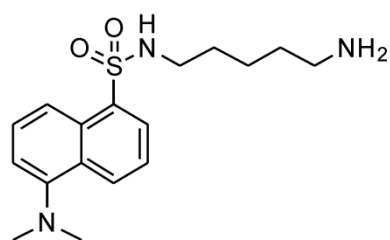
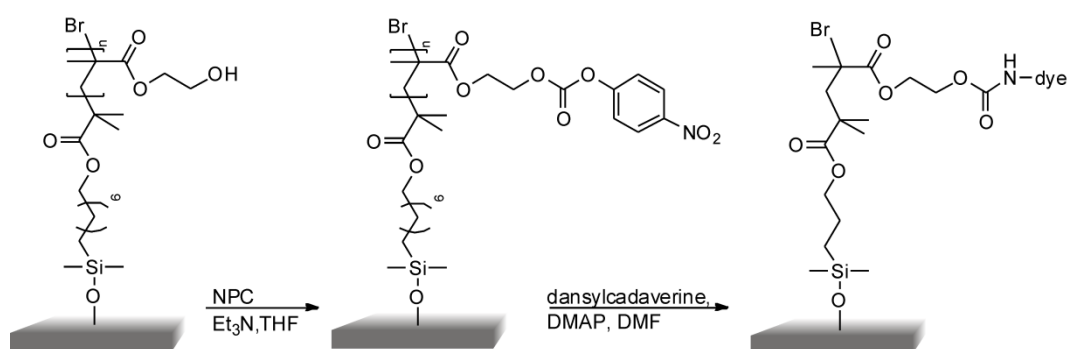


**Figure S1.** Dansylcadaverine structure



**Scheme S1.** Synthetic route for coupling of dansylcadaverine directly to PHEMA brushes

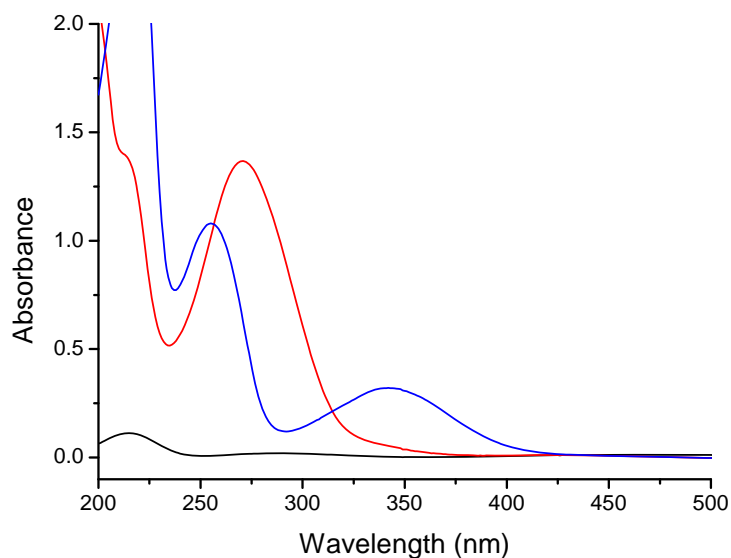


**Figure S2.** UV-Vis spectra of PHEMA (black line); NPC activated PHEMA (red line) and dansylcadaverine modified PHEMA (blue line) with a thickness of the initial PHEMA brush of 97 nm and a grafting density of 100%

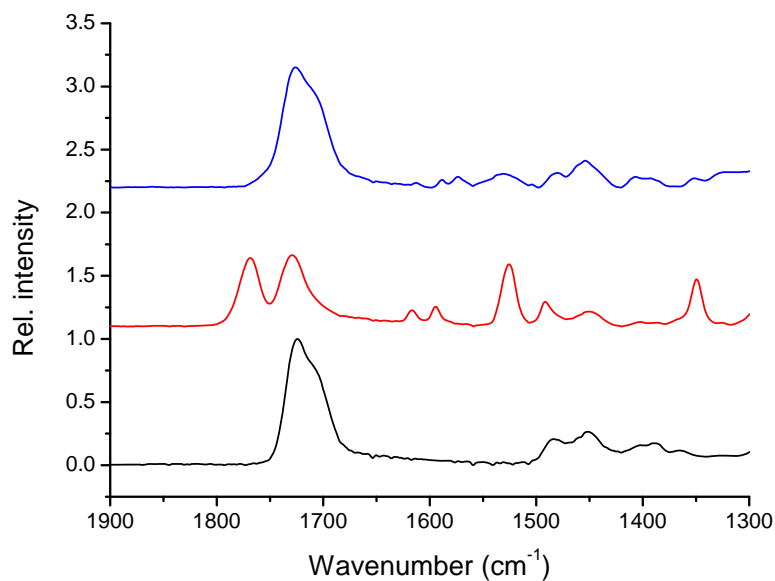


**Figure S3.** FTIR spectra of PHEMA (black line); NPC activated PHEMA (red line) and dansylcadaverine modified PHEMA (blue line) with a thickness of the initial PHEMA brush of 97 nm and a grafting density of 100%

## **5. Synthesis and characterization of hydrolytically degradable polymer brushes**

### **5.1. Introduction**

Biomedical applications of natural or synthetic biodegradable polymers as scaffolds in tissue engineering or for drug delivery systems and therapeutic devices have attracted researchers' interest in the last few years<sup>1-4</sup>. Biodegradable polymers were first introduced in 1980s and there are many criteria for their classification starting with their source: natural or synthetic polymers, chemical composition and synthesis methods, potential applications and processing possibilities. Among the biomaterials, degradable polymers having hydrolytically labile chemical bonds on their backbone are of real interest for applications such as scaffolding matrices for tissue regeneration, bioresorbable implant materials, controlled drug/protein delivery systems, versatile resorbable multifilament sutures.<sup>1-4</sup> Polymer brushes are thin polymeric films with all chains tethered with one end on a surface. There are two main strategies for the synthesis of polymer brushes: "grafting to" in which polymers previously synthesized are bound on a substrate by physisorption or chemisorption, and "grafting from" method involving polymer brush growth from an activated substrate. Although extensively used, the "grafting to" strategy has limitations concerning brush thicknesses and densities, due to steric repulsion hindering the active centers on the surface. "Grafting from" strategy is the most used method in the synthesis of polymer brushes allowing good control over composition and architecture<sup>5-10</sup>. Unfortunately, only few researchers referred in their studies to hydrolytically degradable polymer brushes. Mostly all biodegradable polymer brushes systems are based on polyesters synthesized via surface-initiated ring-opening polymerization of various cyclic ester monomers<sup>8,11-19</sup>. Even if reliable, this route has some limitations due to the laborious steps involved in monomers synthesis and the reduced possibilities to functionalize the obtained polyester brushes. Functional polymer brushes are essential materials for various

biomedical applications, ranging from biopassive or bioactive coatings for different medical devices to coatings for controlled protein/drugs delivery systems<sup>7,10,11</sup>.

Surface-initiated atom transfer radical polymerization (SI-ATRP) is the one of the methods often employed to prepare functional polymer brushes by the “grafting from” strategy<sup>5-10</sup>. Based mainly on an all-carbon backbone, polymer brushes synthesized via ATRP are usually non-biodegradable, therefore somewhat limited in their biomedical applications for which the biodegradability is important<sup>8</sup>. Polymer brushes with poly(ethylene glycol) like properties are known to possess very good bacteria/protein repellency and can undergo further post-modification to allow protein immobilization or mediate cell-adhesion<sup>8,20,21</sup>. Modifying them to be biodegradable can make polymer brushes appropriate for a wider range of biomedical applications, including bioactive coatings on degradable scaffolds for tissue engineering and protein/drugs delivery systems<sup>8</sup>. POEGMA brushes are easy to obtain via SI-ATRP with good control over brush thickness and architecture, but they are intrinsically non-degradable. Recently<sup>8</sup>, a route has been proposed to introduce hydrolysable ester bonds in the backbone using SI-ATRP of 5,6-benzo-2-methylene-1,3-dioxepane (BMDO) and poly(ethylene glycol)methacrylate (POEGMA), proving the obtained brushes are degradable in acidic aqueous solutions, but stable in neutral media. Incorporating the neighboring group moieties with different nucleophilicities in polymers can enhance the rate of ester hydrolysis, and hence to increase the hydrolytic degradability of the resulted products. Therefore, it would be possible to obtain more degradable BMDO based brushes *via* copolymerization with appropriate nucleophilic monomers that can favor hydrolysis through the neighboring group participation. It was proved<sup>22</sup> that tertiary amine containing monomers like 2-(diethylamino)ethyl methacrylate (DEAEMA) can significantly increase the rate of some post-polymerization modification reactions by acting as a local catalyst. Therefore, it can be assumed that polymer brushes based on copolymers of POEGMA, BDMO and DEAEMA could be more sensitive to hydrolytic degradation in physiological conditions involving neutral or slightly acidic media, characteristic for usual implantation sites.

An interesting alternative to address the lack of functionality of polyesters brushes and to enhance their degradability resides in their replacement with polyphosphoesters (PPEs) brushes. PPEs are well-known biomaterials exhibiting good biocompatibility and similarity with biomacromolecules such as naturally occurring nucleic acids and teichoic acids<sup>3,4,23,24</sup>. The polyphosphoesters can be obtained using different techniques including



polyaddition, polycondensation reactions as well as ring opening polymerization (ROP)<sup>3,4</sup>. Phosphate bonds in the polyphosphoesters can be hydrolytically or enzymatically broken under physiological conditions resulting phosphates, alcohols and diols<sup>3</sup>. PPEs have gained in the last decades much interest as biomaterials, due to the presence of pentavalent phosphorous atom in their backbone chain which confers high functionality to these polymers<sup>23,24</sup>, allowing the introduction of bioactive molecules and tuning of the physicochemical properties. Most often PPEs are synthesized in the presence of metallic initiators/catalysts, the most used being aluminum isopropoxide ( $\text{Al}(\text{O}^i\text{Pr})_3$ ) and stannous octoate ( $\text{Sn}(\text{Oct})_2$ ). When biomedical applications are discussed, the cytotoxicity of such compounds has to be considered, such applications imposing a medium free of metallic contaminants<sup>24</sup>. A new route for the synthesis of PPEs using organocatalytic (metal-free) systems for ROP of cyclic monomers has been proposed to address this requirement for biomedical applications<sup>24,25</sup>. To the best of our knowledge although used as biomaterials in various biomedical applications there were not yet attempts to obtain polymer brushes based on polyphosphoesters.

Dedicated to the study of the hydrolytically degradable polymer brushes, this Chapter focuses on two main aspects. First, we carried out the synthesis, characterization and study of the degradation behavior in aqueous media of different pH of polymer brushes obtained by SI-atom transfer radical copolymerization of a cyclic ketene acetal monomer, 5,6-benzo-2-methylene-1,3-dioxepane (BMDO), with POEGMA and DEAEMA. To the best of our knowledge this is the first attempt to incorporate a nucleophilic moiety in a degradable polymer brush that can control the degradation kinetics by neighboring group participation. Secondly, we report for the first time an attempt to synthesize PPE brushes as an alternative to polyester brushes as degradable platforms for biomedical applications as drug/protein delivery systems or scaffolds for tissue engineering. Furthermore, we have used only organocatalysts that ensures biomaterials free of metallic contaminants, known as undesirable in biomedical applications

## 5.2. Experimental Section

### 5.2.1. Materials

All chemicals were purchased from Aldrich and used as received unless stated otherwise. Ethanol and 1,8-diazobicyclo[5.4.0]undec-7-ene (DBU) were dried over calcium hydride at room temperature, followed by distillation under reduced pressure just before use. 1,5,7-Triazabicyclo[4.4.0]dec-5-ene (TBD) was dried overnight under vacuum at room temperature. The inhibitor in OEGMA<sub>6</sub> was removed by passing the monomer through a column of activated, basic aluminum oxide, whereas 2-(diethylamino)ethyl methacrylate was freed from its inhibitor (phenothiazine) via distillation under reduced pressure. Silicon (100) covered with a native silicon oxide layer were used as substrates for surface-initiated polymerization. The synthesis of the ATRP initiator (6-2-(2-Bromo-2-methyl)propionyloxy)hexyldimethylchlorosilane and its immobilization on silicon were performed as described in Chapter 2. Tetrahydrofuran (THF), dichloromethane (DCM) and toluene were purified and dried using a solvent purification system (PureSolv). Ultrahigh quality Milli-Q water was obtained from a Millipore Milli-Q gradient machine fitted with a 0.22 µm filter.

### 5.2.2. Methods

X-ray photoelectron spectroscopy (XPS) was carried out using an Axis Ultra instrument from Kratos Analytical equipped with a conventional hemispheric analyzer. The X-ray source employed was a monochromatic Al K $\alpha$  (1486.6 eV) source operating at 100 W and 10<sup>-9</sup> mbar. All XPS spectra were calibrated on the aliphatic carbon signal at 285.0 eV. Relative sensitivity factors (RSF) of 0.278 (C<sub>1s</sub>), 0.78 (O<sub>1s</sub>) were used to correct peak area ratios. Attenuated total reflectance Fourier transform infrared spectroscopy (ATR-FTIR) was performed on a nitrogen purged Nicolet 6700 FT-IR spectrometer equipped with a SmartiTR™ (Thermo Fisher Scientific Inc., Waltham, MA, USA) accessory and a diamond crystal. Atomic force microscopy (AFM) was performed in tapping mode on a Veeco Multimode Nanoscope IIIa SPM controller (Digital Instruments, Santa Barbara, CA) using NSC14/no Al MikroMasch (Tallinn, Estonia) cantilevers. To determine the layer thicknesses, cross-sectional height profiles of micropatterned polymer brushes on silicon substrates were analysed. Micropatterned initiator-coated substrates were prepared using a protocol previously reported in the literature<sup>26</sup>. Brush thicknesses were also

determined by means of a SOPRA GES-5 ellipsometer working with a He–Ne laser ( $\lambda = 632.8$  nm) at an angle of incidence of  $70^\circ$ . The calculation method was based on a four-layer silicon/initiator/polymer brush/ambient model, assuming the polymer brush to be isotropic and homogeneous. A fixed refractive index value of 1.5 was used for the polymer layer. Water contact angles were determined using a DataPhysics OCA 35 contact angle measurement instrument.  $^1\text{H-NMR}$  spectra were recorded on a Bruker AVANCE-400 Ultra Shield spectrometer.

### 5.2.3. Procedures

#### 5.2.3.1. Synthesis of 1,2-benzenedimethanol

In a three-neck round bottom flask equipped with a reflux column and fitted with a dropping funnel, 315 mL of anhydrous THF were added slowly with stirring to 19.3 g (0.5 mol, 2.5 equiv.) of  $\text{LiAlH}_4$  at  $0^\circ\text{C}$  and under nitrogen. To the  $\text{LiAlH}_4$  slurry was added dropwise a solution of 33.5 g (0.2 mol, 1 equiv.) of *o*-phthalic acid in 215 mL of anhydrous THF. After completion of the addition, the reaction contents were refluxed at  $75^\circ\text{C}$  for 18 hours. Subsequently, the heating was stopped and the solution was allowed to cool. The Steinhardt procedure was used to quench the excess of  $\text{LiAlH}_4$ , namely the mixture was treated at  $0^\circ\text{C}$  by successive dropwise addition of 20 mL of water, 20 mL of 15wt% sodium hydroxide solution, and 60 mL of water leading to the formation of a dry white granular precipitate. After quenching, the solution was stirred at room temperature for an additional 3 hours. The whitish slurry was then filtered at reduced pressure and the precipitate was washed with excess THF. The organic section was extracted with diethylether and was then dried over  $\text{MgSO}_4$ . The solvent was removed under reduced pressure leading to the formation of white crystals which were then dried under the vacuum line.

#### 5.2.3.2. Synthesis of 5,6-Benzo-2-(chloromethyl)-1,3-dioxepane

A mixture of 20 g of 1,2-benzenedimethanol (0.145 mol), 16.48 mL of chloroacetaldehyde dimethyl acetal (0.145 mol) and 100 mg of *p*-toluene sulfonic acid monohydrate was heated at  $120^\circ\text{C}$  for 8 hours under nitrogen in a predried flask fitted with a Claisen-Vigreux, condenser, distillation head and a dropping funnel for collecting the methanol. When almost all the calculated amount of methanol was collected ( $\sim 11.7$  mL), the temperature of the reaction mixture was raised to  $160^\circ\text{C}$ . The crude product was solidified on cooling the reaction mixture to room temperature. The resulting solid was

dissolved in  $\text{CHCl}_3$  and washed with 10%  $\text{NaHCO}_3$  solution and water. After solvent evaporation of the organic section under reduced pressure, the crude product was purified by recrystallization from cyclohexane to give yellow crystals. The crystals were then dried under the vacuum line.

#### 5.2.3.3. Synthesis of 5,6-Benzo-2-methylene-1,3-dioxepane

In a predried flask, a solution made of 10 g (0.05 mol) of 5,6-Benzo-2-(chloromethyl)-1,3-dioxepane in 80 mL of *t*-BuOH was allowed to react with 8.4 g (0.075 mol) of *t*-BuOK at 95 °C for 48 hours under nitrogen. After allowing the reaction mixture to cool, 100 mL of diethylether were added and the mixture was filtered under reduced pressure through silica gel. The filtrate was dried over  $\text{MgSO}_4$  and the solvents were removed under reduced pressure. The crude product was then distilled using a distilling bridge, under vacuum at around 115 °C to give a colorless liquid which solidified to white crystals on standing.

#### 5.2.3.4. Synthesis of Poly(OEGMA<sub>6</sub>-BMDO-DEAEMA) brushes

Surface initiated atom transfer radical polymerizations of OEGMA<sub>6</sub>, BMDO and DEAEMA was performed at 90 °C in bulk using a reaction system consisting of monomers (OEGMA<sub>6</sub>, BMDO and DEAEMA), Cu(I)Cl and 2,2'-bipyridyl in the following molar ratios: 100:1:2. First the monomers and bipy were introduced in a Schlenk tube sealed with a septum and mixed until complete homogenization. Then, the mixture was purged with nitrogen for 1 hour and Cu (I)Cl was added. After homogenization the reaction mixture was heated to 90 °C and transferred with a cannula to a nitrogen purged reactor containing the ATRP initiator modified slides. The reactor was placed in a thermostated oil bath at 90 °C and the reaction was allowed to proceed. After the desired time the polymerization mixture was exposed to air, the slides were removed, washed with water and methanol, dried under a flow of nitrogen and then vacuum.

#### 5.2.3.5. Hydrolytic degradation of Poly(OEGMA<sub>6</sub>-BMDO-DEAEMA) brushes

Degradation studies were carried out on POEGMA, P(OEGMA<sub>75</sub>-BMDO<sub>25</sub>) and P(OEGMA<sub>650</sub>-BMDO<sub>25</sub>-DEAEMA<sub>25</sub>) brushes. The polymer brush coated substrates were kept in aqueous solutions of different pH, which were prepared by dilution of concentrated HCl solutions. At different time intervals, the substrates were taken out of the solutions, washed thoroughly with water and methanol and dried under a flow of

nitrogen and then vacuum. The thicknesses of the polymer brushes were subsequently measured by AFM.

#### **5.2.3.6. Synthesis of 2-ethoxy-2-oxo-1,3,2-dioxaphospholane (EEP)**

2-ethoxy-2-oxo-1,3,2-dioxaphospholane (EEP) was synthesized by esterification of 2-chloro-2-oxo-1,3,2-dioxaphospholane (COP) with ethanol. Briefly, a mixture containing ethanol and triethylamine in dry THF was cooled to 0 °C, and a mixture of 2-chloro-2-oxo-1,3,2-dioxaphospholane in dry THF was added dropwise under stirring with COP/TEA/Alcohol ratio = 1/1/1. After complete addition, the resulting mixture was stirred at 0 °C for 5 hours. The triethylamine hydrochloride salt was removed by filtration, the filtrate was concentrated and the residue was purified by vacuum distillation.

#### **5.2.3.7. Synthesis of the thiourea (TU) cocatalyst**

Cyclohexylamine (1.85 g, 18.5 mmol) was added dropwise at room temperature to a stirring solution of 3,5-bis(trifluoromethyl)phenyl isothiocyanate (5.0 g, 19 mmol) in THF (20 mL). After complete addition, the solution was stirred for 4 hours, the solvent was evaporated and the white residue was recrystallized from chloroform to give a white powder.

#### **5.2.3.8. Synthesis of undecanol modified substrates**

Substrates were first cleaned under ultrasound in ethanol, water and acetone (5 minutes each) and then by oxygen plasma for 10 minutes. The native oxide layer of the silicon oxide was first removed by immersing them in 40% hydrofluoric acid. After 5 minutes the substrates were extensively cleaned with dichloromethane, dried under nitrogen flow and directly used for the UV-induced coupling of undecylenic acid methyl ester (UAME). Six surfaces were covered with a few drops of UAME, covered with a microscopy glass slide and exposed to UV light for 30 minutes. After coupling the substrates were thoroughly washed with acetone and dried overnight under vacuum. The reduction of the ester was carried out as followed; 1.6 g of LiAlH<sub>4</sub> was added slowly to 33 mL of dry THF in a round bottom flask. After dissolution reaction mixture was transferred to a reactor containing the substrates; the reduction was allowed to proceed for 16 hours at room temperature after which the modified surfaces were removed from the reaction mixture,

washed with acetone, 0.5 M HCl, acetone and water. The samples were then dried under a flow of nitrogen and dried over night under vacuum.

#### **5.2.3.9. Synthesis of polyphosphoester brushes**

7.5 mL of 1mM monomer solution in dry toluene were added under nitrogen in a reactor containing the initiator slides (plasma cleaned silicon wafer or undecanol modified silicon wafer). Then using a nitrogen purged syringe 7.5 mL of 0.05 mM catalyst solution (DBU, TBD or DBU+TU) in dry toluene were added and the reaction was allowed to proceed for 4 hours at 0 °C. The polymerization was stopped by transferring the wafers in 40 mL of dry toluene where they were kept for 20 minutes. The slides were then rinsed with ethanol several times and then dried under a stream of nitrogen.

### **5.3. Results and Discussion**

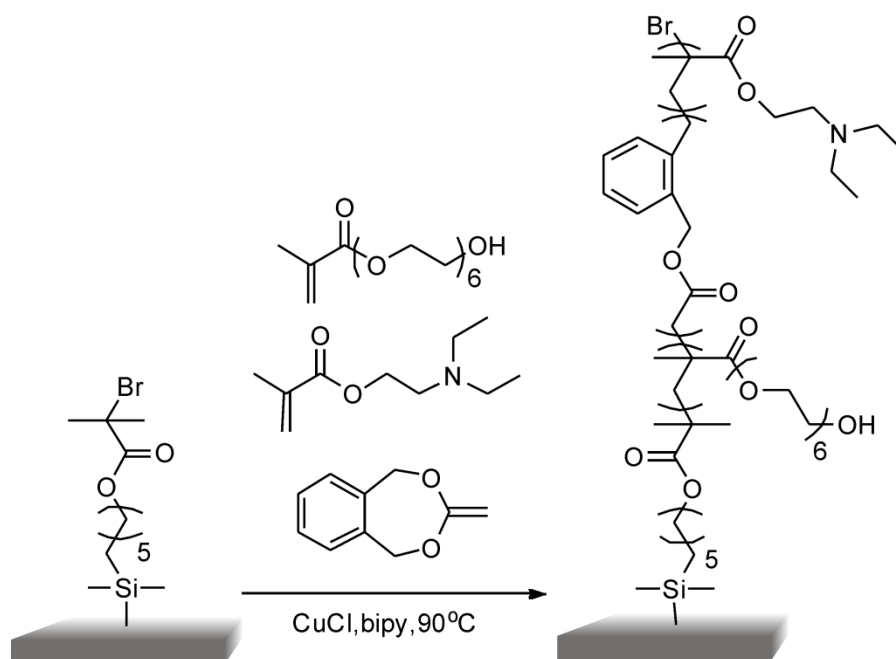
#### **5.3.1. Hydrolytically degradable P(OEGMA-BMDO-DEAEMA) brushes**

SI-ATRP is a method extensively used to obtain HEMA and OEGMA based polymer brushes that are known for their non-fouling properties, but also with limited biomedical applications due to the lack of biodegradability. Recent studies have been performed to render hydrolytic degradability to POEGMA brushes through copolymerization with a cyclic ketene acetal monomer, BDMO, able to introduce hydrolytic/biodegradable ester groups on the polymer backbone. Results proved the obtained copolymer brushes are hydrolytically degraded in acidic conditions, but stable in neutral media<sup>8</sup>. To increase and extend hydrolytic degradability of copolymer brushes based on POEGMA and BMDO we propose herein a new system incorporating DEAEMA as a nucleophile. Polymer brushes able to hydrolytically degrade in neutral or slightly acidic media can find interesting biomedical applications as biopassive or bioactive implant coatings as well as drug delivery system because they met the conditions at the most implantation sites.

##### **5.3.1.1. Synthesis of P(OEGMA-BMDO-DEAEMA) brushes**

5,6-Benzo-2-methylene-1,3-dioxepane (BMDO) was synthesized as presented in Scheme S1 – Supporting Information using a slightly modified literature method<sup>27</sup>, and characterized by <sup>1</sup>H-NMR (Figure S1 to S3, Supporting Information).

The synthesis of P(OEGMA-BMDO-DEAEMA) brushes was performed as presented in Scheme 1. Copolymer brushes were obtained by SI-ATRP, starting with the immobilization of ATRP initiator on previously cleaned silicon wafers. The increase of water contact angle confirmed the successful grafting of the ATRP initiator on the surface, the functionalized surfaces being more hydrophobic. The atom transfer radical copolymerization of BMDO, POEGMA and DEAEMA using a Cu(I)Cl/bipyridyl catalyst system was initiated on the functionalized silicon wafers, at 90 °C. As previously mentioned BMDO was preferentially polymerized and copolymerized by ATRP in solution, and the catalytic system we used was similar with the system reported in literature<sup>8,28</sup>. In parallel, for comparison, POEGMA and P(OEGMA-BDMO) brushes were synthesized, following the same protocol. The monomer feed for the three synthesized polymer brushes was: POEGMA/BMDO/DEAEMA: 100/0/0, 75/25/0 and 50/25/25. For POEGMA brushes the reaction time was 30 minutes, while for the others was 1 hour, and the measured film thickness were 44 nm for POEGMA brushes, 75 nm for (POEGMA-co-BDMO) brushes and 45 nm for (OEGMA-BMDO-DEAEMA) polymer brushes.



**Scheme 1.** Synthetic route for P(OEGMA-BMDO-DEAEMA) brush synthesis

The obtained polymer brushes were characterized by XPS. Figure 1 presents XPS survey and high-resolution elemental scans for POEGMA brush (A), P(OEGMA-BMDO)

brush (B), and P(OEGMA-BMDO-DEAEMA) brush (C). As easily can be noticed, XPS spectra for all brushes evidenced the presence of carbon and oxygen in ratios in concordance with the elemental composition of the monomers in the feed, and furthermore for P(OEGMA-BMDO-DEAEMA) brush the appearance of a 2% nitrogen peak as a clear evidence of DEAEMA presence in the copolymer brushes. Analysis of the high-resolution evidenced the  $C_{1s}$  signal for POEGMA could be fitted with three different components corresponding to three types of carbon atoms: 1 - ester groups units 2 - ethylene glycol units, 3 - aliphatic backbone atoms, with ratios of 2:12:1. These results are in concordance with all previous interpretations of XPS spectra for POEGMA brushes<sup>8,18</sup>. Analyzing the XPS spectrum and high-resolution elemental scan for P(OEGMA-BMDO) brushes the deconvolution of  $C_{1s}$  evidenced a fourth peak at lower energy than aliphatic carbon, assigned to aromatic carbons of BMDO. As expected, adding DEAEMA in the polymer brushes increased the signal corresponding to aliphatic carbons.

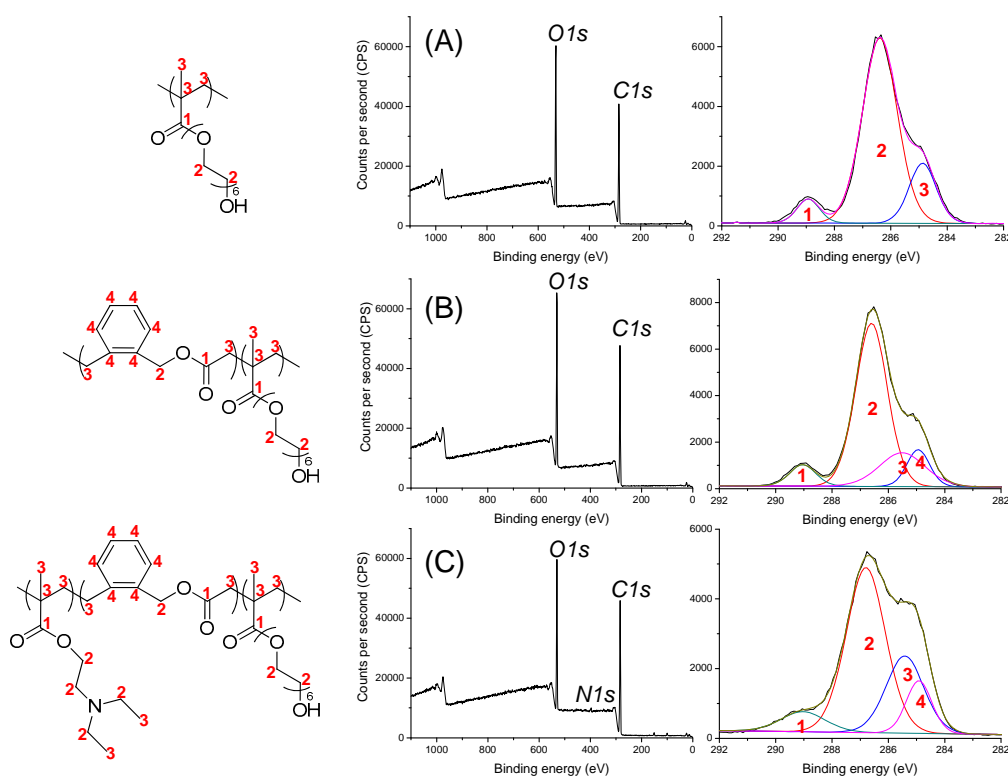
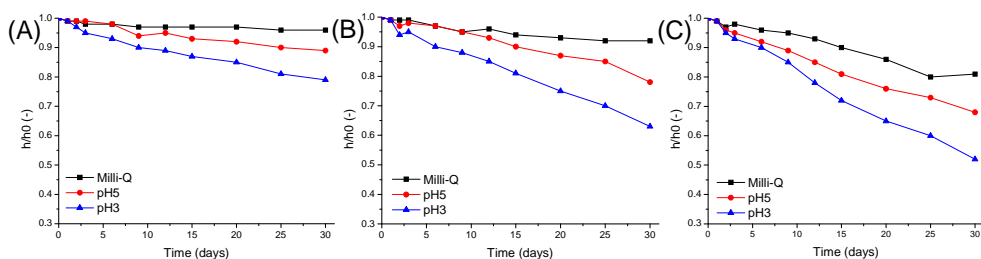


**Figure 1.** XPS survey spectra (left) and high-resolution elemental scans (right) of (A) a 44 nm POEGMA brush, (B) a 75 nm P(OEGMA<sub>75</sub>-BMDO<sub>25</sub>) brush, and (C) a 45 nm P(OEGMA<sub>650</sub>-BMDO<sub>25</sub>-DEAEMA<sub>25</sub>) brush



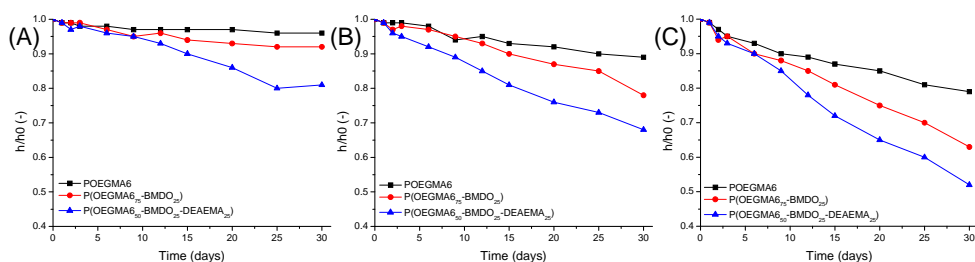
### 5.3.1.2. Degradation kinetics

The degradation kinetics can be evaluated considering the existence of several potential cleavage sites in the synthesized polymer brushes: the ester bonds positioned in the ATRP initiator, on the side chains and in the copolymer main chain, as well as the Si-O-Si link connecting the ATRP initiator with the silicon substrate. To assess their sensitivity to the hydrolytic degradation P(OEGMA-BMDO-DEAEMA) brushes were immersed in aqueous solutions of different pH (Milli-Q water, pH 3 and pH 5) at 20 °C, and the modification in film thickness was monitored for 30 days. The brush thickness was measured by AFM in dry conditions, at various intervals for one month and compared with POEGMA and P(POEGMA-BDMO) brushes. The results are presented in Figure 2 and Figure 3 in which, to simplify the comparison, we used on the y axis the relative thickness defined as the ratio between the measured height and the initial height. Figure 2A evidences the excellent stability of POEGMA brushes in Milli-Q water, even after one month exposure (straight black line). Slight decrease in the POEGMA brush thickness was noticed for water solutions with acidic pH, indication of the degradability dependence on pH. The slight degradation of POEGMA brushes mainly in strong acidic conditions is due to hydrolysis of the side chains, and, also, to scission of the Si-O-Si or ester bonds at the initiator. In concordance with the previous experiments<sup>8</sup>, P(OEGMA-BMDO) brushes were relatively stable in neutral solution (Figure 2B) and lost 21% and 36% thickness at pH 5 and 3, respectively after 30 days due to the introduction of labile ester bonds in the polymer brush backbone thus favoring the hydrolytic degradation of the brushes in acidic solutions. As expected, the copolymer brushes including both BMDO and DEAEMA are the most sensitive to the hydrolytic degradation (Figure 2C) not only for the most acidic conditions, but also in Milli-Q water. The explanation could reside in DEAEMA nucleophilic character and consequently to its effect on the activation of the ability of polymer backbone to be hydrolytically degraded. Moreover, in acidic conditions DEAEMA continues to facilitate the hydrolysis of the ester bonds even if its nucleophilic character may be partially or totally hindered. This could be due to its influence on brush conformation upon exposure to low pH when most likely charges are introduced that could lead to stretching of the polymer brushes, exposing the labile bonds to the hydrolytic attack.



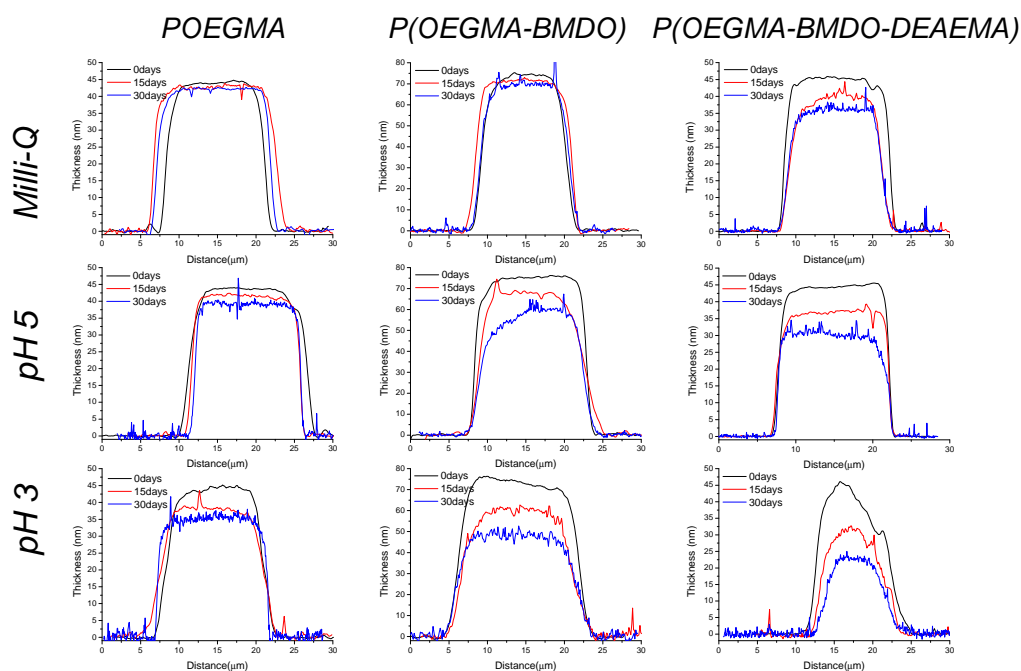
**Figure 2.** Degradation kinetics of (A) a 44 nm POEGMA brush, (B) a 75 nm P(OEGMA<sub>75</sub>-BMDO<sub>25</sub>) brush, and (C) a 45 nm P(OEGMA<sub>650</sub>-BMDO<sub>25</sub>-DEAEMA<sub>25</sub>) brush at 20 °C and different pH conditions

Figure 3 underlines the highest rate of degradability of P(OEGMA-BMDO-DEAEMA) brushes as compared to POEGMA and (POEGMA-*co*-BDMO) brushes for all immersion solutions. The introduction of the third monomer in the copolymer brushes renders the brush degradable even in mild conditions (Milli-Q water) (Figure 3A). Decreasing the pH to 5 (Figure 3B) or 3 (Figure 3C) P(OEGMA-BMDO-DEAEMA) brushes still degrade faster than all the counterparts most likely due to changes in the conformation of polymer brushes. All the representations in Figure 2 and Figure 3 emphasize the degradation kinetics is strongly dependent on pH. It is worth mentioning that introducing the nucleophilic moieties in the copolymer brushes facilitates the hydrolysis of labile bonds in all experimental conditions by means of neighboring group participation or its influence on the brush conformation. Hydrolytically degradable polymer brushes also sensitive in mild conditions can be obtained by tailoring the brush composition.



**Figure 3.** Degradation kinetics of polymer brushes with different compositions in (A) Milli-Q, (B) pH 5 solution, and (C) pH 3 solution at 20 °C

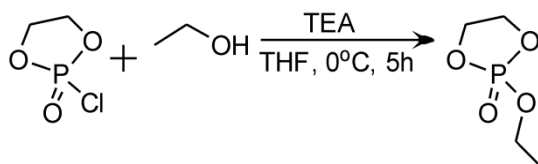
Figure 4 illustrates the 2D cross-sectional profiles for all synthesized copolymer brushes before and after 15 and 30 days of exposure to a Milli-Q, pH 5 and pH 3 solutions at 20 °C. The AFM images complement all the previous observations and sustain the higher hydrolytic degradation of copolymer (OEGMA-BMDO-DEAEMA) brushes in all incubation solutions. If almost no variation in the brush thickness could be noticed for POEGMA and P(OEGMA-BMDO) brushes in Milli-Q even after 30 days exposure, clear modification appeared for DEAEMA containing copolymer brushes after 15 and 30 days. The effect is more evident in acidic conditions being obvious that for DEAEMA containing copolymer brushes significant decreases in film thickness could be noticed. Therefore we can conclude that the introduction of the third comonomer increases the sensitivity of the resulted polymer brushes to hydrolytic degradation even in very mild conditions.



**Figure 4.** AFM 2D cross-sectional profiles of the studied polymer brushes at different time intervals upon exposure to a Milli-Q, pH 5 and pH 3 solution at 20 °C. Cross-sectional profiles: black lines, before degradation; red lines, after 15 days; blue lines, after 30 days

### 5.3.2. Synthesis and characterization of polyphosphoester polymer brushes

Due to the repeating phosphoester bonds in their backbone chain, sensitivity to hydrolytic and enzymatic degradation, polyphosphoesters are materials intensively studied for biomedical applications. In the last few years more attention has been paid to controlled syntheses through ROP to produce PPEs with tailored properties. Moreover, due to the presence of pentavalent phosphorous atom, unlike aliphatic polyesters, they can be functionalized allowing the introduction of bioactive molecules or tuning of the physico-chemical properties. Consequently, we decided to propose PPEs brushes as an attractive alternative of hydrolytically degradable coating with potential interesting applications as scaffolds in tissue engineering or as drug delivery systems. Usually, metallic compounds are used as polymerization catalysts in the PPEs synthesis<sup>23</sup>. Being focused on the potential biomedical applications of the synthesized PPE brush systems we had to consider the cytotoxicity of such compounds and the requirement for the lack of residual metal contaminants in biomaterials. Therefore we decided to adopt for PPEs synthesis a strategy based on organocatalysts like 1,5,7-triazabicyclo[4.4.0]undec-5-ene (TBD), *N*-methylated TBD (MTBD), and 1,8-diazabicyclo[5.4.0]undec-7-ene (DBU) that have been reported to be efficient catalysts in ROP of several lactones<sup>24,29,30</sup>. Due to the commercial availability for our systems we chose to try DBU and TBD knowing that DBU is a monofunctional organocatalyst activating only the alcohol of the initiator, while TBD is able of a dual activation of both the monomer and the alcohol<sup>24</sup>. As monomer we selected 2-ethoxy-2-oxo-1,3,2-dioxaphospholane (EEP) since it the simplest and most easy to synthesize cyclic phosphate monomer. EEP was synthesized by esterification of 2-chloro-2-oxo-1,3,2-dioxaphospholane (COP) with ethanol following a slightly modified procedure from literature<sup>24</sup> (Scheme 2). The structure was confirmed by <sup>1</sup>H-NMR (Figure 5). Instead of ethanol, other bifunctional molecules containing a hydroxyl group can be used for esterification to introduce more functionalities in the monomer.



**Scheme 2.** Synthesis of 2-ethoxy-2-oxo-1,3,2-dioxaphospholane (EEP)

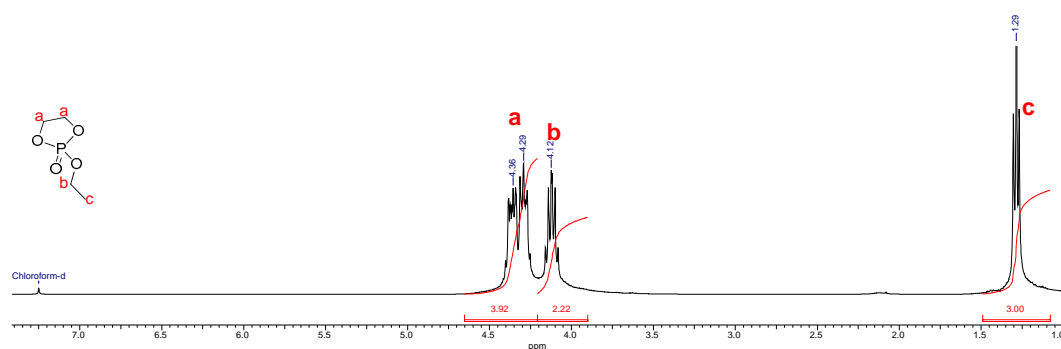
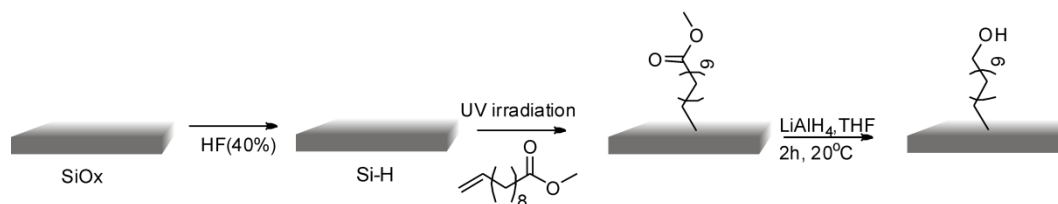


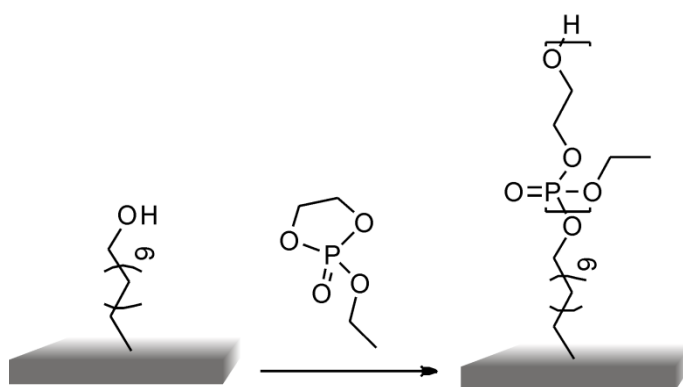
**Figure 5.**  $^1\text{H-NMR}$  of 2-ethoxy-2-oxo-1,3,2-dioxaphospholane (EEP)

For the surface initiated ring opening polymerization of EEP we tried to assess the possibility of using the hydroxyl from plasma cleaned silicon wafers as initiator while using DBU or TBD as catalyst. FTIR and ellipsometry were employed to evaluate if the brushes were grown from Si-OH substrate and the results are presented in Table 1. Unfortunately, the ellipsometric measured thickness was 0 in both cases and no specific FTIR signal ( $\text{P=O}$  at  $1250\text{ cm}^{-1}$  and  $\text{P-O-C}$  at  $950\text{ cm}^{-1}$ ) was observed suggesting that no brush was obtained. From these results we concluded the Si-OH substrate cannot initiate the ROP of the cyclic monomer and decided to modify the substrate, adding a longer spacer between the substrate and the hydroxyl group. This could be achieved by modifying the silicon wafers with undecanol following a slightly modified literature procedure<sup>31</sup> that is presented in Scheme 3. The undecanol modified surfaces were characterized by XPS and water contact angle (WCA) and the results are presented in Table S1 – Supporting Information. As expected, after the reduction of the ester, the water contact angle decreased from  $80^\circ$  to  $65^\circ$ . From the XPS data we can notice that the area of the oxygen and carbon peaks is also decreasing suggesting the successful reduction of the ester. The undecanol modified surface was then used to initiate the ring opening polymerization of EEP with DBU or TBD as catalyst. The reaction followed the procedure presented in Scheme 4. The thickness of the polymer brushes was measured by ellipsometry (Table 1). Even for the modified silicon wafers, the reaction was not successful when TBD was used as catalyst. For the DBU catalytic system polymer brushes with 2 nm thickness were obtained. In order to improve the polymer brush growth a new catalytic system was used consisting of DBU and a thiourea (TU) cocatalyst that has been previously reported to add better control of the polymerization of both lactides<sup>31</sup> and PPE<sup>24</sup>. The TU cocatalyst was synthesized starting from

bis(trifluoromethyl)phenyl isothiocyanate and cyclohexylamine and the reaction is presented in Scheme 5. The TU structure was confirmed by  $^1\text{H-NMR}$  and the results are presented in Figure 6.



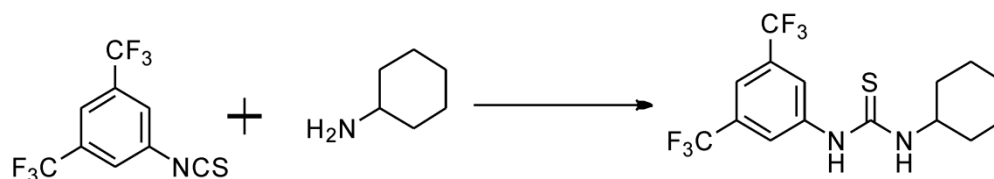
**Scheme 3.** Schematic representation of undecanol coupling to silicon wafers



**Scheme 4.** Synthetic route of PPE polymerization from undecanol modified silicon wafers

**Table 1.** Characterization of all the systems tried for PPE synthesis

Surface	Catalyst system	Thickness (nm)	WCA (°)	Surface composition		
				C (%)	O (%)	P (%)
Si-OH	DBU	0	20	-		
Si-OH	DBU+TU	0	20	-		
Si-OH	TBD	0	20	-		
Si-(CH <sub>2</sub> ) <sub>11</sub> -OH	DBU	1.8±0.17	50	44.5	40.9	14.5
Si-(CH <sub>2</sub> ) <sub>11</sub> -OH	TBD	0	85	-		
Si-(CH <sub>2</sub> ) <sub>11</sub> -OH	DBU+TU	6.2 ±0.12	50	34.5	46.9	18.5



**Scheme 5.** Synthesis of the thiourea (TU) cocatalyst

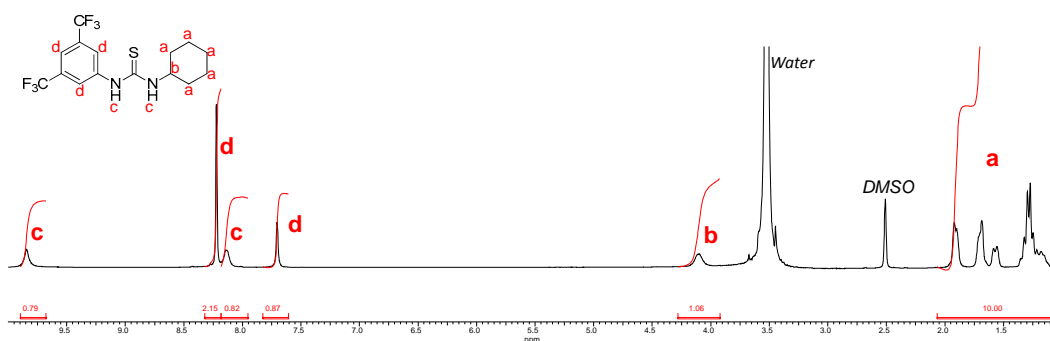


**Figure 6.** <sup>1</sup>H-NMR of the thiourea (TU) cocatalyst

We tried to grow polyphosphoester brushes using the new catalytic system consisting of DBU and TU both from the Si-OH substrate and undecanol modified surfaces. FTIR and ellipsometry were used to characterize the obtained polymer surfaces. Even using this catalytic system no change could be observed for the Si-OH substrate, but for the first time on undecanol modified substrate we could observe from the FTIR spectrum the appearance of the P=O peak at 1250 cm<sup>-1</sup> (Figure 7). This indicates that undecanol modified surface was able to initiate the polymerization in these conditions. The ellipsometric thickness measured for this case was about three times higher compared to the one obtained for the DBU catalytic system. This observation is in concordance with literature data for ROP of the cyclic phosphate monomers in solution<sup>24</sup> for which was proved that DBU can initiate the polymerization reaction through the basic activation of propagating alcoholic chain end, but with a reduced reaction rate. The addition of a cocatalyst able to activate the monomer hastens the reaction, and, in our case, thicker polymer brushes were obtained. It is obvious that a dual system able to activate both the monomer and the initiator is the most efficient catalytic system for the ROP of cyclic phosphoesters on surfaces. There are data proving this system works for the polymerization of lactones<sup>32,33</sup> and CPMS<sup>24</sup> in solution and we succeeded to prove it is valid also for cyclic phosphoesters on surface. The low thickness obtained for the

polyphosphoester brushes could be due to low grafting density of the polymer, the collapsed conformation of the grafted polymers, EEP polymers having a  $T_g$  around  $-40$  °C according to literature<sup>24,34</sup>, or to some still unclear, side reactions. Nevertheless, the thickness is in concordance with literature data for polyester brushes, that had an ellipsometrically determined thickness of approx.  $80\text{--}100\text{\AA}$ <sup>35</sup>. The modification of the water contact angle (Table 1) also indicates the successful grafting of the polyphosphoesters on the surface.

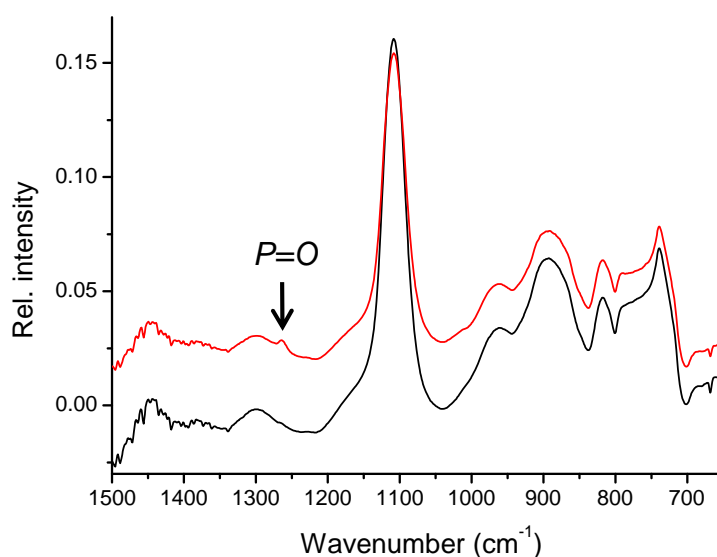


**Figure 7.** FTIR spectra of undecanol modified silicon wafers (A) and polyphosphoester brushes synthesized with DBU+TU cocatalyst system (B)

The obtained polymer brushes were characterized by XPS. Figure 8 presents XPS survey and high-resolution elemental scans for undecanol silicon modified surfaces (A), and polyphosphoester brushes grafted on surface (B). As easily can be noticed, XPS spectra evidenced the presence of phosphorus on the surface at 137 eV. High resolution  $C_{1s}$  for the undecanol modified silicon surface could be fitted with the two corresponding components one for the aliphatic carbon and the second for the carbon next to the oxygen. As expected, for the polyphosphoester modified surfaces an increase in the second component could be noticed, further confirming the structure of the polymer brush. Even if the thickness of the synthesized brushes was quite low they can find potential



applications as building blocks for biodegradable antibacterial platforms, scaffolds for tissue engineering or protein/drug release systems<sup>23,34</sup>.

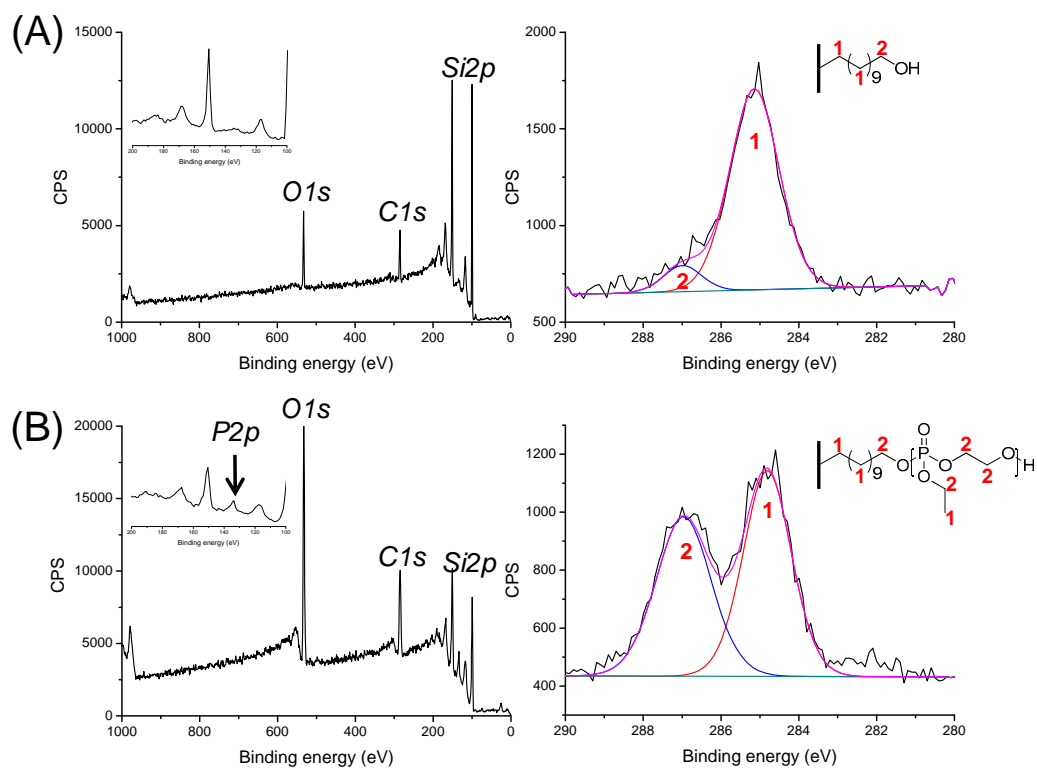


**Figure 8.** XPS survey spectra (left) and high-resolution elemental scans (right) of (A) undecanol silicon modified surfaces (B) polyphosphoester brushes synthesized with DBU+TU cocatalyst system

## **5.4. Conclusions**

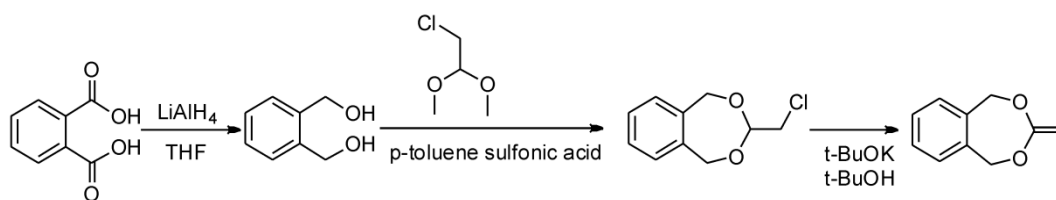
This Chapter centered on the possibility to obtain hydrolytically degradable platforms based on polymer brushes. Two strategies were explored one focused on improving the degradability of existing polymer brushes and the second by proposing an alternative to polyesters. The first approach refers to enhancing the degradability of polymer brushes based on 5,6-benzo-2-methylene-1,3-dioxepane (BMDO) by introducing a DEAEMA nucleophilic moiety. SI-ATRP was used to obtain POEGMA-BMDO-DEAEMA copolymers and their degradability in neutral or acidic conditions was evaluated. XPS was used for surface characterization and it evidenced the incorporation of DEAEMA monomer. It was proved that adding a nucleophilic to brushes makes the systems more sensitive to hydrolytic degradation in Milli-Q water as well as in acidic conditions. The second approach reported, for the first time, the synthesis of the polyphosphoester brushes as an alternative to degradable polyester brushes. Polyphosphoesters, known as degradable, functional polymers, obtained till now only in solution, proved suitable for interesting biomedical applications. The polyphosphoester brushes were synthesized by surface-initiated ring opening polymerization from undecanol modified silicon wafers using DBU+TU co-catalytic system. The structure of the brushes was confirmed by XPS and a 6.2 nm thickness was determined by ellipsometry. It is envisioned that such brush based coatings could have interesting biomedical applications in controlling processes at surfaces or as scaffolds in tissue engineering. Moreover the design of thin, biodegradable polymer brush layers can ensure functional building blocks for platforms suitable for antibacterial applications as implants coatings, as well as controlled release devices applicable in drug delivery systems or tissue engineering.

## 5.5. References

- (1) Ghanbarzadeh, B.; Almasi, H. *Chapter 6 – Biodegradable Polymers, in Biodegradation - Life of Science*, Edited by Rolando Chamy and Francisca Rosenkranz, Publisher: InTech, **2013**
- (2) Vroman, I.; Tighzert, L. *Materials* **2009**, *2*, 307
- (3) Lakshmi S. Nair, L. S.; Cato T. Laurencin, C. T. *Prog. Polym. Sci.* **2007**, *32*, 762
- (4) Tian, H.; Tang, Z.; Zhuang, X.; Chen, X.; Jing, X. *Progress in Polymer Science* **2012**, *37*, 237
- (5) Edmondson, S.; Osborne, V. L.; Huck, W. T. S. *Chem. Soc. Rev.* **2004**, *33*, 14
- (6) Olivier, A.; Meyer, F.; Raquez, J.-M.; Damman, P.; Dubois, P. *Progress in Polymer Science* **2012**, *37*, 157
- (7) Barbey, R.; Lavanant, L.; Paripovic, D.; Schuwer, N.; Sugnaux, C.; Tugulu, S.; Klok, H.-A. *Chem. Rev.* **2009**, *109*, 5437
- (8) Riachi, C.; Schüwer, N.; Klok, H.-A. *Macromolecules* **2009**, *42*, 8076
- (9) Xua, F. J.; Neoh, K. G.; Kang, E. T. *Prog. Polym. Sci.* **2009**, *34*, 719
- (10) Siegwart, D. J.; Oh, J. K.; Matyjaszewski, K. *Progress in Polymer Science* **2012**, *37*, 18
- (11) Choi, I. S.; Langer, R. *Macromolecules* **2001**, *34*, 5361
- (12) Yoon, K. R.; Koh, Y. J.; Choi, I. S. *Macromol. Rapid Commun.* **2003**, *24*, 207
- (13) Yoon, K. R.; Yoon, O. J.; Chi, Y. S.; Choi, I. S. *Macromol. Res.* **2006**, *14*, 205
- (14) Yoon, K. R.; Lee, Y.-W.; Lee, J. K.; Choi, I. S. *Macromol. Rapid Commun.* **2004**, *25*, 1510
- (15) Zeng, H.; Gao, C.; Yan, D. *Adv. Funct. Mater.* **2006**, *16*, 812
- (16) Möller, M.; Nederberg, F.; Lim, L. S.; Kånge, R.; Hawker, C. J.; Hedrick, J. L.; Gu, Y. D.; Shah, R.; Abbott, N. L. *J. Polym. Sci., Part A: Polym. Chem.* **2001**, *39*, 3529
- (17) Husemann, M.; Mecerreyes, D.; Hawker, C. J.; Hedrick, J. L.; Shah, R.; Abbott, N. L. *Angew. Chem., Int. Ed.* **1999**, *38*, 647
- (18) Xu, L.; Gorman, C. B. *J. Polym. Sci., Part A: Polym. Chem.* **2010**, *48*, 3362
- (19) Hu, X Hu, G.; Crawford, K.; Gorman, C. B. *J. Polym. Sci., Part A: Polym. Chem.* **2013**, *51*, 4643
- (20) Tugulu, S.; Arnold, A.; Sielaff, I.; Johnsson, K.; Klok, H.A. *Biomacromolecules* **2005**, *6*, 1602
- (21) Tugulu, S.; Silacci, P.; Stergiopoulos, N.; Klok, H.A. *Biomaterials* **2007**, *28*, 2536

- (22) Barbey, R.; Klok, H.-A. *Langmuir* **2010**, *26*, 18219
- (23) Wang, Y.-C.; Yuan, Y.-Y.; Du, J.-Z.; Yang, X.-Z.; Wang, J. *Macromol. Biosci.* **2009**, *9*, 1154
- (24) Clément, B.; Grignard, B.; Koole, L.; Jérôme, C.; Lecomte, P. *Macromolecules* **2012**, *45*, 4476
- (25) Kiesewetter, M. K.; Shin, E. J.; Hedrick, J. L.; Waymouth, R. M. *Macromolecules* **2010**, *43*, 2093
- (26) Tugulu, S.; Harms, M.; Fricke, M.; Volkmer, D.; Klok, H.-A. *Angew. Chem, Int. Ed.* **2006**, *45*, 7458
- (27) Wickel, H.; Agarwal, S. *Macromolecules* **2003**, *36*, 6152
- (28) Lutz, J. F.; Andrieu, J.; Üzgüün, S.; Rudolph, C.; Agarwal, S., *Macromolecules* **2007**, *40*, 8540
- (29) Lohmeijer, B. G. G.; Pratt, R. C.; Leibfarth, F.; Logan, J. W.; Long, D. A.; Dove, A. P.; Nederberg, F.; Choi, J.; Wade, C.; Waymouth, R. M.; Hedrick, J. L. *Macromolecules* **2006**, *39*, 8574
- (30) Pratt, R. C.; Lohmeijer, B. G. G.; Long, D. A.; Waymouth, R. M.; Hedrick, J. L. *J. Am. Chem. Soc.* **2006**, *128*, 4556
- (31) Wang, X.; Ruther, R. E.; Streifer, J. A.; Hamers, R. J. *J. Am. Chem. Soc.* **2010**, *132*, 4048
- (32) Pratt, R. C.; Lohmeijer, B. G. G.; Long, D. A.; Lundberg, P. N. P.; Dove, A. P.; Li, H.; Wade, C. G.; Waymouth, R. M.; Hedrick, J. L. *Macromolecules* **2006**, *39*, 7863
- (33) Iwasaki, Y.; Wachiralapphathoon, C.; Akiyoshi, K., *Macromolecules* **2007**, *40*, 8136
- (34) Zhang, F.; Smolen, J. A.; Zhang, S.; Li, R.; Shah, P. N.; Cho, S.; Wang, H.; Raymond, J. E.; Cannon, C. L.; Wooley, K. L. *Nanoscale* **2015**
- (35) Hu, X.; Gorman, C. B. *Acta Biomaterialia* **2014**, *10*, 3497

## 5.6. Supporting Information



Scheme S1. Synthetic route of BMDO synthesis

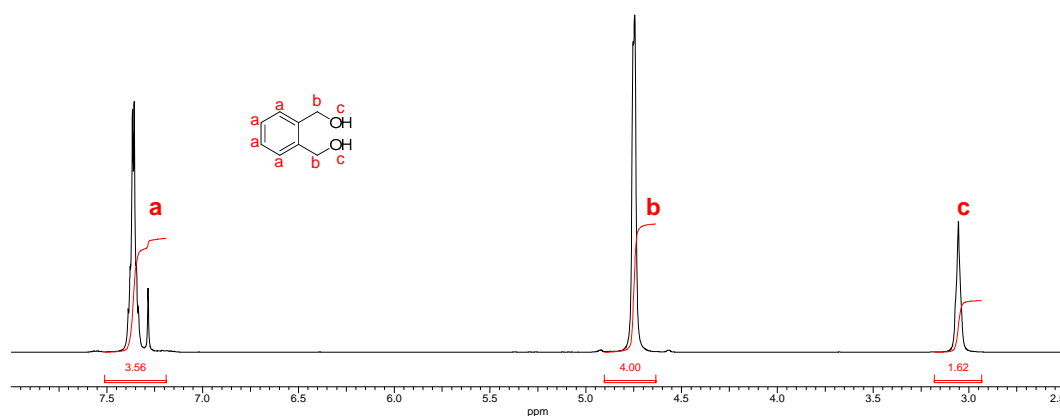


Figure S1. <sup>1</sup>H-NMR of benzodimethanol

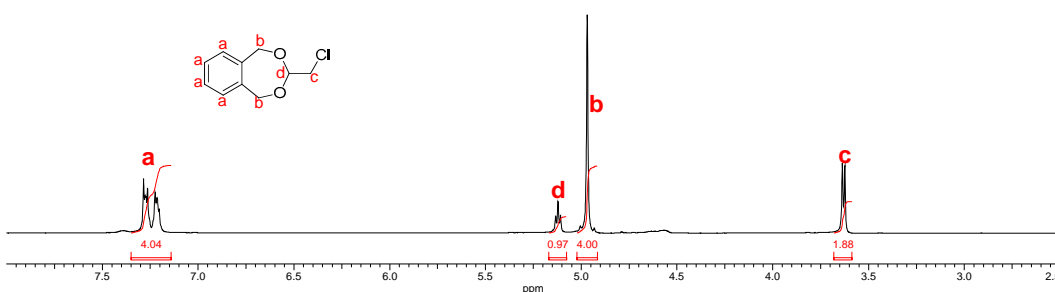


Figure S2. <sup>1</sup>H-NMR of 3-(chloromethyl)-1,5-dihydrobenzo[e][1,3]dioxepine

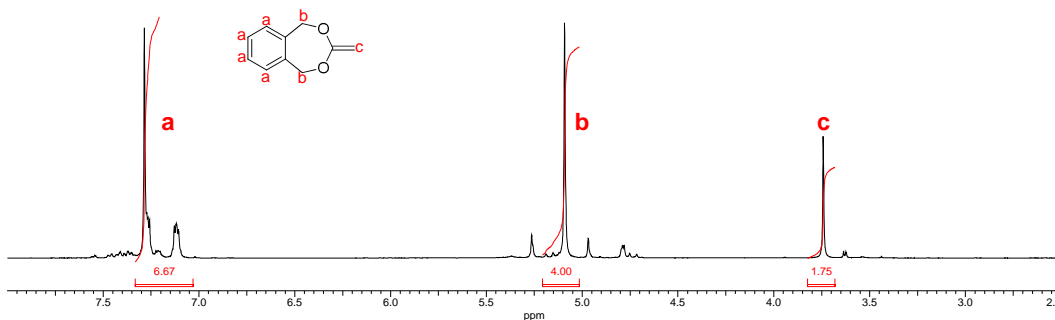


Figure S3. <sup>1</sup>H-NMR of BMDO

**Table S1.** XPS and WCA characterization of undecanol modified surfaces and its precursor

	XPS peak	Sample	
		Si-UAME	Si-undecanol
XPS atomic concentration (%)	O 1s	13.28	10.91
	C 1s	23.02	20.75
	Si 2p	63.70	68.34
WCA	-	80	65

## 6. Conclusions and Perspectives

New approaches addressing antibacterial protection of implantable medical devices are of paramount importance for the reduction of the incidence of biomaterial-related infections. Based on deep understanding of biofilm formation and growth mechanism, the new strategies have to consider both potential antifouling and bactericidal action of the newly synthesized materials. Polymer brushes can be obtained through a variety of controlled polymerization methods and may represent an interesting alternative for the development of versatile and reliable platforms for antibacterial applications. Polymer brushes can be synthesized with fine tuned physicochemical properties, controlled architecture and functionalities to address various requirements imposed by applications as antibacterial coatings for implant surfaces. This Thesis exploited the possibilities provided by surface-initiated controlled radical polymerization to synthesize both non-fouling and antibacterial polymer brush surfaces and to offer new perspectives for the development of new multifunctional antimicrobial platforms.

**Chapter 2** considered the high impact of *Staphylococcus epidermidis* in hospital-acquired infections and tested, for the first time, the resistance against *S. epidermidis* adhesion of HEMA and OEGMA polymer brushes. Polymer brushes were successfully synthesized by SI-ATRP with good control over grafting densities and thicknesses. This allowed the preparation of a large library of polymer brushes and to study the influence of these parameters on the bacteria repellent property. All prepared samples were compared with PEG brushes considered as “gold standard” material in the preparation of antifouling surfaces. Crystal Violet staining was employed as method to assess bacterial adhesion on the synthesized surfaces. All surfaces proved antibacterial proprieties against *S. epidermidis* at least comparable with PEG brushes regardless the grafting density and thickness. The only exception was the case of surfaces with very low grafting densities at short polymerization times where insufficient surface coverage reduces the ability of the coating to prevent bacteria adhesion. Both HEMA and OEGMA polymer brushes proved suitable for tailoring surfaces able to delay or avoid bacteria attachment, altering the biological response of the pristine surface. This study is particularly interesting offering interesting perspectives involving the possibility to exploit the functionalities present on the polymer side-chain for coupling a broad range of bioactive compounds, including antimicrobials. Moreover, such functionalities can facilitate the development of attractive

platforms for drug delivery systems. Further studies can focus on the design of particular nonfouling coatings appropriate for specific bacterial strains and on *in vivo* testing of the efficiency of the obtained surfaces. Also, an in-depth study should be realized to clarify the correlation between non specific protein adsorption and bacterial antiadhesive properties for a wide range of polymer brush surfaces and relevant bacterial strains.

In **the third Chapter** we explored the possibility to obtain dual biopassive-bioactive coatings based on the antifouling character of the polymer brushes and the active bacteria killing effect of an antibiotic immobilized on the surface. Vancomycin was immobilized on the polymer brush surfaces both via the glycosidic primary amine and the carboxyl group. ELISA testing and XPS were used to evidence the coupling of vancomycin on surfaces. All surfaces were tested against *S. epidermidis* using SYTO9/PI staining. Upon modification with vancomycin, both via the primary amine or carboxylic group, PHEMA brushes lost their nonfouling properties and no bactericidal effect could be noticed. Vancomycin modified POEGMA brushes with the antibiotic coupled via the C-terminal carboxylic acid led to dual-functional bacteria repellent – bactericidal surfaces although the bactericidal effect was smaller than expected. For the coupling of the vancomycin via the primary amine group to OEGMA polymer brushes no bactericidal effect could be revealed but the brushes kept their antifouling properties. This is the first successful attempt to create polymer brush based surfaces exhibiting both bacteria repellent and bactericidal effect, offering the premises to develop more complex systems able to combine the biopassive properties of the polymer brushes with different bactericidal compounds. More research can reveal the interaction mechanism between the antibiotic modified polymer brushes and the microorganisms as well as the influence of polymer brush architecture on the activity of the antibacterial agent. An interesting perspective is to use antimicrobial peptides (AMPs) as bactericidal agents as long as they proved to be effective against different bacterial strains. Further research should aim at elucidating the influence of the PEG side-chain length on the ability of the active compound to reach and kill the approaching bacteria. Moreover, supplementary studies can explain how the coupled antimicrobial agent affects the nonfouling properties of the polymer brush surface as well as the complex reciprocal influences between the coating nonfouling character and the activity of the bactericidal compound.

The main goal of **the fourth Chapter** was to study different approaches based on polymer brushes to release an active component only in the presence of infection or approaching bacteria. As bacteria signals specific enzymes (Autolysins and  $\beta$ -lactamases)



secreted by bacteria able to cleave a linker connecting the active compound to polymer brushes were selected. The ability of autolysins to induce the cleavage of a peptide linker and to release a fluorescent (7-Methoxycoumarin-4-yl)-acetyl (Mca) dye linked to polymer brushes was analyzed. Also, we evaluated the capacity of  $\beta$ -lactamase to cleave a cephalosporine-like linker (7-HACA) and release the bound dansylcadaverine dye. Autolysins successfully induced the dye release only for low grafting density thin polymer brushes which seem to be more stable in the selected experimental conditions, while no dye release was observed for  $\beta$ -lactamase. It was proved that a bacteria triggered release system can be obtained using polymer brushes. Supplementary studies on the conformation and architecture of the polymer brush, linker structure, as well as, on the properties of the active component could lead to a more efficient system. Moreover, in further experiments it would be interesting to use the autolysin developed platform to link an antibiotic and study its release kinetics and bactericidal properties. Of real interest are antibiotics with proven activity both in solution as well as immobilized, for comparing the influence of the polymer brush surfaces on their effectiveness against various bacterial strains.

**Chapter 5** studied the possibility to obtain hydrolytically degradable platforms based on polymer brushes, first by trying to enhance the degradability of P(OEGMA-BMDO) brushes and second by proposing an alternative to polyester brushes. In the first case it was proved that introducing DEAEMA moiety can increase the degradability of copolymer brushes not only in acidic conditions but also in neutral or slightly acidic media. Although the results are promising, more studies are required to understand the catalytic effect of the nucleophilic moiety and the effect of the polymer brush conformation on the degradability of the system. Moreover this method can be successfully employed for controlling and tailoring the hydrolytic degradation of other degradable polymer brushes in different media. In the second case, we reported for the first time the synthesis of the polyphosphoester brushes as an alternative to polyester brushes. Even if the thickness of the synthesized brushes was quite low they can find potential applications as building blocks for biodegradable antibacterial platforms, scaffolds for tissue engineering or protein/drug release systems. Polymer brushes surfaces with improved hydrolytic degradability can be further used as modular platforms in the release of a wide range of bactericidal agents. More studies can elucidate the biodegradability mechanisms of different copolymer brushes analyzing the influence of various systems on the activity of a wide range of bactericidal agents.

Overall this Thesis successfully highlighted the possibility of using polymer brush surfaces as versatile and reliable platforms for multiple antibacterial applications. It has been proved that by the appropriate design of the system the polymer brushes could exhibit bacteria repellent properties, bactericidal activity as well as degradability. All these properties could be used and combined for the future design of more specialized antibacterial coatings.

## Curriculum vitae

### IBĂNESCU SORIN-ALEXANDRU

Date of birth: 6 May 1983

Place of birth: Iasi (RO)

Nationality: Romanian

Marital status: married

#### *Education & Professional Experience*

Since May 2010: Ph. D. Thesis in the group of Prof. H.-A. Klok, Polymers Laboratory, École Polytechnique Fédérale de Lausanne (EPFL) (Switzerland).

Ph. D. thesis: *Surface Grafted Polymer Brushes: A Versatile Platform for Antibacterial Applications*

- 2007 – 2008    **Master of Science – specialization *Polymeric Biomaterials***, “Gheorghe Asachi” Technical University of Iasi, Faculty of Chemical Engineering and Environmental Protection, Master Thesis: *Rheological studies of dough based products*
- 2002 – 2007    **Diploma engineer** “Gheorghe Asachi” Technical University of Iasi, Faculty of Chemical Engineering and Environmental Protection, Major in *Macromolecular Compounds Engineering and Chemistry*
- 1998 - 2002    **Baccalaureate**, “Grigore Moisil” High school, Iasi, Romania, Diploma as *Computer Programmer*

#### *Employment*

- 2007 – 2010    Research assistant at “Petru Poni” Institute of Macromolecular Chemistry, Iasi, Romania
- 2006 – 2007    Research technician at “Petru Poni” Institute of Macromolecular Chemistry Iasi, Romania
- 2003 - 2006    PC operator, S.C. Management Proiect Consult, Iasi, Romania

#### *Technical skills*

- Working experience in organic and polymer synthesis (ATRP, SI-ATRP, SET-LRP, RAFT, SI-RAFT)
- Functionalization of polymers with different biomolecules; bacteria adhesion tests

- Working experience with various instrumental techniques for polymer and surface characterization such as FTIR spectroscopy, XPS spectroscopy, Atomic Force Microscopy, ellipsometry, dynamic mechanical analysis, rheometry, thermogravimetric analysis, differential scanning calorimetry, UV-Vis spectroscopy, spectrofluorometry; contact angle measurement
- Strong research, analytical and writing skills
- Experience in maintaining at troubleshooting scientific instrumentation

### *Languages*

- Romanian (mother tongue)
- English (fluent)
- French (intermediate)

### *Selected publications, posters and talks*

1. **HEMA/OEGMA Polymer Brushes - An Attractive Platform to Prevent Bacteria Adhesion**, S. Ibanescu, J. Nowakowska, N. Khanna, R. Landmann, H.-A. Klok, *in preparation*
2. **Stimuli Responsive Graft Polysiloxanes**, A. D. Rusu (Hodorog), C. Ibanescu, E. Resmerita, A. B. Simionescu, M. Danu, V. Hurduc, S. Ibănescu, *Revista de Chimie*, 64(6), 667-671, 2013
3. **Rheology of gelatin – starch systems. I. Influence of system composition**, A. B. Simionescu, S. Ibănescu, M. Danu, I. Rotaru, C. Ibănescu, *Revista de Chimie*, 64(8), 909-913, 2013
4. **Gluten content influence on rheological behavior of starch-gluten networks**, M. Danu, I. Rotaru, C. Ibănescu, N. Hurduc, S. Ibănescu, B. C. Simionescu, *EEMJ*, 11(11), 1883-1888, 2012
5. **Thermal, dynamic mechanical, and dielectric analyses of some polyurethane biocomposites**, D. Macocinschi, D. Filip, S. Vlad, M. Cristea, V. Musteata, S. Ibanescu, *Journal of Biomaterials Applications*, 27(2), 119-129, 2012
6. **Effect of montmorillonite content in nanocomposites of segmented polyurethanes with poly(2-alkyl-2-oxazoline) sequences**, G. David, B. C. Simionescu, S. Ibanescu, F. Vearba, *High Performance Polymers*, 23(1), 74-84, 2011
7. **Dynamic Mechanical Analysis of Polyurethane-Epoxy Interpenetrating Polymer Networks**, M. Cristea, S. Ibanescu, C. N. Cascaval, D. Rosu, *High Performance Polymers*; 21(5), 608 – 623, 2009.

### *Oral Presentations:*

1. **Nouveaux polyurethane/montmorillonite nanocomposites. Rapport structure-propriétés**, G. David, B. C. Simionescu, S. Ibănescu, G. Lisă, *IXème Colloque Franco - Roumain sur les Polymères - Alba Iulia*, 26-29 august 2009

2. **Polyurethane based nanocomposites**, G. David, S. Ibănescu, G. Lisă, F. Vearbă, *Zilele Facultății de Inginerie Chimică și Protecția Mediului, New Frontiers in Chemistry and Chemical Engineering*, Iasi, 18-20 Nov. 2009
3. **Dynamic mechanical analysis. Rheology or thermal method for polymer characterization** (plenary lecture), M. Cristea, D. Ionita, S. Ibănescu, B. C. Simionescu, *ZILELE ACADEMICE IEȘENE, a XXII-a sesiune de comunicări științifice a Institutului de Chimie Macromoleculară "Petru Poni", Progrese în știința compușilor organici și macromoleculari*, Iași, 8 - 10 octombrie 2009
4. **DMTA Study of Polyurethane-Epoxy Interpenetrating Polymer Networks**, S. Ibănescu, M. Cristea, D. Ionită, B. C. Simionescu, *ZILELE ACADEMICE IEȘENE, a XXII-a sesiune de comunicări științifice a Institutului de Chimie Macromoleculară "Petru Poni", Progrese în știința compușilor organici și macromoleculari*, Iași, 8 - 10 octombrie 2009

**Posters:**

1. **Termogravimetric analysis of mineral and synthetic oils**, S. Ibănescu, M. Danu, C. Ibănescu, G. Lisă, *Zilele Facultății de Inginerie Chimică și Protecția Mediului, New Frontiers in Chemistry and Chemical Engineering*, Iasi, 18-20 Nov. 2009
2. **Frequency-induced phenomena in polymers as revealed by dynamic mechanical analysis**, D. Ionita, S. Ibănescu, M. Cristea, B. C. Simionescu, *Frontiers in Macromolecular and Supramolecular Chemistry, The Second Cristofor I. Simionescu Symposium*, Iasi 2-3 June 2009
3. **Viscoelastic properties of polymer dispersed liquid crystals based on polysulfone udel and thermotropic azomethines** (poster), S. Ibănescu, D. Ionită, M. Cristea, V. Cozan, *ZILELE ACADEMICE IEȘENE, a XXII-a sesiune de comunicări științifice a Institutului de Chimie Macromoleculară "Petru Poni", Progrese în știința compușilor organici și macromoleculari*, Iași, 8 - 10 octombrie 2009